Dynamics of Mobile Impurities in One-Dimensional Quantum Liquids

A DISSERTATION
SUBMITTED TO THE FACULTY OF THE GRADUATE SCHOOL
OF THE UNIVERSITY OF MINNESOTA
BY

Michael Schecter

IN PARTIAL FULFILLMENT OF THE REQUIREMENTS
FOR THE DEGREE OF
Doctor of Philosophy

Alex Kamenev

August, 2014

Acknowledgements

It is a great pleasure to thank all those who helped contribute to my understanding of impurity motion in one-dimensional systems. The material presented in this dissertation has certainly benefited from numerous discussions with many talented students and postdocs as well as my collaborators during the course of my graduate studies. I would like to mention in particular O. Gamayun, D. M. Gangardt, S. Gopalakrishnan, M. Knap, A. Lamacraft, A. Levchenko, O. Lychkovskiy, T. Price, R. Schmidt, and D. Schneble.

Finally, I would like to express my sincere gratitude towards A. Kamenev who first introduced me to the fascinating world of physics in one dimension and whose patience, guidance and support substantially enriched my time at the University of Minnesota.

Dedication

To my family, especially my mother Gina, for all of their unconditional support throughout the years.

To my wife Carly, for her remarkable strength, patience and encouragement during the hardest of times.

Abstract

We study the dynamics of mobile impurities in a one-dimensional quantum liquid. Due to singular scattering with low-energy excitations of the host liquid, the impurity spectral properties become strongly renormalized even at weak coupling. This leads to universal phenomena with no higher-dimensional counterparts, such as lattice-free Bloch oscillations, power-law threshold behavior in the impurity spectral function and a quantum phase transition as the impurity mass exceeds a critical value. The additional possibility of integrability in one-dimension leads to the absence of thermal viscosity at special points in parameter space. The vanishing of the phonon-mediated Casimir interaction between separate impurities can be understood on the same footing.

We explore these remarkable phenomena by developing an effective low-energy theory that identifies the proper collective coordinates of the dressed impurity, and their coupling to the low-energy excitations of the host liquid. The main appeal of our approach lies in its ability to describe a dynamic response using effective parameters which obey exact thermodynamic relations. The latter may be extracted using powerful numerical or analytical techniques available in one-dimension, yielding asymptotically exact results for the low-energy impurity dynamics.

Contents

List of Tables

List of Figures

Chapter 1

Introduction

Impurity disorder holds a special place in the history of condensed matter physics – the "physics of dirt"[1] . Its unavoidable and usually undesirable presence has forced us to closely examine its influence, which in turn, provided an opportunity to discover a remarkable wealth of surprising phenomena not possible in its absence. Well-known examples from the solid-state include Anderson localization, the Quantum Hall effect, Kondo effect and orthogonality catastrophe. Even several decades since their discovery, the concepts originating from these phenomena continue to guide our understanding of modern experiments and pave the way for new avenues of research. Indeed, as we shall see, some of these ideas provide the key to understanding peculiar features of *mobile* impurities immersed in one-dimensional (1d) quantum liquids.

The earliest studies of impurities in quantum liquids began when it was realized that a dilute component of ^{3}He remains miscible in the superfluid phase of ^{4}He in a certain range of temperature and concentration. This system stimulated studies of the ultimate limits of viscosity at low temperatures and produced the only well-understood unconventional fermionic superfluid – ^{3}He. However, similar to many other solid state systems, the impurity coordinates are analyzed only in a certain average sense, with the traditional goal to understand how their concentration modifies bulk transport or thermodynamic properties of otherwise pure systems. The reverse paradigm – to determine the effect of the surrounding medium on the motion of individual impurities – has become increasingly relevant with the emergence of the field of ultracold atomic

[1] An adorning perspective by Pauli.

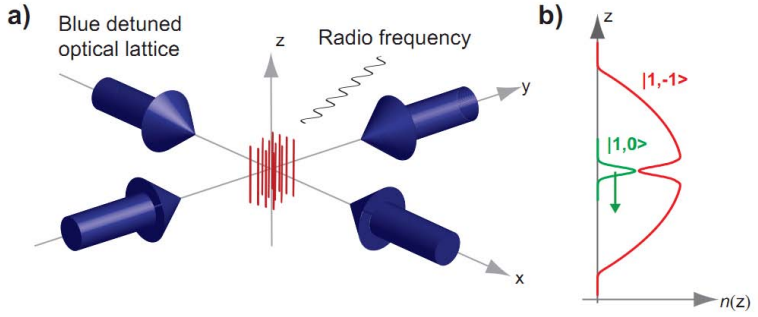

Figure 1.1: **a)** Creation of impurities in a 2d array of independent 1d tubes parallel to the vertical. The atoms are prepared in the hyperfine ground state $|F = 1, m_f = -1\rangle$ which allows vertical suspension against gravity using a magnetic harmonic potential. **b)** A radio frequency pulse resonant with a local hyperfine splitting creates impurities in the untrapped $|F = 1, m_f = 0\rangle$ state which then fall under the influence of gravity. Adapted from [2].

gases [1]. In the last decade, this field has witnessed tremendous progress in fabricating and manipulating dilute impurities immersed in bosonic or fermionic superfluids subject to tunable spatial dimensionality, lattice configuration and interaction strength. As opposed to the essentially bulk resolution of many standard condensed matter experiments, this platform allows one to detect the real-time dynamic response of individual impurity atoms subject to a variety of external manipulation protocols and quantum environments. The wide range of tunability and control provided by ultracold atomic systems thus serve as a powerful tool for discovering novel effects while continually challenging our understanding of complicated many-body or dynamical phenomena.

Recent experiments [2, 3, 4, 5, 6, 7] were able to study impurities in the quasi-1d regime where atoms occupy the lowest transverse channel of an atomic wave-guide. This can be realized by loading quantum gases in 1d optical lattices [8, 9, 10, 11, 12] or using the magnetic confinement on atom chips [5]. A hyperfine state of a few atoms can be switched locally with the help of a radio frequency magnetic field pulse and may be thought of as an effective "spin-flip" in a polarized two-component system [2, 5], see Fig. (1.1). As a result, these atoms become distinguishable from the rest of the quantum liquid and thus may be considered as mobile impurities. One may also use mixtures of different atomic species (*e.g.*, ^{87}Rb and ^{41}K in Ref. [6, 7]) with one dilute component.

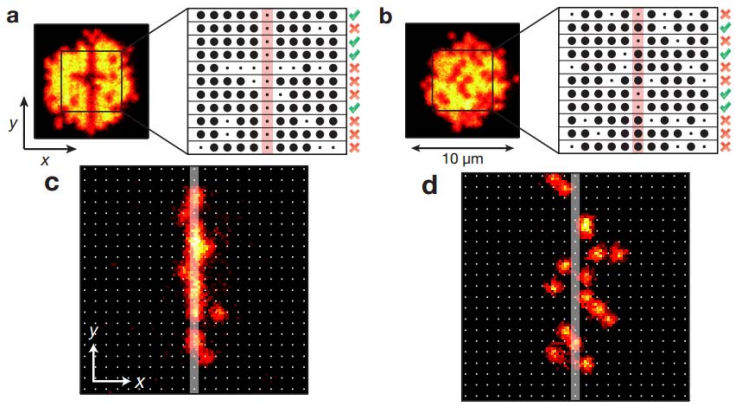

Figure 1.2: Top panel: **a** 'Negative' fluorescence imaging of atoms with single-site resolution. Here impurities appear as dark holes in the Mott insulating state (the vertical red stripe shows their initial position). The 1d systems are oriented horizontally. **b** Same as in **a** but after an evolution time of 60 ms. The green check-marks indicate low-temperature realizations where only one empty lattice site is produced. Bottom panel: **c** 'Positive' imaging of impurities, now appearing as bright spots, can be used to explore the superfluid regime where the majority particles exhibit large fluctuations of the on-site occupation numbers. **d** Same as in **c** but after an evolution time of 1 ms. Adapted from [14].

This gives route to impurities of mass M different from the mass m of the host particles. Another promising realization is achieved by placing *ions* of Yb^+, Ba^+ or Rb^+ in the Bose-Einstein condensate of neutral ^{87}Rb atoms [3, 4].

Remarkably, the impurities may be selectively acted upon with the help of external forces. In the case of neutral atoms the external force is gravity, being uncompensated by the force from the vertical magnetic trap (impurity atoms are created in magnetically untrapped states). In the case of an ion, the selective force is an applied electric field. These setups thus allow one to drive the non-equilibrium dynamics of mobile impurities immersed in a 1d quantum liquid. By releasing the trap after a certain delay time, one can monitor the resulting density and velocity distributions of impurities.

Finally, the most recent experimental advance occured with the achievement of the long-sought ability to address individual atoms with single-site resolution [13]. Using a tightly focused laser-beam together with a microwave pulse resonant with the local hyperfine splitting, the authors of Ref. [14] were able to create and detect the motion

of individual impurity atoms in a 1d lattice populated by a majority component, see Fig. (1.2). In this way they were able to monitor, with single-site resolution, the evolution of the squared impurity wave-function as it moves through the quantum liquid. The above experiments have opened the door for a rather new and exciting possibility in the study of the mobile impurity problem, where the dynamical response of the impurity degrees of freedom take front stage and can be explored with unprecendented precision and control.

In higher dimensions, the dynamics of mobile impurities in quantum liquids is an old subject pioneered by Landau and Khalatnikov [15, 16] and Bardeen, Baym, Pines and Ebner [17, 18, 19, 20, 21, 22] in their studies of ^{3}He atoms in superfluid ^{4}He. These authors realized that at finite temperature the impurities experience a viscous force from the normal component of the liquid, even if their speed is less than the critical superfluid velocity. The mechanism leading to such a viscous force was shown to be that of Raman scattering of thermal excitations of the superfluid, *i.e.* thermal phonons, off the impurity ^{3}He atoms. It was found [15, 16, 22] that the corresponding friction coefficient scales with temperature as T^8 in the low temperature limit. It was later discussed by Castro-Neto and Fisher [23] that in 1d the Raman mechanism leads to the friction force proportional to T^4 due to phase-space considerations. The same mechanism governs the temperature-induced acceleration of grey solitons in weakly interacting condensates [24]. Recently, the authors of Ref. [25, 26] showed that, in addition to phase-space effects, the friction is extremely sensitive to the details of the interactions between impurity and the background liquid and vanishes for exactly solvable 1d models. The friction, therefore, may be rather small in the spin-flip setup if the parameters are near the Yang-Gaudin [27, 28] integrable case where $M = m$ and the short-range impurity-host interaction strength is equal to that between host particles. As discussed later in Ch. 2, this work was generalized in Refs. [29, 30] to include the full range of total momenta.

Due to one-dimensional kinematics, the slowly moving impurity tends to deplete the host liquid, creating density and current gradients in its vicinity. At small momenta the dispersion of the impurity can still be described by the quadratic law $E = P^2/2M^*$ with effective mass M^* of the impurity atom [31, 32]. In the weakly interacting regime, and for sufficiently small momenta, the depletion of the host liquid can be studied within the framework of the Bogoliubov theory. The resulting excitations, polarons, consist

of impurities surrounded by a cloud of linear excitations of the condensate and were studied in Ref. [33] and later in Refs. [34, 35]. However, even for a weakly interacting liquid, the induced depletion becomes essentially *non-linear* at larger momenta or strong impurity-liquid coupling. This brings a qualitative change of the dispersion relation and we introduce a quasiparticle, the *depleton*, describing the impurity dressed by this non-linear depletion cloud.

The remarkable property of the depleton dispersion is that it is a *periodic* function of the momentum P with the period $2\pi\hbar n$, where n is the density of the 1d host liquid [36]. To explain this feature it is worth noticing that, being quadratic at small momenta, the depleton energy is less than any of the excitations of the host liquid (see Fig. 1.3). Indeed, the low-energy excitations of the host liquid have a sound-like nature with the energy $cP > P^2/2M^*$, where c is the speed of sound. Therefore the dressed impurity excitation provides the cheapest way for the system to accommodate a small momentum. This means that the depleton dispersion relation is *defined* as the lowest possible many-body excitation energy of the system with a given momentum. An example of such dispersion is shown in Fig. 1.3. Above the depleton energy there is a continuum of many-body excitations comprised of the moving impurity and a certain number of phonons. This spectral edge is characterized by power-law threshold behavior of the zero-temperature correlation functions and can be understood as a consequence of the orthogonality catastrophe [32, 36, 37, 38, 39, 40].

One may argue now that in the infinite system the ground-state energy with a given momentum is a periodic function of the latter with the period $2\pi\hbar n$. Indeed, it is easy to see that the ground-state energy with momentum $2\pi\hbar n$ vanishes in the thermodynamic limit. To this end, consider a ring of length L where the spectrum of the momentum operator is quantized in units of $2\pi\hbar/L$. If the momentum of each particle is boosted by one quantized unit, the total momentum of the system is $2\pi\hbar n$, while the total energy vanishes thanks to the total mass of the liquid diverging in the thermodynamic limit. We thus conclude that the ground-state for a given momentum P, which is the dispersion relation $E(P)$ of the dressed impurity, is a periodic function of momentum. Explicit examples are provided by exactly solvable models [36, 37], the weakly interacting Bose-liquid and an impurity weakly coupled to free fermions, considered in detail in Appendix A.2.

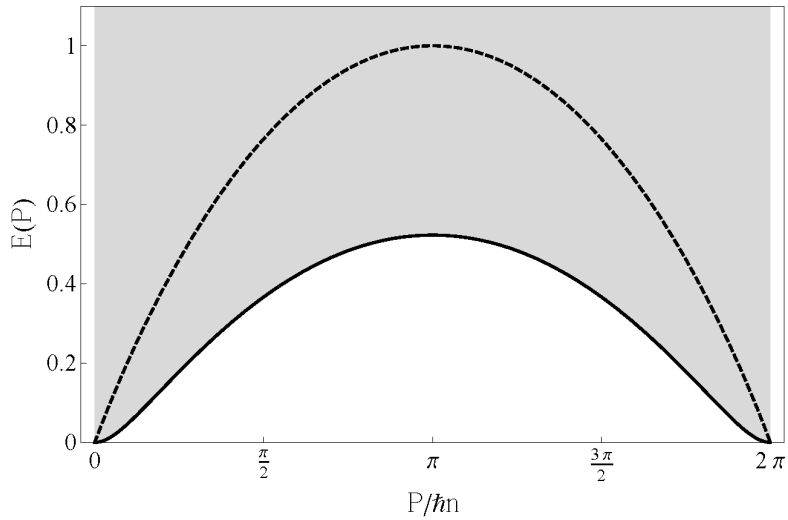

Figure 1.3: Schematic dispersion relation for a mobile impurity in a 1d quantum liquid. The dispersion defines the lower bound of the many-particle excitation spectrum. In the region above the dispersion (shaded gray) there exists a continuum of many-body states. For comparison, the lower bound in the absence of the impurity is defined by the soliton/hole excitation, shown by the dashed line (its maximum defines the energy unit).

The physics behind the periodic dispersion relation is most readily understood in the case of a quasi-condensate host. In that case the effect stems from the transfer of momentum from the accelerated impurity to the supercurrent of the background liquid: similarly to the density depletion, the moving impurity creates a sharp phase drop Φ across it. To satisfy periodic boundary conditions, the rest of the liquid must sustain the phase gradient Φ/L, resulting in the supercurrent which carries momentum $\hbar n\Phi$. While the supercurrent is absorbing momentum, it does not contribute to the energy. Indeed, as it was already mentioned, in the thermodynamic limit the bulk of the liquid is infinitely heavy and thus can accommodate any momentum at no energy cost. As a result, the energy and momentum of the depleton core, being periodic functions of the phase drop Φ with the period 2π, oscillate as functions of the total momentum with the period $2\pi\hbar n$, while the rest of the momentum goes into the supercurrent. A similar periodic dispersion relation would arise if the host liquid were regarded as a rigid crystal with the lattice spacing $a = 1/n$. Then the momentum interval between $P = -\hbar\pi n$ and $P = \hbar\pi n$ would be nothing but the Brillouin zone of such a crystal, while the impurity

dispersion, discussed above, would be its lowest Bloch band.

Although the above considerations completely disregard the absence of the true long-range order in the 1d liquid (either superfluid or crystalline) and thus should be taken with care, the periodicity of the dispersion suggests the possibility of Bloch oscillations of the impurity atom subject to an external force [25]. Indeed, if an external force F is applied to the impurity atom (*e.g.*, an electric field acting on an ion) the *total* momentum of the system changes linearly with time, $P = Ft$. For an infinitesimal force this leads to an adiabatic change of the energy $E(P)$ and the velocity $V = \partial E/\partial P$ of the depleton which become periodic functions of time with the period $2\pi\hbar n/F$. It is quite remarkable that in such a process, on average, the impurity does not accelerate; moreover, it does not even move. Instead, it channels the momentum into the collective motion of the liquid, *i.e.*, the supercurrent, and in the process oscillates around a fixed location. As a result, *no energy* is transferred, on average, to the system from the external potential.

This spectacular phenomenon is present at zero temperature and under an infinitesimal external force. Both finite temperature and a finite force complicate the picture in a substantial way. A main aim of this dissertation is to clarify the influence of these two factors on the observability of the Bloch oscillations. In brief, our conclusions are as follows: at a sufficiently low temperature there is a parametrically wide range of external forces $F_{\min}(T) < F < F_{\max}$, where the Bloch oscillations *are observable*. Contrary to the adiabatic picture, they are accompanied by a *drift* and exhibit a certain amplitude and period renormalization.

The drift manifests itself in the appearance of an average velocity $V_{\rm D}$ superimposed on top of the periodic Bloch oscillations, and is a result of heating the system. The principle of adiabaticity thus implies that $V_{\rm D}$ must vanish in the limit $F \to 0$, but gives no indication of how this may occur. The simplest possibility is that the rate of heating, being insensitive to the sign of F, scales as F^2 in the leading order. Since the work done on the system is $W \propto F^2 = FV_{\rm D}$, one finds a linear relation between the drift and the force, allowing one to define the impurity *mobility* σ, as $V_D = \sigma F$. Another intriguing scenario is possible when the impurity mass exceeds a critical threshold: the rate of heating and thus drift become non-analytic functions of the applied force: $V_{\rm D} \propto F^{1/(1+\alpha)}$ [41]. As we discuss in detail in Ch. 3, this occurs when the impurity

dispersion undergoes a quantum phase transition by developing non-analytic cusps at momenta $j\pi\hbar n$ where j is an odd integer, accompanied by metastable branches within the many-body continuum. The remarkable consequence of this transition appears as a divergence in the transport coefficient (mobility), and is deeply related to the mechanism by which the impurity is able to reverse its velocity despite being accelerated by a directed force.

The dissipated energy goes to the emitted long wavelength phonons, which run away from the impurity with the sound velocity c. The maximal force can then be roughly estimated by solving $c = V_{\rm D}(F_{\rm max})$, where for finite mobility we obtain the simple result $F_{\rm max} \approx c/\sigma$. At a larger force the drift velocity exceeds c, leading to Cherenkov radiation of phonons. The phonons take a substantial part of the momentum and thus ruin the Bloch oscillation mechanism, discussed above. The impurity motion is then either incoherent drift, or an unlimited acceleration, depending on the parameters. In this regime we expect a Boltzmann kinetic equation approach to be applicable since at high energies binary collisions between the impurity and background particles becomes more important than scattering off the low-energy collective excitations. This approach, although not applicable at small F, has been used recently to study impurity dynamics in a free fermi gas [42].

We derive the *exact* analytic expression for the drift mobility σ expressed in terms of the equilibrium dispersion relation of the impurity. It is worth noticing that the mobility σ is *not* a linear response property, despite the possibility of a linear relation between the drift velocity and the external force. Indeed, the motion of depleton in this regime is characterized by drift superimposed with essentially non-linear Bloch oscillations, in which the particle explores the entire range of momenta. It is therefore not immediately obvious that the mobility σ may be expressed in terms of the equilibrium properties. Nevertheless we prove that such a relation does exist.

The true linear response is associated with the thermally induced Landau-Khalatnikov friction force $F_{\rm fr}(V) \propto -T^4 V$, which arises due to the Raman scattering of phonons discussed above. It provides the lower limitation on the externally applied force $F_{\rm min}(T) = F_{\rm fr}(V_c)$, where V_c is the maximal equilibrium velocity given by the maximum slope of the depleton dispersion, Fig. 1.3. Indeed, at smaller external forces the velocity saturates and therefore the depleton dynamics is confined to small momenta and Bloch

oscillations do not occur.

The friction coefficient in the small momentum regime was discussed in Ref. [25] and found to be vanishing in exactly solvable cases. The reason behind it is the presence of an infinite number of conservation laws, which prevent a non-equilibrium state from thermalization. Here we extend those calculations to the entire range of momenta and derive an exact result for the full momentum dependence of the friction force. Quite naturally, it vanishes in exactly solvable cases too.

The above discussion has so far focused on the case where one is concerned only in the dynamics of a single, isolated impurity. While this is appropriate in the dilute limit considered here, it neglects the possibility of inter-impurity correlations induced by coupling to one and the same quantum liquid. This can be important for a variety of reasons. In addition to obtaining the leading low-impurity-density corrections to the single-impurity response characteristics, one is also able to directly investigate the induced interaction law between two separate impurities. Certainly in higher dimensions this issue is of fundamental importance: induced interactions caused by the medium can drive instabilities into entirely new phases of matter. This effect is also relevant in 1d where instead of an instability, one may be interested in the hybridization between separate, effectively 2-level, atoms or quantum dots embedded in a tunable quantum environment which have potential application for quantum information processing [43].

We find that the interaction mediated by the 1d quantum liquid has essentially two leading components. The first is a single-phonon exchange interaction which can be understood in terms of the classical mattress effect: a given impurity creates a density depletion in its vicinity which in turn is felt by another nearby impurity. Since the density distortion is restored exponentially on the scale of the healing length, this effect is spatially *local*. The second component results from a two-phonon process whereby virtual phonons perpetually scatter between impurities, in analogy with the Casimir effect [44]. As is well-known from the electromagnetic Casimir effect the induced interaction is a power-law, rather than exponential, and therefore dominates over the spatially local interaction at large separations. In our case, we find a universal phonon-mediated Casimir interaction scaling as $1/r^3$, where r is the impurity separation[2] . The coefficient of the Casimir interaction is non-universal and depends on the product

[2] This result also applies to static impurities in 1d superfluids.

of impurity-phonon scattering amplitudes. As a result, it is controlled by the *same* parameter as the thermal viscosity, an effect also arising from impurity-phonon scattering. We thus conclude that when the underlying model is integrable both the thermal viscosity and the Casimir interaction vanish identically. This presents the intriguing possibility of changing the *sign* of the interaction by independently tuning impurities to lie on opposite sides of integrability. By developing equations of motion for the impurities we find that the Casimir interaction is in fact only the real part of the total induced interaction. The imaginary part is related by causality (Kramers-Kronigs) to the Casimir interaction and is responsible for a *correlated* friction. This effect can lead to an enhancement or suppression of the center of mass damping, depending on the relative separation of the impurities.

1.1 Outline of the Dissertation

We shall conclude the introduction by summarizing the main achievements of this dissertation, which is organized as follows[3] .

- Chapter 2 provides the general framework for the description of impurity dynamics in 1d quantum liquids. It follows closely the work of Ref. [29]. In Section 2.1 we give a qualitative description of the depleton quasiparticles and the mechanism of coupling to linear sound excitations, or phonons, of the background liquid. Section 2.2 is devoted to the formal derivation of the depleton Lagrangian based on superfluid thermodynamics. We discuss the coupling of the depleton with the phonon subsystem and derive a set of stochastic equations of motion for the depleton dynamics in Section 2.3. In the case where the impurity mass is subcritical, these equations are then used to study radiation losses and derive an expression for the depleton mobility in Section 2.4 and the thermal friction in Section 2.5. The main results are summarized in Section 2.6.

- Chapter 3 discusses the quantum phase transition associated with the impurity mass exceeding a critical threshold and follows Ref. [41]. In Sections 3.1 and 3.2

[3] The analysis and results of this dissertation closely follow several previous works of the author [29, 41, 44, 45].

we show that the development of cusps in the impurity dispersion is accompanied by metastable branches in the continuum and estimate the value of the critical mass. In Section 3.3 we calculate the decay rate from the metastable branches and establish the exact criterion for the occurence of the quantum phase transition. Section 3.4 discusses how these features affect the impurity response to an external force.

- Chapter 4 discusses the induced interaction between impurities immersed in a 1d quantum liquid and follows Ref. [44]. Section 4.1 discusses the qualitative aspects of the Casimir interaction and explains why the effect was missed in previous studies. In Sections 4.2 and 4.3 we build on the ideas of Ch. 2 to derive an effective low-energy theory from which we derive semiclassical equations of motion that show the existence of a long-range phonon-mediated Casimir interaction between impurities. Finally, in Section 4.4 we estimate the magnitude of the Casimir interaction and describe a simple experiment in which our results can be verified.

- Appendix A outlines the analysis of several illustrative impurity models. Section A.1 discusses grey soliton solutions of the Gross Pitaevskii equation, which governs the dynamics of weakly interacting bosons. Section A.2 discusses a point impurity coupled to weakly interacting bosons at zero temperature. Section A.3 discusses an impurity weakly coupled to a free fermi gas following Ref. [45]. In Sections A.2 and A.3 we demonstrate the existence of a non-perturbative impurity-soliton and impurity-hole bound states, respectively.

- Appendix B contains technical details of several calculations used throughout the dissertation. In particular, Section B.3 discusses various forms of the impurity-phonon back-scattering amplitude, while Section B.4 discusses the power-law threshold behavior of the impurity spectral function.

Chapter 2

Phenomenology of impurity dynamics

In this Chapter we develop the framework to discuss the low-energy dynamics of a mobile impurity moving in a one-dimensional quantum liquid. In certain momentum intervals the impurity induces a strong, non-linear depletion of the liquid around it, even at weak coupling. The non-perturbative nature of this effect calls for an effective low-energy theory that incorporates such processes from the start. Our approach allows one to study a wide-range of universal phenomena unique to 1d, all while expressing the results in terms of a few independently measurable thermodynamic characteristics. We focus on the case where the impurity mass is sub-critical and derive exact results for the radiation-induced mobility as well as the thermal friction force. These results show that there is a wide range of external forces where Bloch oscillations exist and may be observed experimentally.

2.1 Qualitative analysis

The key to understanding the impurity dynamics is in its interactions with the phonons of the host liquid. This problem is rather non-trivial even if the impurity is weakly coupled to the liquid. Indeed, no matter how weak the interactions are, the impurity develops local depletion, which become appreciable when the impurity momentum approaches πn (we set $\hbar = 1$ throughout the rest of the dissertation). To visualize

this process it is useful to adopt a semiclassical picture of the background, valid for a weakly interacting Bose liquid. In this regime, to accommodate the total momentum πn, the depletion cloud takes the form of a dark soliton [46]. The dark soliton is an essentially non-linear mesoscopic object, which includes a large number of particles and a complete depletion of the liquid density. It is exactly the soliton formation which is responsible for channeling momentum into the supercurrent and thus for the Bloch oscillations. It is also the soliton which determines the interactions of the impurity with the dynamically induced phonons. Therefore the non-equilibrium dynamics of the quantum impurity cannot be separated from the dynamics of the essentially non-linear soliton-like depletion cloud.

What makes the problem analytically tractable is the scale separation between the spatial extent of the local soliton-like cloud and the characteristic phonon wavelength. The former is given by the healing length $\xi = 1/mc$. The latter appears to be much longer than ξ, if the temperature is sufficiently low and the external force is not too strong. One can thus separate the near-field mesoscopic region, which contains the quantum impurity and its depletion cloud, from the far-field region, supporting the radiation emitted by the impurity. Since the depletion is restored exponentially at the healing length away from the impurity, the precise position of the boundary between the near-field and the far-field regions is of no importance.

Because of the wide difference in their spatial scales, the impurity together with its entire non-linear depletion cloud represents a dynamic *point-like* scatterer for the long wavelength phonons. From the viewpoint of such phonons any point scatterer may be entirely described by two phase shifts. These two phase shifts are the discontinuities of the phonon displacement and momentum fields across the scatterer. They may be expressed through the number of depleted particles N and the phase drop Φ across the depleton quasiparticle. Therefore, out of many degrees of freedom of the near-field region, only N and Φ interact with the phononic sub-system.

What remains is to describe the dynamics of the local depletion cloud with certain fixed values of N and Φ. The solution of this problem is facilitated by the fact that the characteristic equilibration rate of the cloud, estimated as $1/\tau = c/\xi$, is much faster than the relevant phononic frequencies. As a result, the cloud may be treated as being in the state of *local equilibrium*, conditioned to certain values of the slow collective coordinates

N and Φ. The fact that there are two such slow variables is due to the presence of two conservation laws: the number of particles and momentum. The fast internal equilibration of the near-field region is therefore conditioned by the instantaneous values of the two conserved quantities.

The slow change (compared to the fast time scale of τ) in the number of depleted particles N and the phase drop Φ are due to the fact that the *local* chemical potential μ and the local current j at the position of the impurity are both affected by the state of the global phononic sub-system. As a result, one may express the Lagrangian of the near-field region as a function of N and Φ through the equilibrium thermodynamic potential which is a function of μ and j. The latter function may be independently measured or analytically evaluated in certain limiting cases and for exactly solvable models.

These considerations allow one to separate the local, non-linear but *equilibrium* problem, from the global, non-equilibrium but *linear* one. The latter statement implies that the host liquid sufficiently far away from the impurity may be treated as linear, *i.e.*, as a Luttinger liquid [47, 48]. This is certainly an approximation which disregards the possibility of the moving impurity emitting non-linear excitations, such as grey solitons or shock waves. The train of solitons emitted by the impurity moving with a constant supercritical velocity was indeed observed in simulations of Ref. [49]. The kinematics of this process suggests that it is only possible if the drift velocity is close to the speed of sound c. We therefore assume that as long as $F < F_{\max}$, one may disregard solitons emission and treat the liquid away from the impurity as the linear one. This is essentially the same criterion which allows us to separate the depletion cloud from the long wavelength phonons.

Adopting these approximations, one is able to integrate out the phononic degrees of freedom characterizing the liquid away from the impurity. It reduces the problem to the dynamics of the impurity described by its coordinate $X(t)$ and momentum $P(t)$ along with the dynamics of its near-field depletion cloud fully described by the two collective coordinates: the number of depleted particles $N(t)$ and the phase drop $\Phi(t)$. We derive an effective action written in terms of such an extended set of degrees of freedom. This action leads to a coupled system of quantum Langevin equations governing the dynamics of the depleton.

Away from equilibrium, for $F > F_{\min}$, the equations of motion yield the pattern of Bloch oscillations. The deterministic part of these equations provides information about the drift velocity, amplitude and shape of the velocity oscillations, as well as their period. The stochastic part results in the dephasing of the oscillations amongst an ensemble of identically prepared systems. It is interesting to notice that the stochastic part is manifestly different from the equilibrium noise prescribed by the fluctuation-dissipation theorem. As a consequence, the exactly integrable models lose their special status and their non-equilibrium dynamics appear to be not qualitatively different from the dynamics of generic non-integrable models.

2.2 Lagrangian of the mobile impurity

Let us first consider the background liquid in the absence of an impurity, employing the hydrodynamical description proposed by Popov [47]. Its Lagrangian is expressed in terms of the slowly varying chemical potential μ and density n as an integral of the local thermodynamic pressure

$$L_0(\mu, n) = \int dx\, p_0(\mu, n) = \int dx \left[\mu n - e_0(n)\right]. \tag{2.1}$$

Here $e_0(n)$ is the energy density of the liquid. In thermodynamic equilibrium the density is a function of the chemical potential, given by the solution of the following equation: $\mu = \mu(n) = \partial e_0/\partial n$, which is a result of the minimization of this functional with respect to n. This way one defines the grandcanonical thermodynamic potential of the host liquid as

$$\Omega_0(\mu) = -L_0(\mu, n(\mu))\,. \tag{2.2}$$

For a uniform system the Lagrangian and the corresponding thermodynamic potential are both proportional to the length of the system.

Consider now an impurity of mass M having a coordinate X and moving through the liquid with velocity $V = \dot{X}$ as measured in the laboratory reference frame. It is convenient to choose the reference frame where the impurity is at rest and the liquid flows with the velocity $-V$, as shown in Fig. 2.1. In this co-moving frame the impurity experiences the supercurrent j' and the chemical potential μ'. Hereafter primes denote

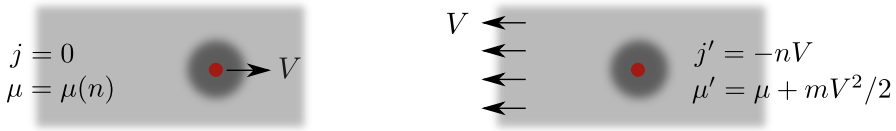

Figure 2.1: Transformation to the co-moving frame.

physical quantities defined in the co-moving frame to distinguish them from the corresponding quantities in the laboratory frame. We employ a Galilean transformation into the moving frame which gives

$$j' = -nV, \qquad \mu' = \mu + mV^2/2. \tag{2.3}$$

Together with the Galilean transformation of the energy density $e_0' = e_0 + mV^2/2$, the transformation (2.3) combined with Eqs. (2.1) and (2.2) show the invariance of the background grandcanonical potential $\Omega_0'(\mu') = \Omega_0(\mu)$. As expected from the Galilean invariance, the latter is independent of the velocity V and the supercurrent j'.

We now introduce the impurity into the flowing liquid maintaining *both* j' *and* μ' *fixed* and let it equilibrate. Its motion distorts the host liquid density and velocity fields, forming the depletion cloud moving along with the impurity. The grandcanonical potential increases by an amount $\Omega_{\rm d}'(j', \mu') = E_{\rm d}' - \mu' N_{\rm d}$, where $E_{\rm d}'$ and $N_{\rm d}$ are the corresponding changes in energy and number of particles. Using the Galilean invariance one can relate the energy $E_{\rm d}' = E_{\rm d} - P_{\rm d}V + mN_{\rm d}V^2/2$ to the energy $E_{\rm d}$ and momentum $P_{\rm d}$ induced by the moving impurity in the laboratory frame. This fact and relations (2.3) allows one to identify, in the spirit of Popov's approach, the Lagrangian of the depletion cloud with the negative change of the grandcanonical potential

$$L_{\rm d}(V, n) \;\; = \;\; P_{\rm d}V - E_{\rm d} + \mu N_{\rm d} = -E_{\rm d}' + \mu' N_{\rm d} = -\Omega_{\rm d}'(j', \mu')\,. \tag{2.4}$$

This relation is quite remarkable as the left hand side describes the dynamics of the depletion cloud moving with the velocity V, while its right hand side is a thermodynamic quantity. The link between them comes from the Galilean transformation, Eqs. (2.3). The relation between the Lagrangian and the grandcanonical potential, Eq. (2.4), can

be viewed as a generalization of the Popov relation, Eq. (2.2), to the case of mobile impurities.

Two remarks are in order. First, in assuming the thermodynamic equilibrium at nonzero supercurrent j' flowing through the impurity we rely on superfluidity. Second, we note that the increase in energy $E'_{\rm d}$, momentum $P_{\rm d}$, number of particles $N_{\rm d}$ and the grandcanonical potential $\Omega'_{\rm d}$ due to the presence of a *single impurity* are finite size corrections to the corresponding extensive quantities.

2.2.1 Collective degrees of freedom of the depleton

Variations of the so far fixed parameters j' and μ' of the background liquid induce changes in the thermodynamic potential of the depletion cloud. It can be written with the help of the corresponding response functions as

$$\mathrm{d}\Omega'_{\rm d} = \Phi\,\mathrm{d}j' + N\mathrm{d}\mu'\,, \qquad \Phi = \partial_{j'}\Omega'\,, \quad N = \partial_{\mu'}\Omega'. \tag{2.5}$$

The response to the variation of the chemical potential $N = -N_{\rm d}$ is identified with the number of particles *expelled* from the liquid by the impurity (hence the minus sign). The response Φ to the change of the supercurrent j' is the superfluid phase and has no analogy in classical thermodynamics. In the state of the global thermodynamic equilibrium both Φ and N are rigidly locked to j' and μ' and, consequently, to V and n. This is denoted by writing $\Phi = \Phi_0(V,n)$ and $N = N_0(V,n)$. These functions can be obtained from the derivatives of the Lagrangian defined in Eq. (2.4) as described in the next subsection.

In the nonequilibrium situations, where the supercurrent and chemical potential fluctuate, it is convenient to treat Φ and N as *independent variables*. We perform the standard Legendre transformation to a new thermodynamic potential,

$$H_{\rm d}(\Phi,N) = \Omega'_{\rm d} - j'\Phi - \mu' N, \qquad \mathrm{d}H_{\rm d} = -j'\mathrm{d}\Phi - \mu'\mathrm{d}N. \tag{2.6}$$

The independent variables Φ and N describe the state of the depleted liquid in the immediate vicinity of the impurity which may or may not be in equilibrium with globally imposed j' and μ'. In the equilibrium situation $H_{\rm d}(\Phi,N)$ does not contain any additional information with respect to the thermodynamic potential $\Omega'_{\rm d}(j',\mu')$, which is in turn related to the depletion cloud Lagrangian $L_{\rm d}(V,n)$ by Eq. (2.4). The aim of introducing

$H_{\rm d}(\Phi, N)$ is to allow for interactions of the depletion cloud with the long wavelength phonons. As we shall see in Section 2.3 the latter may change the number of particles and the momentum of the depletion cloud, forcing it to equilibrate to some new values of Φ and N. Before turning to phonons, it is instructive to rewrite the impurity Lagrangian (2.4) by substituting into it Eq. (2.6) and considering Φ and N as independent vaiables,

$$L_{\rm d} = \frac{1}{2}\, MV^2 - j'\Phi - \mu' N - H_{\rm d}(\Phi, N)\,. \tag{2.7}$$

Expressing j', μ' through V, n using Eq. (2.3), we finally obtain the Lagrangian of the depleton

$$L(V, \Phi, N) = \frac{1}{2}\,(M - mN)V^2 + nV\Phi - \mu N - H_{\rm d}(\Phi, N)\,, \tag{2.8}$$

where $\mu = \mu(n)$ is the equilibrium chemical potential of the host liquid in the laboratory frame and we have added the bare kinetic energy proportional to the impurity mass M. The momentum of the depleton is obtained by the standard procedure

$$P = \frac{\partial L}{\partial V} = (M - mN)V + n\Phi\,, \tag{2.9}$$

The last term describes the supercurrent momentum $n\Phi$ stored in the background. The first term is proportional to the reduced mass $M - mN$, expressing the fact that the mass mN is *removed* from the local vicinity of the moving impurity. This quantity should not be confused with the *effective* mass M^* characterizing the curvature the equilibrium dispersion, Eq. (2.15), given by Eq. (2.19).

We can use Eq. (2.9) to express velocity of the depleton as a function of its momentum,

$$\dot{X} = V = V(P, \Phi, N) = \frac{P - n\Phi}{M - mN}. \tag{2.10}$$

Combining Eq. (2.10) and the Lagrangian (2.8) leads to the Hamiltonian

$$H(P, \Phi, N) \;=\; PV - L = \frac{1}{2}\,\frac{(P - n\Phi)^2}{M - mN} + \mu N + H_{\rm d}(\Phi, N)\,. \tag{2.11}$$

This Hamiltonian generates the following equations of motion

$$\dot{P} \;=\; 0 \tag{2.12}$$

$$0 \;=\; -\partial_\Phi H = nV - \partial_\Phi H_{\rm d} \tag{2.13}$$

$$0 \;=\; -\partial_N H = -\mu - mV^2/2 - \partial_N H_{\rm d} \tag{2.14}$$

in addition to Eq. (2.10). The first equation is the momentum conservation expected in the absence of external forces and for homogeneous background. The two other equations are in fact *static constraints*. This is a manifestation of the already mentioned fact that, without phonons, Φ and N are rigidly locked constants and do not have independent dynamics.

2.2.2 Equilibrium values of the collective variables and internal energy

As we shall see in Section 2.3, the coordinates canonically conjugated to Φ, N are the phononic displacement and phase at the location of the impurity. In the absence of these degrees of freedom the only consistent solution of Eqs. (2.13), (2.14) corresponds to the *static*, or *equilibrium*, relations $\Phi = \Phi_0(P, n)$, $N = N_0(P, n)$. Substituting them back into the Hamiltonian (2.11) leads to the equilibrium dispersion relation of the dressed impurity (depleton),

$$H(P, \Phi_0(P, n), N_0(P, n)) = E(P, n)\,. \tag{2.15}$$

The corresponding "equilibrium Lagrangian" can be obtained as $L(V, n) = PV - E$ by expressing the momentum as a function of the velocity with the help of $V = \partial E/\partial P$. In most situations it is rather these quantities and not the "internal energy" $H_{\rm d}(\Phi, N)$ which represent the physical input about the dynamics of the dressed impurity. They can be obtained from solving the equilibrium problem for the impurity moving with the constant momentum P, or velocity V, through the liquid with the asymptotic density n. Below we show explicitly how collective variables Φ and N and the corresponding energy $H_{\rm d}$ can be obtained from the knowledge of $E(P, n)$ or $L(V, n)$.

We start with the situation when the velocity V is a control parameter. In this case finding $H_{\rm d}(\Phi, N)$ amounts to performing the Legendre transformation Eq. (2.6) by exploiting the definition (2.4) of the Lagrangian $L_{\rm d} = L - MV^2/2$ of the depletion cloud in terms of the thermodynamic potential $\Omega'_{\rm d}$ and using the pair (V, n) instead of the thermodynamical variables (j', μ'). To achieve this goal we use Eqs. (2.3) to relate the corresponding partial derivatives by the linear transform

$$\begin{pmatrix} \partial_V \\ \partial_n \end{pmatrix} = \begin{pmatrix} -n & mV \\ -V & mc^2/n \end{pmatrix} \begin{pmatrix} \partial_{j'} \\ \partial_{\mu'} \end{pmatrix}. \tag{2.16}$$

Here we have used the relation $\partial\mu/\partial n = mc^2/n$ between the compressibility and the sound velocity c. Using the definitions Eqs. (2.5) and Eqs. (2.16) we can express the derivatives of $L(V,n)$ in terms of collective variables Φ, N

$$\frac{\partial L}{\partial V} - MV = P - MV = n\Phi - mVN \tag{2.17}$$

$$\frac{\partial L}{\partial n} = V\Phi - \frac{mc^2}{n}N. \tag{2.18}$$

Solving these equations yield equilibrium values, $\Phi_0(V,n)$ and $N_0(V,n)$. Equation (2.17) can be otherwise obtained by simply substituting $\Phi_0(V,n)$ and $N_0(V,n)$ into the definition of the momentum, Eq. (2.9). This is a consequence of the equations of motion (2.13), (2.14). The quantities involving second derivatives of the Lagrangian do not enjoy this property. The most obvious case is the effective mass

$$M^* = \frac{\partial P}{\partial V} = M - mN - mV\frac{\partial N_0}{\partial V} + n\frac{\partial \Phi_0}{\partial V}\,, \tag{2.19}$$

which differs from the expression $M - mN$ obtained by taking the partial derivative of Eq. (2.9) with respect to velocity.

The equilibrium relations $\Phi_0(V,n)$ and $N_0(V,n)$ can be inverted to find the velocity $V_0(\Phi,N)$, and density $n_0(\Phi,N)$ for given values of Φ and N. Substituting them into Eq. (2.8) gives

$$H_{\rm d}(\Phi,N) = -L(V_0,n_0) + \frac{MV_0^2}{2} + n_0V_0\Phi - \left(\mu(n_0) + \frac{mV_0^2}{2}\right)N\,. \tag{2.20}$$

Conversely, we can use the momentum P as a control parameter. Again, using equations of motion Eqs (2.13), (2.14) one is able to show the equivalence of the derivatives $\partial H(P,\Phi,N)/\partial n = \partial E(P,n)/\partial n$ and $\partial H(P,\Phi,N)/\partial P = \partial E(P,n)/\partial P$. The latter defines the velocity $V_0(P,n)$. Using these facts and differentiating explicitly Eq. (2.11) we have the following system of equations

$$V_0(P,n) = \frac{P - n\Phi}{M - mN}; \qquad \frac{\partial E(P,n)}{\partial n} = \frac{mc^2}{n}N - V_0(P,n)\Phi, \tag{2.21}$$

which are equivalent to Eqs. (2.17), (2.18) by virtue of the fact that $(\partial L/\partial n)_V = -(\partial E/\partial n)_P$. Solving Eqs. (2.21) yield equilibrium values $\Phi_0(P,n)$, $N_0(P,n)$ as functions of P and n. Next, we invert these relations to obtain $P_0(\Phi,N), n_0(\Phi,N)$ as functions of Φ, N. Using Eq. (2.15) and Eq. (2.11) we obtain the expression for the core energy

$$H_{\rm d}(\Phi,N) = E(P_0,n_0) - \mu(n_0)N - \frac{1}{2}\frac{(P_0 - n_0\Phi)^2}{M - mN}. \tag{2.22}$$

in terms of the dispersion $E(P, n)$ and its derivatives.

To illustrate this procedure we use two cases, where the energy $H_{\rm d}(\Phi, N)$ possesses a simple form. One is the grey soliton in a weakly interacting Bose-Einstein condensate describing a massless, $M = 0$, impurity propagating in a weakly interacting Bose liquid with the coupling constant g. The standard results [46, 50] for the soliton dynamics are provided in Appendix A.1 and lead to

$$H_{\rm d}(\Phi, N) = \frac{1}{8}\, m g^2 N^3 \left[\frac{1}{3} - \left(\sin\frac{\Phi}{2}\right)^{-2}\right]. \tag{2.23}$$

Another example is provided by a strongly interacting impurity [32, 51]. In this case the number of expelled particles N is almost independent of the state of the impurity and may be considered as a non-dynamic constant. The remaining dependence of the energy on the superfluid phase Φ has a standard Josephson form

$$H_{\rm d}(\Phi) = -E_{\rm J}\cos\Phi. \tag{2.24}$$

The Josephson energy $E_{\rm J} = nV_{\rm c}$ is expressed through the corresponding critical velocity $V_{\rm c}$, which in this case is much smaller than the sound velocity c.

Expressions (2.20) or (2.22) provide the core energy of the locally equilibrium depletion cloud as a function of its slow variables Φ and N. This procedure emphasizes the fact that the introduction of Φ and N does not rely on the semiclassical interpretation of the condensate wavefunction. In fact, they may be defined even away from the semiclassical, weakly interacting regime where the phase of the condensate as well as its depletion are not well defined.

2.3 Coupling to phonons

An external force F acting on the impurity drives the system away from equilibrium, making the impurity radiate energy and momentum. For a sufficiently weak force such a radiation takes the form of long wavelength phonons, *i.e.*, small deviations of density $\rho(x, t)$ and velocity $u(x, t)$ fields from their equilibrium values, see Fig. 2.2. Below we show how coupling to phonons can be formulated in terms of the collective variables Φ, N. It turns out that this procedure is based solely on the principles of gauge and

Galilean invariance, *i.e.*, the conservation of number of particles and momentum, and leads to universal results.

2.3.1 Hydrodynamic description of phononic bath

We start by considering the Lagrangian governing dynamics of the phonon fields in the bulk of the liquid. To this end it is convenient to parameterize them by introducing the superfluid phase $\varphi(x,t)$ and the displacement field $\vartheta(x,t)$ such that $u = \partial_x\varphi/m$ and $\rho = \partial_x\vartheta/\pi$. The dynamics of these variables can be described following the method of Popov [47] by considering the slow change of the density $n \to n + \rho(x,t)$ and, independently, the change of the chemical potential,

$$\mu \to \mu - \dot{\varphi}(x,t) - \frac{mu^2(x,t)}{2}. \tag{2.25}$$

Substituting them into Eq. (2.1) yields the Lagrangian of phonons,

$$\begin{aligned} L_{\rm ph} &= \int dx \Big[p_0(\mu(x,t), n(x,t)) - p_0(\mu, n) \Big] \\ &= \int dx \left[-\rho\dot{\varphi} - \frac{m(n+\rho)u^2}{2} - \Big(e_0(n+\rho) - e_0(n) - \mu\rho \Big) \right]. \end{aligned} \tag{2.26}$$

For nonzero phononic fields, the impurity is subject to the modified local supercurrent and chemical potential in the co-moving reference frame

$$\mu' = \mu - \dot{\varphi} - \frac{mu^2}{2} + \frac{m(V-u)^2}{2} = \mu(n) + \frac{mV^2}{2} - (\dot{\varphi} + V\partial_x\varphi)\,; \tag{2.27}$$

$$j' = -(n+\rho)(V-u) = -nV - \frac{1}{\pi}(\dot{\vartheta} + V\partial_x\vartheta)\,, \tag{2.28}$$

where the phonon variables are taken at the instantaneous spatial position $X(t)$ of the impurity. Equation (2.27) follows from Eq. (2.25) and the fact that in the presence of the background flow $u = \partial_x\varphi/m$ the velocity of impurity with respect to the liquid is changed to $V - u$. To derive expression (2.28) for the modified supercurrent we have

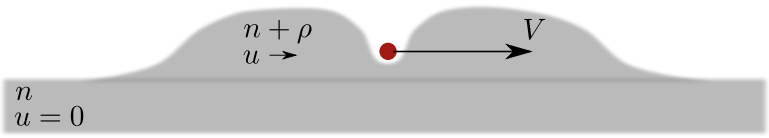

Figure 2.2: Impurity propagating in a local environment.

used the continuity equation in the form $\dot{\vartheta}/\pi = -(n+\rho)u$. This relation is an exact statement, which follows from the gauge invariance and is valid for any configuration of the fields.

Substituting the modified supercurrent and chemical potential, Eqs. (2.27), (2.28), into Eq. (2.7) and subtracting the corresponding equilibrium values, results in the following universal form of the interaction Lagrangian,

$$L_{\rm int} = \frac{1}{\pi}\,\Phi\,\frac{\mathrm{d}}{\mathrm{d}t}\vartheta(X,t) + N\frac{\mathrm{d}}{\mathrm{d}t}\varphi(X,t). \tag{2.29}$$

It is the *full time derivative* $\mathrm{d}/\mathrm{d}t = \partial_t + \dot{X}\partial_x = \partial_t + V\partial_x$ which enters the interaction term, as follows from Eqs. (2.27), (2.28).

The interaction Lagrangian, Eq. (2.29) provides dynamics of the collective coordinates N and Φ. It shows that the corresponding canonical momenta are the phonon degrees of freedom at the location of the impurity, *i.e.*, $\varphi(X,t)$ and $\vartheta(X,t)$, correspondingly. Through the gradient terms in Eq. (2.26) these two local variables are coupled to the phonon fields elsewhere and it is the dynamical properties of these phonons which determine the behavior of the impurity. For example, if the spectrum of phonons is discrete, one expects coherent oscillations of few modes. In the infinite system the continuous spectrum of the background modes leads to dissipation similar to that of the Caldeira-Leggett model [52].

2.3.2 Linear phonons and transformation to chiral fields

Away from this interaction region the excitations of the liquid may be considered as linear ones. Therefore one should keep only the quadratic terms in the phononic Lagrangian Eq. (2.26). For the kinetic energy in Eq. (2.26) one thus retains the leading term $mnu^2/2$, while the potential energy is expanded as $e_0(n+\rho) - e_0(n) - \mu\rho \simeq (\partial\mu/\partial n)\rho^2/2 = (mc^2/2n)\rho^2$, using the thermodynamic relation between the compressibility and the sound velocity c. As a result, one obtains the quadratic Luttinger liquid Lagrangian

$$L_{\rm ph} = \frac{1}{\pi}\int dx\left[-\partial_x\vartheta\partial_t\varphi - \frac{c}{2K}(\partial_x\vartheta)^2 - \frac{cK}{2}\left(\partial_x\varphi\right)^2\right]. \tag{2.30}$$

Besides the sound velocity c the Lagrangian in Eq. (2.30) is characterized by the dimensionless Luttinger parameter $K = \pi n/mc$, which depends on the degree of correlations

in the host liquid [48]. For a liquid of weakly repulsive bosons the Luttinger parameter K is large, $K \gg 1$ but can be reduced down to the limiting value $K = 1$ by increasing the repulsive interactions or decreasing the density of the particles [53]. The combination $\pi c/K = mc^2/n$ entering Eq. (2.30) contains information about interactions between the particles in the liquid, while the combination $cK/\pi = c\kappa = n/m$ is independent of the interactions as a consequence of Galilean invariance.

To gain additional insight into the physics of the depleton–phonon interaction, the phononic fields can be decomposed into a doublet of right- and left-moving chiral components with the help of the linear transformation

$$\begin{pmatrix} \vartheta/\pi \\ \varphi \end{pmatrix} = \mathsf{T}\chi = \mathsf{T}\begin{pmatrix} \chi_+ \\ \chi_- \end{pmatrix}, \qquad \mathsf{T} = \frac{1}{\sqrt{2}}\begin{pmatrix} \sqrt{\kappa} & \sqrt{\kappa} \\ \frac{1}{\sqrt{\kappa}} & -\frac{1}{\sqrt{\kappa}} \end{pmatrix}, \tag{2.31}$$

where $\kappa = K/\pi = n/mc$. In terms of the chiral fields the Lagrangian, Eq. (2.30) splits into a sum of two independent contributions,

$$L_{\rm ph}[\chi] = \frac{1}{2}\int dx\, \left[\chi_+(\partial_x\partial_t + c\partial_x^2)\chi_+ + \chi_-(-\partial_x\partial_t + c\partial_x^2)\chi_-\right] = \frac{1}{4}\int dx\, \chi^\dagger \mathsf{D}^{-1}\chi\,. \tag{2.32}$$

The matrix of the inverse phonon propagator is defined by its Fourier representation,

$$\delta(x)\delta(t)\mathsf{D}^{-1} = \int \frac{\mathrm{d}q}{2\pi}\frac{\mathrm{d}\omega}{2\pi}\, e^{iqx - i\omega t}\mathsf{D}^{-1}(q,\omega),\ \mathsf{D}^{-1}(q,\omega) = 2\begin{pmatrix} q(\omega - cq) & 0 \\ 0 & -q(\omega + cq) \end{pmatrix} \tag{2.33}$$

The equation of motion following from the Lagrangian (2.32) dictates a simple coordinate and time dependence, $\chi_\pm(x,t) = \chi_\pm(x \mp ct)$. Using this fact one can show that for uniformly moving reference point $X = Vt$ one has

$$\frac{\mathrm{d}}{\mathrm{d}t}\chi_\pm(X,t) = (V \mp c)\partial_x\chi_\pm(X,t)\,. \tag{2.34}$$

This property is in fact a statement about the correlation functions of the fields $\chi_\pm$ calculated with the Gaussian action, Eq. (2.32) which enforces classical equations of motion; the path integration is performed over arbitrary configurations of the fields. The interaction term, Eq. (2.29) may be conveniently rewritten by introducing chiral collective variables

$$\Lambda = \begin{pmatrix} \Lambda_+ \\ \Lambda_- \end{pmatrix} = \mathsf{T}^\dagger \begin{pmatrix} \Phi \\ N \end{pmatrix}. \tag{2.35}$$

In the static limit the quantities $\Lambda_\pm$ are proportional, up to a factor of $\sqrt{2\pi}$, to the chiral phase shifts $\delta_\pm$ introduced in Refs.[38, 40, 54]. In the presence of an external force F they acquire dynamics, which is governed by the total Lagrangian of the depleton interacting with the phonons

$$L_{\rm tot} = P\dot{X} - H(P,\Lambda) - U(X) - \dot{\Lambda}^\dagger(t)\,\chi(X,t) + L_{\rm ph}[\chi] \tag{2.36}$$

where the impurity Hamiltonian $H(P,\Lambda)$ is obtained from Eq. (2.11) by using the linear relation, Eq. (2.35) between the chiral phase shifts Λ and collective variables Φ and N, and $L_{\rm ph}$ is given by Eq. (2.32). Here $U(X)$ is an external potential acting on the impurity only and $F = -\partial U/\partial X$ is the external force.

2.3.3 Integrating out the phonons

We now have all the necessary ingredients for describing the dynamics of the depleton coupled through the interaction term, Eq. (2.29) to the phononic bath. The presence of the impurity is felt by phonons through time-dependent boundary conditions at $x = X(t)$ parameterized by the collective variables $N(t)$ and $\Phi(t)$, or equivalently by chiral phases $\Lambda_\pm(t)$. Here we simplify our description even further by solving the phononic linear equations of motion for any variation of these collective variables and substituting the obtained solution back into the action. This procedure leads to the dynamics of the impurity expressed in terms of collective variables only and is equivalent to exact integration of the Gaussian phononic action.

To this end we employ the Keldysh formalism [55, 56] and extend the dynamical variables $X(t)$, $P(t)$, $\Lambda_\pm(t)$ as well as phononic fields $\chi_\pm(x,t)$ to forward and backward parts of the closed time contour $t \to t_\pm$. Performing the Keldysh rotation, we write $X(t_\pm) = X_{\rm cl} \pm X_{\rm q}$, $\Lambda(t_\pm) = \Lambda_{\rm cl} \pm \Lambda_{\rm q}$, and $\chi(t_\pm) = \chi_{\rm cl} \pm \chi_{\rm q}$ with the help of symmetric ("classical", cl) and antisymmetric ("quantum", q) combinations. The coupling term Eq. (2.29) then becomes

$$L_{\rm int} = 2\left[\dot{\Lambda}^\dagger_{\rm cl}(t)\chi_{\rm q}(X_{\rm cl},t) + \dot{\Lambda}^\dagger_{\rm q}(t)\chi_{\rm cl}(X_{\rm cl},t) + \dot{\Lambda}^\dagger_{\rm cl}(t)X_q(t)\,\partial_x\chi_{\rm cl}(X_{\rm cl},t)\right] \tag{2.37}$$

up to terms linear in $X_{\rm q}$. The advantage of the chiral fields introduced in Eq. (2.31) is that one can use the property (2.34) together with classical trajectory $X_{\rm cl} = Vt$ to

simplify the interactions, Eq. (2.37) as

$$L_{\rm int} = -2\dot{\Lambda}^\dagger_{\rm cl}\chi_{\rm q} + 2\left(\Lambda^\dagger_{\rm q} + X_{\rm q}\dot{\Lambda}^\dagger_{\rm cl}\mathsf{V}^{-1}\right)\frac{{\rm d}\chi_{\rm cl}}{{\rm d}t} \tag{2.38}$$

where we have introduced the matrix

$$\mathsf{V}^{-1} = \begin{pmatrix} \frac{1}{c-V} & 0 \\ 0 & -\frac{1}{c+V} \end{pmatrix}. \tag{2.39}$$

The interaction term, Eq. (2.38) is linear in phononic fields so that a Gaussian integration with quadratic action, Eq. (2.36) can be performed by standard methods as explained in Appendix B.1. It leads to a quadratic, though nonlocal in time, effective action for the collective variables,

$$\begin{aligned} S_{\rm eff} &= -\int {\rm d}t\ \dot{\Lambda}^\dagger_{\rm cl}(t)\ \left[\Lambda_{\rm q}(t) + \mathsf{V}^{-1}\dot{\Lambda}_{\rm cl}(t)X_{\rm q}(t)\right] \\ &+ \int {\rm d}t{\rm d}t'\ \left[\Lambda^\dagger_{\rm q} + X_{\rm q}\dot{\Lambda}^\dagger_{\rm cl}\mathsf{V}^{-1}\right]_t \partial_t\mathsf{F}(t-t')\left[\Lambda_{\rm q} + \mathsf{V}^{-1}\dot{\Lambda}_{\rm cl}X_{\rm q}\right]_{t'}, \end{aligned} \tag{2.40}$$

where, assuming thermal equilibrium of the phononic subsystem, the matrix $\mathsf{F}(t)$ is related by inverse Fourier transform to the matrix

$$\mathsf{F}(\omega) = \begin{pmatrix} \coth\frac{\omega}{2T_+} & 0 \\ 0 & \coth\frac{\omega}{2T_-} \end{pmatrix}, \tag{2.41}$$

of the thermal distribution of the chiral bosons with the temperatures $T_\pm = T(1 \mp V/c)$ modified by the corresponding Doppler shifts.

One should supplement the action Eq. (2.40) with the Keldysh analogue of the action corresponding to the depleton Hamiltonian, Eq. (2.11),

$$S = 2\int dt\left[\left(\dot{X}_{\rm cl} - \partial_P H\right)P_{\rm q} - \left(\dot{P}_{\rm cl} + \partial_X U\right)X_{\rm q} - \nabla_\Lambda H\cdot\Lambda_{\rm q}\right], \tag{2.42}$$

where we kept only terms linear in the quantum components and $H = H(P_{\rm cl}, \Lambda_{\rm cl})$. Notice that quadratic terms in quantum fields are absent in Eq. (2.42) while cubic and higher orders are omitted in the spirit of the semiclassical approximation.

The second line in the effective action Eq. (2.40) may be split with the help of the Hubbard-Stratonovich transformation, which introduces two real, uncorrelated Gaussian noises $\xi_+(t), \xi_-(t)$. Their correlation matrix in the frequency representation takes

the standard Ohmic form (see, *e.g.* [52]),

$$\left\langle \xi(\omega)\xi^{\dagger}(\omega')\right\rangle = \pi\omega\mathsf{F}(\omega)\delta(\omega-\omega')\,, \qquad \xi = \begin{pmatrix}\xi_+\\ \xi_-\end{pmatrix} \tag{2.43}$$

The action, Eq. (2.40) becomes local in time,

$$S_{\rm eff} = -\int \mathrm{d}t\, \left(\dot{\Lambda}^{\dagger}_{\rm cl} - 2\xi^{\dagger}\right)\left(\Lambda_{\rm q} + \mathsf{V}^{-1}\dot{\Lambda}_{\rm cl}X_{\rm q}\right). \tag{2.44}$$

Now the entire semiclassical action is linear in quantum components and integration over them enforces the delta-functions of the equation of motions. While Eq. (2.10) remains intact, due to the absence of $P_{\rm q}$ in the effective action (2.44), Eqs. (2.12), (2.13) and (2.14) are modified by the phonons:

$$\dot{P} = F - \frac{1}{2}\dot{\Lambda}^{\dagger}\mathsf{V}^{-1}\dot{\Lambda} + \xi^{\dagger}\mathsf{V}^{-1}\dot{\Lambda}\,, \tag{2.45}$$

$$\frac{1}{2}\dot{\Lambda} = -\nabla_{\Lambda}H + \xi\,, \tag{2.46}$$

where we have dropped subscripts for clarity. The obtained equations include additional dissipative terms involving time derivatives of the collective variables Λ. They also include fluctuations coming from the pair of Gaussian noises $\xi_{\pm}(t)$ correlated according to Eq. (2.43).

2.4 Depleton dynamics at zero temperature

Our goal is to discuss the non-equilibrium solutions of the equations of motion in the presence of a constant external force F. Neglecting the fluctuation terms and using the transformation Eq. (2.35), the equations of motion, Eqs. (2.45), (2.46), can be rewritten in terms of the collective variables Φ and N as follows,

$$\begin{aligned}\dot{P} &= F - \frac{1}{2}\left(\dot{\Phi},\dot{N}\right)\mathsf{T}\mathsf{V}^{-1}\mathsf{T}^{\dagger}\begin{pmatrix}\dot{\Phi}\\ \dot{N}\end{pmatrix}\\ &= F - \frac{c}{c^2-V^2}\left(\frac{\kappa V}{2c}\dot{\Phi}^2 + \dot{\Phi}\dot{N} + \frac{V}{2\kappa c}\dot{N}^2\right) \qquad (2.47)\\ \frac{\kappa\dot{\Phi}}{2} &= -\partial_{\Phi}H = nV - \partial_{\Phi}H_{\rm d} \qquad (2.48)\\ \frac{\dot{N}}{2\kappa} &= -\partial_N H = -mV^2/2 - \mu(n) - \partial_N H_{\rm d}\,. \qquad (2.49)\end{aligned}$$

The rate of energy radiated by phonons is obtained by taking derivative with respect to time of the total impurity energy,

$$W = \dot{H} - F\dot{X} = V(\dot{P} - F) - \dot{\Lambda}^{\dagger} \cdot \nabla_{\Lambda} H = V(\dot{P} - F) + \dot{\Phi}\partial_{\Phi} H + \dot{N}\partial_{N} H. \quad (2.50)$$

Using Eq. (2.10) and equations of motion either in the form (2.45–2.46) or (2.47–2.49) we obtain

$$W = -\frac{1}{2}\dot{\Lambda}^{\dagger}\left[1 + V\,\mathsf{V}^{-1}\right]\dot{\Lambda} = -\frac{c^2}{c^2 - V^2}\left(\frac{\kappa}{2}\dot{\Phi}^2 + \frac{V}{c}\dot{\Phi}\dot{N} + \frac{1}{2\kappa}\dot{N}^2\right), \quad (2.51)$$

The dissipation of momentum, Eq. (2.47) and energy, Eq. (2.51) is a generalization of Eqs. (22),(23) in Ref.[57] (up to a factor of two), where they were derived in the context of grey solitons dynamics.

According to Eqs. (2.12)–(2.14), in the absence of the external force $F = 0$ there is a family of stationary solutions of the equations of motion, which are characterized by a constant velocity V below some critical velocity V_{c}. These solutions describe the dissipationless motion of the impurity consistent with superfluidity. Indeed, by neglecting the fluctuation terms we effectively put the temperature to be zero, thus making the one-dimensional liquid superfluid.

At first glance one can just solve the set of the evolutionary equations (2.10), (2.47)–(2.49) to fully describe the impurities dynamics. One needs to be careful, though, because Eqs. (2.48), (2.49) correspond to the motion in the vicinity of the *maximum* of the Hamiltonian H and therefore exhibit a runaway instability. A further look at this instability shows that its characteristic rate is of the order $mc^2 \sim \mu$, which is well outside the frequency range of applicability of the theory developed above. In fact this high-frequency instability of Φ and N evolution is a direct analog of the well-known spurious self-acceleration of charges due to the back reaction of the electromagnetic field [58]. The recipe to overcome it is, of course, also well-known: instead of trying to solve equations of motion directly, one should perturbatively find how radiation corrections influence the dynamics [59]. This strategy offers a convenient analytical approach to treat the dynamics described by Eqs. (2.10) and (2.47)–(2.49). Below we apply it to study modifications to Bloch oscillations which arise due to the phonon radiation.

2.4.1 Radiative corrections to Bloch oscillations

At zero temperature with a sufficiently small applied force one expects the system to adiabatically stay in the ground state with total momentum $P = Ft$. In this zeroth approximation, the motion is nothing but a tracing of the dispersion relation $E(P, n)$ and the phononic subsystem gains no share of the work done on the system by F. The velocity is simply

$$V^{(0)}(t) = V_0(Ft, n) = \partial E(P, n)/\partial P\Big|_{P=Ft}. \tag{2.52}$$

Since the dispersion relation displays periodic behavior, one immediately obtains Bloch oscillations with period $\tau_{\rm B}^{(0)} = 2\pi n/F$, amplitude $V_{\rm c}$ and zero drift. In reality, the slow acceleration of the impurity over the course of a Bloch cycle gives rise to a soft radiation of low energy phonons, which serve to renormalize the period, amplitude and drift from the zeroth order approximations.

To study the corrections to the depleton trajectory, let us assume it exhibits a steady-state motion such that $V(t + \tau_{\rm B}) = V(t)$, $N(t + \tau_{\rm B}) = N(t)$ and $\Phi(t + \tau_{\rm B}) = \Phi(t) + 2\pi$. Then it follows from Eq. (2.9) that $P(t + \tau_{\rm B}) = P(t) + 2\pi n$. Here $\tau_{\rm B}$ is the, *a priori* unknown, true period of the motion, not to be confused with the zeroth approximation $\tau_{\rm B}^{(0)}$. To find it we integrate Eq. (2.47) over a single Bloch cycle

$$2\pi n = \int_0^{\tau_{\rm B}} dt\dot{P} = F\tau_{\rm B} - \frac{1}{2}\int_0^{\tau_{\rm B}} dt \frac{1}{c^2 - V^2}\left(\kappa V\dot{\Phi}^2 + 2c\dot{\Phi}\dot{N} + \kappa^{-1}V\dot{N}^2\right) = \tau_{\rm B}(F - F_{\rm rad}) \tag{2.53}$$

where $F_{\rm rad}$ is the average radiative friction force exerted on the impurity over a single Bloch cycle. Since the radiative frictional force tends to reduce the applied force, Eq. (2.53) indicates that the true period of oscillation is *larger* than the zeroth approximation $\tau_{\rm B}^{(0)}$.

The work of the external force per unit time is given by

$$FV = \dot{E}(P, n) - W. \tag{2.54}$$

The first term on the r.h.s. of this equation is the reversible change in energy of the impurity, while the second term, owing to Eq. (2.51), is the rate of energy channeled into the phonon system. We average Eq. (2.54) over a single Bloch cycle, noticing

that $\langle \dot{E} \rangle = 0$ due to the periodicity of the dispersion relation. The remaining term corresponds to the power radiated into phononic bath and leads to the *drift velocity*:

$$V_{\rm D} = -\langle W \rangle / F. \tag{2.55}$$

Assuming the energy pumped into the phonon system per Bloch cycle is small, we may use the bare trajectories $V_0(P,n)$, $\Phi_0(P,n)$, $N_0(P,n)$ in Eq. (2.51). This approximation is justified for small forces such that $F < F_{\rm max}$. In this limit, one may use the fact that $dt = dP/F$ to show that

$$V_{\rm D} = \sigma F. \tag{2.56}$$

Here σ is the $T = 0$ mobility of the impurity, given by the average over the Brillouin zone

$$\sigma = \frac{1}{2\pi n} \int\limits_{-\pi n}^{\pi n} dP \left(\frac{c^2}{c^2 - V_0^2} \right) \left[\frac{\kappa}{2} \left(\frac{\partial \Phi_0}{\partial P} \right)^2 + \frac{V_0}{c} \left(\frac{\partial N_0}{\partial P} \right) \left(\frac{\partial \Phi_0}{\partial P} \right) + \frac{1}{2\kappa} \left(\frac{\partial N_0}{\partial P} \right)^2 \right]. \tag{2.57}$$

It was mentioned in Sec. 2.2.2 that the equilibrium functions $\Phi_0(P,n)$ and $N_0(P,n)$ can be obtained directly from partial derivatives of the equilibrium dispersion relation $E(P,n)$. Since $V_0 = \partial E/\partial P$, the mobility may be expressed entirely in terms of $E(P,n)$ and the Luttinger parameter $K = \pi\kappa$.

The fact that the mobility can be expressed through equilibrium properties is reminiscent of the Kubo linear response formulation. It is crucial to mention, however, that we are *not* discussing a linear response property in the Kubo sense. The Kubo linear response takes place at finite temperature in non-integrable systems, see Section 2.5. At $T = 0$ the liquid is superfluid and the impurity undergoes Bloch oscillations with amplitude V_c at an arbitrarily small external force F. It means that the response is essentially non-linear, as the total velocity (drift *plus* oscillations) is not proportional to the force. As we shall see in Section 2.5, this remains true even at *finite* temperatures if the system is integrable. The mobility σ describes the average (over one period) shift of the oscillation center due to the energy radiated in the course of such *non-linear* oscillations. The fact that it may be fully expressed through the equilibrium properties is rather remarkable in its own right.

The result in Eq. (2.56) holds for sufficiently weak external perturbation $F < F_{\rm max}$. One can estimate $F_{\rm max}$ by comparing the corresponding drift velocity with the velocity

of sound. From Eq. (2.56) we have

$$F_{\max} = c/\sigma. \tag{2.58}$$

As the force increases past this upper bound, the separation of length and energy scales used to define the depleton dynamics cannot be justified. In other words, for a strongly perturbed system the *equilibrium* dispersion relation $E(P, n)$ ceases to be a meaningful concept.

Below we use a model of an impurity coupled via delta-function interaction with strength G to the background particles to illustrate the dynamical properties of a depleton discussed above. We discuss two regimes: the strong coupling regime, where the interactions in the liquid can be of arbitrary strength and the weak coupling regime where the dynamics of the depletion cloud is governed by Gross-Pitaevskii equation. In the latter case one is restricted to a weakly interacting bosonic background.

Strong coupling regime $G/c \gg 1$

The impurity expels a large number $N \gg 1$ of particles from its vicinity. Thus, one can neglect the dynamics of N and use the Josephson form, Eq. (2.24) for the remaining dependence of the energy on the superfluid phase. Due to the fact that the velocity is bounded by the critical value $V_{\rm c}$, the impurity is slow $V \leq V_{\rm c} \ll c$. Indeed, the calculation for a weakly interacting bosonic background, Eq. (A.22) (see also Ref.[60]) gives $V_c = c^2/2G \ll c$. Therefore, if the impurity is not too heavy, $M \sim m$, we can neglect the second term in the momentum, Eq. (2.9) and we are left with the superfluid contribution $P = n\Phi$ only. Using this fact in Eq. (2.57) gives the universal result for the mobility

$$\sigma = \frac{\kappa}{2\hbar n^2} = \frac{K}{hn^2} = \frac{1}{2nmc}\,, \tag{2.59}$$

where we restored $\hbar = h/2\pi$. Note that in the strong coupling limit, the mobility is *independent* of the impurity parameters and *only* depends on the parameters of the host liquid, namely the Luttinger parameter K and the asymptotic density n. This result has been obtained by Castro-Neto and Fisher [23] by using the linear response approach in the limit $V_c = 0$, where the non-linear Bloch oscillation reponse does not occur.

For the case of impenetrable bosons, or free fermions corresponding to $K = 1$, one can use an analogy from electronic transport. Suppose the background is made of

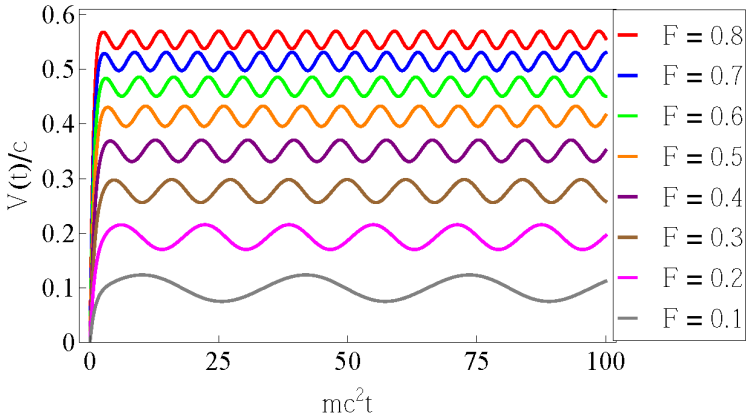

Figure 2.3: Velocity as a function of time for various forces listed in the legend (F in units of $F_{\max} = 2nmc^2$). Here $\kappa = 20$, $G/c = 20$ and $M = 40m$. The dashed lines correspond to the drift velocity plotted in Fig. 2.4. One notices that as F increases, the drift velocity and frequency of oscillations increases, while the velocity amplitude (as measured from $V_{\rm D}$) decreases.

non-interacting fermions each carrying electric charge e. In the frame co-moving with the impurity a current $I = enV_{\rm D}$ flows through the wire, whose quantum resistance is R. The latter is given by the Landauer formula, which for the spinless case reads as $R = h/e^2$. The ohmic power transferred to the system, I^2R, must be supplied by the external force, $FV_{\rm D} = hn^2V_{\rm D}^2$ giving the result in Eq. (2.59) for $K = 1$. For $K > 1$ one recalls that $R = h/Ke^2$ [61] leading again to Eq. (2.59). Notice that the discussion of Ref. [62] claiming an interaction-independent mobility is not applicable here, since we always assume that the system length is much larger than the characteristic wavelength of phonons.

Scaling with K, the mobility grows with weaker interactions and diverges in the free-boson limit. To understand this result, notice that the moving impenetrable impurity experiences $nV_{\rm D}$ collisions per unit time. A given collision results in the momentum transfer $mV_{\rm D}$ to the boson of the gas. The balance of forces $F = nmV_{\rm D}^2$ then implies $V_{\rm D} = F/\sqrt{nmF}$ leading to $\sigma = 1/\sqrt{nmF} \to \infty$ as $F \to 0$, in agreement with non-interacting limit of Eq. (2.59).

Turning to the period of oscillations, Eq. (2.53) we use the relations $V \approx V_{\rm D} =$

$\kappa F/2n^2$, $\dot{\Phi} \approx F/n$ to obtain the renormalized period of Bloch oscillations,

$$\tau_{\rm B} \approx \frac{2\pi n}{F}\left[1+\left(\frac{F}{2nmc^2}\right)^2\right]. \tag{2.60}$$

The characteristic force entering Eq. (2.60) coincides with the upper bound $F_{\rm max} = 2nmc^2$ obtained from Eq. (2.58) using the result (2.59) for the mobility. Indeed, the frequency of the motion $\omega \approx F/n$ should be small compared to the typical phonon frequency mc^2 in order to justify the large scale separation employed in Sec. 2.1.

To go beyond lowest order in F we devise a numerical approach to the strongly coupled impurity based on the Josephson form, Eq. (2.24) for the energy. Using it in Eq. (2.48) and recalling Eq. (2.47) gives,

$$\dot{P} = F - \frac{1}{2}\frac{\kappa V}{c^2-V^2}\dot{\Phi}^2; \qquad \frac{\kappa\dot{\Phi}}{2n} = V - V_c\sin\Phi, \tag{2.61}$$

where P is given by Eq. (2.9). The second of Eqs. (2.61) relates the change in Φ with the deviation of the impurity velocity V from its equilibrium value $V_c\sin\Phi$. The velocity $V(t)$ is obtained by solving Eqs. (2.61) numerically and the results depicted in Figs. 2.3 agree well with the ansatz (2.62). As one can see, the precise choice of initial conditions is essentially irrelevant to the ensuing discussion, where we focus only on the asymptotic, steady state behavior of the functions $\Phi(t)$ and $V(t)$.

After a sufficiently long time the system reaches the regime of steady Bloch oscillations, where its velocity is given by

$$V(t) = V_{\rm D} + V_{\rm B}\cos(\omega_{\rm B}t+\delta)\,. \tag{2.62}$$

Here the parameters $V_{\rm D}$, $V_{\rm B}$, $\omega_{\rm B} = 2\pi/\tau_{\rm B}$ and δ depend on the ratio of the external force F to the critical force $F_{\rm max}$.

To find the drift velocity and period of Bloch oscillations we substitute the ansatz $V = V_{\rm D}$ and $\dot{P} = n\dot{\Phi} = n\omega_{\rm B}$ into Eqs. (2.61) to obtain a closed set of equations,

$$n\omega_{\rm B} = F - \frac{1}{2}\frac{\kappa V_{\rm D}\omega_{\rm B}^2}{c^2-V_{\rm D}^2}; \qquad \frac{\omega_{\rm B}}{2mc^2} = V_{\rm D}/c \tag{2.63}$$

which are solved to give

$$\frac{V_{\rm D}}{c} = \frac{\omega_{\rm B}}{2mc^2} = \frac{F_{\rm max}}{2F}\left(\sqrt{1+\left(\frac{2F}{F_{\rm max}}\right)^2}-1\right). \tag{2.64}$$

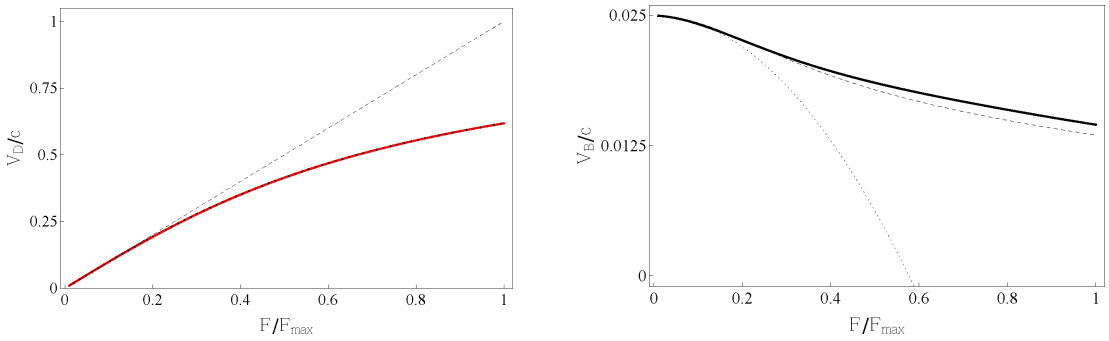

Figure 2.4: Drift velocity $V_{\rm D}$ (left panel) and amplitude $V_{\rm B}$ (right panel) as functions of the applied force F corresponding to the same set of parameters as in Fig. 2.3. The solid curve in the left panel is indistinguishable from the analytic prediction, Eq. (2.64), while the dashed curve is the small force result Eq. (2.56) with mobility $\sigma = \kappa/2\hbar n^2$. In the right panel the solid curve is produced numerically, the dashed curve is Eq. (B.17), and the dotted curve corresponds to the small F limit, Eq. (2.65).

Expanding the expression for $\omega_{\rm B} = 2\pi/\tau_{\rm B}$ for small $F/F_{\rm max}$ one recovers the result (2.60) obtained by a different method. The results for the drift velocity are plotted in Fig. 2.4a and are in excellent agreement with the numerical solution of Eqs. (2.61).

The Bloch amplitude $V_{\rm B}$ can also be estimated from Eqs. (2.61). In Appendix B.2 it is shown that for $F \ll F_{\rm max}$

$$V_{\rm B} = V_{\rm c}\left\{1 - \left[1 + \frac{1}{2}\left(\frac{M - mN}{m\kappa}\right)^2\right]\left(\frac{F}{F_{\rm max}}\right)^2\right\}. \tag{2.65}$$

Thus, Eq. (2.65) predicts a decrease of the Bloch amplitude $V_{\rm B}$ with increasing F (see Fig. 2.4b). Physically sensible, this result implies that as the force increases, the ideal equilibrium tracing of the dispersion relation is, to a degree, lost. This is due to the phononic subsystem gaining a proportionately larger share of the work done by the external force. Expression (2.65) is compared with results of the numerical solution of Eqs. (2.61) and the results presented in the right panel of Fig. 2.4b show good agreement.

Weakly interacting background bosons and weak coupling regime $G/c \ll 1$

We deal with the case of the background made of weakly interacting bosons by using the Gross-Pitaevskii equation for the background Bose liquid as explained in Appendix A.2. By calculating numerically the dispersion relation of the impurity, see *e.g.* Fig. 1.3, we

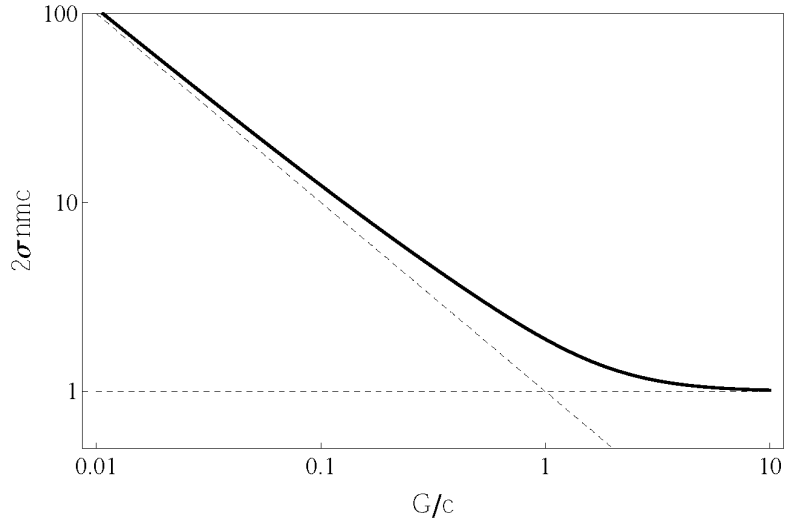

Figure 2.5: Log-log plot of the *zero temperature* mobility σ as a function of the impurity coupling G in a weakly interacting superfluid (solid line). The dashed lines correspond to the asymptotic values of σ in the strong and weak coupling limits given by Eqs. (2.59) and (2.68), respectively. The Luttinger parameter for the liquid is taken to be $\kappa = n/mc = 20$, while $M = m$.

obtain the functions N_0 and Φ_0 for all values of the impurity-background coupling G. The results of numerical evaluation of Eq. (2.57) are shown in Fig. 2.5.

Let us turn now to the case of weak coupling $G \ll c$, where particles can tunnel through the semi-transparent impurity. In such a case one expects the mobility to increase as the impurity becomes more transparent. For weak coupling, the main contribution to the integral in Eq. (2.57) comes from the region where the velocity of the impurity is maximal, *i.e.* $V \sim V_c$. It corresponds to the inflection points of the dispersion, Fig. 1.3. Beyond this point the dispersion follows closely the dispersion of grey solitons, Eq. (A.4) and one can use the expressions (A.5) to estimate the mobility. As the momentum P_c corresponding to maximum velocity $V(P_c) = V_c$ is small, we simplify Eqs. (A.4), (A.5) and write

$$\frac{V(\Phi)}{c} \simeq 1 - \frac{1}{2}\left(\frac{\Phi}{2}\right)^2; \qquad \frac{P(\Phi)}{n} = \Phi - \sin\Phi \simeq \frac{\Phi^3}{6} \tag{2.66}$$

or, equivalently,

$$\Phi(P) = (6P/n)^{1/3}; \qquad \frac{V(P)}{c} = 1 - \frac{(6P/n)^{2/3}}{8}\,. \tag{2.67}$$

Substituting these expressions into Eq. (2.57) we can estimate the mobility as

$$\sigma \sim \frac{\kappa}{n}\int_{P_c}\frac{dP}{1-V^2/c^2}\left(\frac{\partial\Phi}{\partial P}\right)^2 \sim \frac{\kappa}{n^2}\int_{\Lambda}\frac{dP/n}{(P/n)^2} \sim \frac{\kappa}{n^2}\frac{c}{G} = 1/nmG\,. \tag{2.68}$$

Here we have estimated the momentum cutoff $\Lambda = P_c/n \sim G/c$ using Eq. (A.20) for the critical velocity and the second equation in (2.67). The coefficient in Eq. (2.68) is fixed from the numerics and was found to be very close to one for $M = m$. Interestingly, in the weak coupling limit σ is *independent* of the correlations within the liquid (provided the liquid is weakly interacting, $G \ll c$), diverging in the limit of a completely transparent impurity. Thus, in the weak coupling limit, the upper critical force $F_{\max} = nGmc$ corresponds to energy difference Gn per healing length $\xi = 1/mc$.

2.5 Depleton Dynamics at Finite Temperature

At a finite temperature, even in the absence of an external force, the collective coordinates fluctuate around their equilibrium position $\Lambda_{\pm}^{(0)}$, found from the condition $\partial_\Lambda H = 0$. Assuming these fluctuations are small, one may linearize Eq. (2.46) near its equilibrium point. Transformed to the frequency representation, the linearized matrix equation of motion takes the form

$$\left(-\frac{i\omega}{2} + 2\mathsf{\Gamma}^{-1}\right)\Lambda(\omega) \;\;=\;\; \xi(\omega)\,, \tag{2.69}$$

where $\mathsf{\Gamma}$ is the Hessian matrix of the second derivatives of the impurity Hamiltonian *at fixed momentum* P. Its matrix elements are

$$\mathsf{\Gamma}^{-1} = \begin{pmatrix}\Gamma_{++} & \Gamma_{+-}\\ \Gamma_{-+} & \Gamma_{--}\end{pmatrix}^{-1} = \frac{1}{2}\begin{pmatrix}H_{\Lambda_+\Lambda_+} & H_{\Lambda_+\Lambda_-}\\ H_{\Lambda_-\Lambda_+} & H_{\Lambda_-\Lambda_-}\end{pmatrix}\Bigg|_{\Lambda=\Lambda^{(0)}} \tag{2.70}$$

The solution of equation (2.69) takes the form

$$\Lambda(\omega) = \frac{1}{2}\left(1 - \frac{i\omega}{4}\mathsf{\Gamma}\right)^{-1}\mathsf{\Gamma}\,\xi(\omega) = \frac{1}{2}\mathsf{\Gamma}\,\xi(\omega) + \frac{i\omega}{8}\mathsf{\Gamma}^2\,\xi(\omega) + \dots\,, \tag{2.71}$$

where we consider it as a perturbative sequence in frequency, to avoid the spurious instabilities mentioned in Section 2.4. Substituting this solution into the right hand

side of Eq. (2.45) and averaging it over the Gaussian noise (2.43), one finds for the momentum loss rate

$$\dot{P} = F_{\rm fr} = -\frac{1}{16}\int \frac{d\omega}{2\pi}\,\omega^3\,{\rm Tr}\Big\{\mathsf{F}(\omega)\big[\Gamma^\dagger,\mathsf{V}^{-1}\big]\Gamma\Big\}\,, \tag{2.72}$$

where we kept only the leading order in frequency. The matrix-valued function $\mathsf{F}(\omega)$ is odd in frequency, selecting only odd powers of ω from the expression it is multiplied by. Equation (2.72) provides the expression for the viscous friction force acting on the impurity from the normal component of the liquid. It can be identified with the Raman two-phonon scattering mechanism [15, 16, 25, 26, 24].

Substituting the explicit form of the Ohmic noise correlator (2.41) and performing the frequency integration, one finds for the friction force

$$\begin{aligned} F_{\rm fr} &= -\frac{\left|\Gamma_{+-}\right|^2}{8}\frac{c}{c^2-V^2}\int\frac{d\omega}{2\pi}\,\omega^3\left(\coth\frac{\omega}{2T_-}-\coth\frac{\omega}{2T_+}\right) \\ &= -\frac{2\pi^3}{15}\left|\Gamma_{+-}\right|^2\frac{T^4}{c^2}\left(\frac{c^2+V^2}{c^2-V^2}\right)V\,. \end{aligned} \tag{2.73}$$

The T^4 dependence of the friction force was reported in [23] and is a direct consequence of the phase space for two-phonon scattering. It can be also viewed as a one-dimensional version of the Khalatnikov-Landau result [15, 16] for the viscosity of liquid helium. It should be noted that the friction force (2.73) is proportional to the off-diagonal matrix element Γ_{+-} which represents backscattering of phonons by the depleton. It depends on the momentum P and, consequently velocity V, of the mobile impurity in addition to the parameters of the impurity-background interactions. Below we derive the general expression for the backscattering amplitude and relate it to the equilibrium dispersion $E(P,n)$ of the depleton.

2.5.1 Backscattering amplitude

The detailed information about the microscopic impurity-liquid interactions is contained in the off-diagonal matrix element Γ_{+-} which represents the effective vertex for two-phonon scattering. In the spirit of our phenomenological approach it may be expressed, as explained in Appendix B.3, through partial derivatives of the equilibrium functions $\Phi_0(V,n)$ and $N_0(V,n)$,

$$\Gamma_{+-} = -\frac{\kappa m}{M^*}\left[\frac{M-mN}{mn}\left(\frac{\partial\Phi_0}{\partial V}+m\frac{\partial N_0}{\partial n}\right)+\left(\frac{\partial\Phi_0}{\partial V}\frac{\partial N_0}{\partial n}-\frac{\partial\Phi_0}{\partial n}\frac{\partial N_0}{\partial V}\right)\right]. \tag{2.74}$$

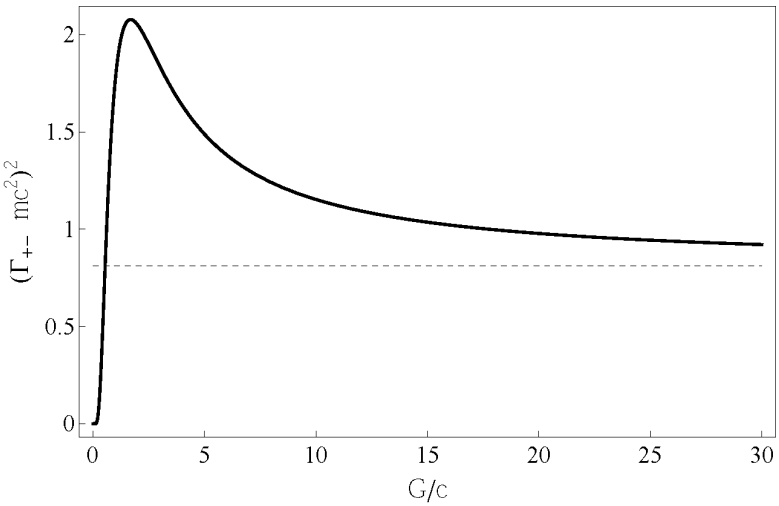

Figure 2.6: $V = 0$ and $\Phi = 0$ (*i.e.*, $P = 0$) square of the backscattering amplitude as a function of the impurity coupling G for $\kappa = 10$ and $M = m$ (solid line). The dashed line corresponds to the strong coupling $G \gg c$ limit, Eq. (2.76).

Treating collective variables $\Phi_0 = \Phi_0(P, n)$ and $N_0 = N_0(P, n)$ as functions of momentum rather than velocity and calculating the corresponding derivatives as explained in Appendix B.3 we find an alternative representation

$$\Gamma_{+-}(P, n) \;=\; -\frac{1}{c}\left(\frac{M}{m}\frac{\partial \Phi_0}{\partial P} + \Phi_0\frac{\partial N_0}{\partial P} - N_0\frac{\partial \Phi_0}{\partial P} + \frac{\partial N_0}{\partial n}\right). \tag{2.75}$$

The functions Φ_0 and N_0 are obtained from the equilibrium dispersion $E(P, n)$ as explained in Section 2.2.2 (see, *e.g.* Eq. (2.21)). These relations can be used to obtain an equivalent representation for the backscattering amplitude Γ_{+-} given by Eq. (B.29) in Appendix B.3.

Two remarks are in order. First, it should be noted that the backscattering amplitude given by Eqs. (2.74), (2.75) depends on the velocity V or momentum P of the depleton. While the momentum dependence is unambiguous, there can be different regimes corresponding to the *same* velocity characterized by different values of the superfluid phase Φ. Second, it can be shown by calculating the dispersion $E(P, n)$ by the Bethe Ansatz method that the off-diagonal matrix element Γ_{+-} vanishes identically for integrable mobile impurities, such as lowest excitation branch in Lieb-Liniger [63], the Yang-Gaudin model [27, 28], an equal mass impurity coupled to a free fermi gas [51] and

the soliton of the Gross-Pitaevskii equation [64] (see Appendix A.1). We postpone the details of these exact calculations to another publication. Below we use the semiclassical approach valid for the weakly interacting bosonic background which provides results for backscattering amplitude in a wide range of parameters relevant to experiments.

Strongly coupled impurity, $G/c \gg 1$, in a weakly interacting liquid, $K \gg 1$

In the strong coupling regime the leading terms in the the number of depleted particles, the second equation in (A.22) is a constant, $N_0 = 2\kappa \gg 1$ and the momentum iss dominated by the supercurrent and $P = n\Phi$. These observations simplify greatly the expression (2.75) for backscattering amplitude and one obtains

$$\Gamma_{+-} = \frac{1}{mc^2}\left[1 - \frac{M}{\kappa m}\right], \tag{2.76}$$

where we have used the fact that $\partial\kappa/\partial n = \kappa/2n$. The expression (2.76) is a momentum and velocity independent constant, equal to $1/mc^2$ for a not too heavy impurity $M \ll \kappa m$.

Weakly coupled, slow impurity, $G/c \ll 1$

In the weak coupling regime the backscattering amplitude varies strongly with the velocity of the depleton. Here we present results for a slow impurity which can be found by evaluating Γ_{+-} at $V = 0$.

There are two distinct physical regimes corresponding to a slow impurity: one, corresponding to the solution with $\Phi_0 \simeq 0$ and momentum $P \simeq MV \simeq 0$, dominated by the bare impurity, and one corresponding to $\Phi_0 \simeq \pi$ and momentum $P \simeq \pi n$, dominated by the background supercurrent. For $\Phi \approx 0$ we have

$$N_0(V,n) = 2\kappa\left(1 + \frac{G}{2c} - \sqrt{1 + \left(\frac{G}{2c}\right)^2}\right),\ \Phi_0(V,n) = 2\frac{V}{c}\left(-1 + \frac{G}{2c} + \sqrt{1 + \left(\frac{G}{2c}\right)^2}\right), \tag{2.77}$$

while near $\Phi = \pi$, we find

$$N_0(V,n) = 2\kappa\,, \qquad \Phi_0(V,n) = \pi - 2\frac{V}{c}\left(1 + \frac{G}{c}\right). \tag{2.78}$$

These expressions are correct up to terms $\mathcal{O}(V^2)$ for the number of particles and $\mathcal{O}(V^3)$ for the phase.

In the case $\Phi_0 \simeq 0$ we use Eqs. (2.77) to calculate Γ_{+-}. For weak coupling to the leading order in both $g/c = 1/\kappa$ and G/c we have,

$$\Gamma_{+-} = \frac{1}{mc^2}\left(\frac{G}{c}\right)\left(\frac{mG}{Mg} - 1\right), \qquad G/c \ll 1. \tag{2.79}$$

This result agrees with Eq.(5) in Ref. [25] and indicates that friction vanishes near the integrable point $M = m$ and $G = g$, at least for small velocities near $\Phi = 0$. The results for arbitrary coupling G/c are presented in Figs. 2.6.

In the case $\Phi_0 \simeq \pi$, we use Eqs.(2.78) and calculate the effective mass $M^* = M - mN + n\partial_V\Phi = M - 2\kappa m - 2\kappa m(1+G/c)$. Using Eq.(2.74) we find for arbitrary coupling

$$\Gamma_{+-} = \frac{1}{mc^2}\frac{(M/\kappa m)\,(1+2G/c) - 2G/c}{M/\kappa m - 2G/c - 4}, \tag{2.80}$$

It comes as no surprise that Eq.(2.80) vanishes in the limit $M, G \to 0$, where one recovers the dark soliton result from Appendix A.1. Indeed, there it is mentioned that such soliton excitation is transparent for phonons due to its integrability and, consequently, $\Gamma_{+-} = 0$ for all velocities. In the limit of weak coupling Eq.(2.80) becomes

$$\Gamma_{+-} = \frac{1}{mc^2}\left(\frac{2G}{c} - \frac{M}{\kappa m}\right). \tag{2.81}$$

At the Yang-Gaudin integrable point ([27, 28], see also [37]) of the *quantum* system defined as $M = m$ and $G = g$, the corresponding limit of the second equation in (2.81) is proportional $g/c = 1/\kappa$ which is a small parameter in the semiclassical limit and therefore our calculation goes beyond the accuracy of the approximations adopted above.

2.5.2 Bloch oscillations in the presence of viscous friction

Imagine the impurity is dragged by a weak external force F. There is a velocity $V < V_{\rm c}$ such that $F + F_{\rm fr}(V) = 0$ and the system reaches a steady state with constant drift velocity $V_{\rm D}$ and *no* oscillations, $V_{\rm B} = 0$. If the applied force is very small, the drift velocity can be found from the small velocity limit of Eq. (2.73) in the linear response

form, $V_{\rm D} = \sigma_T F$, where the finite temperature mobility is given by

$$\sigma_T^{-1} = \frac{2\pi^3}{15}\frac{T^4}{c^2}\left|\Gamma_{+-}(V=0)\right|^2. \tag{2.82}$$

in accordance with [23, 25]. Increasing the external force leads to a slightly non-linear dependence of the drift velocity on F (due to the non-linear velocity dependence of $F_{\rm fr}(V)$, cf. Eq. (2.73)), until the the maximal possible velocity $V_{\rm c}$ is reached for $F = F_{\rm min} = -F_{\rm fr}(V_c)$. Beyond this critical force no steady state solution can be found and the impurity performs Bloch oscillations on top of a uniform drift. In such a non-linear regime the amplitude, period of the oscillations, drift velocity, as well as the momentum-dependent viscous backscattering amplitude, Eq. (2.75), are controlled by the equilibrium dispersion relation.

We illustrate the above scenario using the model of a strongly coupled impurity in a weakly interacting liquid (such a scenario is not near an integrable point and thus demonstrates the influence of non-zero thermal friction). In this case the critical velocity is small and the backscattering amplitude is velocity-independent. The critical force is then found from the linear response as $F_{\rm min} = V_{\rm c}/\sigma_T$. We can use the relation $V = V_{\rm c}\sin\Phi + \kappa\dot{\Phi}/2n$ (i.e., the second of Eqs. (2.61)) and the fact that $P = n\Phi$ to write down the equation of motion for the superfluid phase,

$$\dot{\Phi} = \frac{F_{\rm min}}{n(1+\kappa/2\sigma_T n^2)}\Big(\lambda - \sin\Phi\Big)\,, \tag{2.83}$$

where $\lambda = F/F_{\rm min}$. Equation (2.83) is formally equivalent to an overdamped, driven pendulum where Φ plays the role of the angle from the vertical. Introducing the dimensionless time variable $s = (F_{\rm min}/n(1+\kappa/2\sigma_T n^2))t$ and assuming, without loss of generality, $\Phi(0) = 0$, the solution of Eq. (2.83) is found to be

$$\tan\frac{\Phi}{2} = \frac{\lambda\tanh\left(\frac{\sqrt{1-\lambda^2}}{2}s\right)}{\sqrt{1-\lambda^2}+\tanh\left(\frac{\sqrt{1-\lambda^2}}{2}s\right)} \tag{2.84}$$

For $\lambda < 1$ it describes the velocity approaching its limiting value $V_\infty = V_{\rm c}\sin\Phi(\infty) = \lambda V_{\rm c}$. For $\lambda > 1$ Eq. (2.84) describes a periodic function with period

$$\tau_{\rm B} = \frac{t}{s}\frac{2\pi}{\sqrt{\lambda^2-1}} = \frac{2\pi n(1+\kappa/2\sigma_T n^2)}{\sqrt{F^2-F_{\rm min}^2}}\,. \tag{2.85}$$

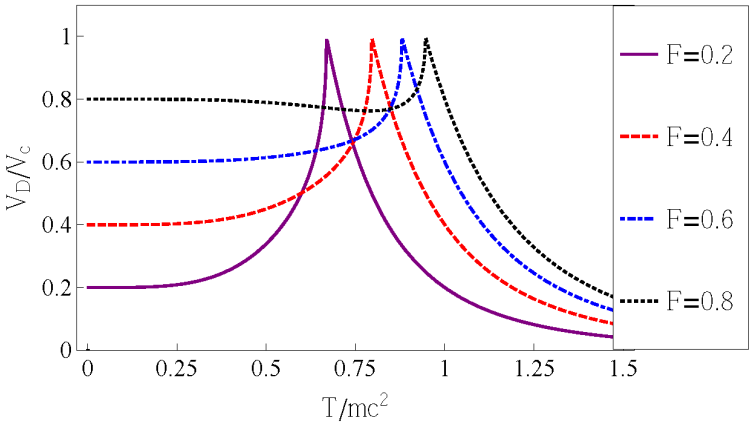

Figure 2.7: Drift velocity of a strongly coupled impurity in a weakly interacting bose liquid as a function of temperature T for various forces as predicted by Eq. (2.86). F is given in units of $F_{\max}V_c/c$, while the Luttinger parameter is taken to be $K = \pi\kappa = \pi^4/15 \approx 6.5$ so that, to a good approximation, $F_{\min}(T = mc^2) = F_{\max}V_c/c$.

The corresponding drift velocity for $F > F_{\min}$ can be found by averaging the momentum relation $n\dot{\Phi} = F - V/\sigma_T$ over a single period with the result

$$V_{\rm D} = V_c \left(\frac{F}{F_{\min}} - \frac{\sqrt{F^2/F_{\min}^2 - 1}}{1 + \kappa/2\sigma_T n^2} \right). \tag{2.86}$$

For $F_{\min} \ll F \ll F_{\max}$, one may expand Eq. (2.86) to obtain a small temperature correction

$$V_{\rm D}/c \approx \frac{F}{F_{\max}} + \frac{c}{V_c}\frac{F_{\min}}{F}\left(\frac{1}{2}V_c^2/c^2 - (F/F_{\max})^2 \right), \tag{2.87}$$

which gives the previous result Eq. (2.59) in the limit of small T, or more specifically, small $F_{\min}$. Interestingly, Eq. (2.87) predicts an *increase* in the drift with increasing T if $F/F_{\max} \lesssim V_c/c$. This suggests that for a small enough force, a significant *drop* in the drift velocity may occur as the system is cooled below the critical temperature, when the impurity enters the regime of Bloch oscillations, see Fig. 2.7.

The above analysis demonstrates, *inter alia*, a non-monotonic dependence of the drift velocity on the parameter $F/F_{\min}$ as it is increases past 1 and enters the regime of Bloch oscillations. This may occur either by fixing the temperature and increasing the force, or by fixing the external force and cooling the system. In contrast to the

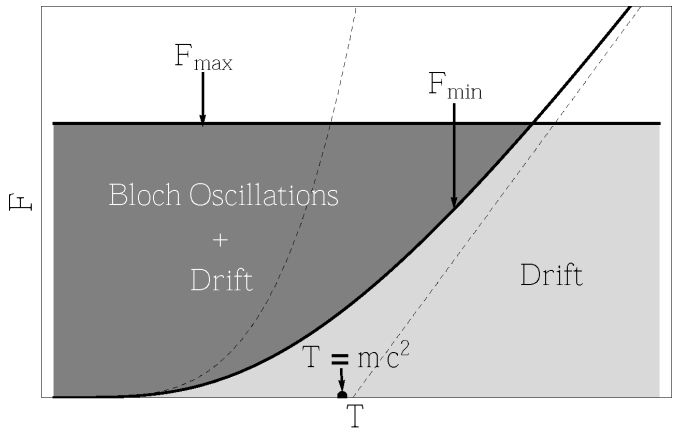

Figure 2.8: Schematic force vs. temperature diagram of impurity motion in a 1D quantum liquid. In the region $F < F_{\min}$ (light gray) the impurity drifts with mobility $\sigma_T \propto T^{-4}$ for $T \ll mc^2$. For $T \gg mc^2$, the mobility scales $\sigma_T \propto T^{-1}$ (dashed are the small and large temperature asymptotics). For $F_{\min} < F < F_{\max}$ (dark gray) one has Bloch oscillations + drift. Above $F_{\max}$, our theory is inapplicable and we expect an incoherent motion, possibly corresponding to a supersonic impurity which has *escaped* its self-induced depletion cloud.

vanishing amplitude $V_{\rm B}$ near $F_{\max}$, indicated by the second equation in (2.64), it is rather the divergent period, Eq. (2.85) for F approaching $F_{\min}$ from above which leads to the disappearance of Bloch oscillations.

2.6 Discussion of the results

The coupling with phonons governed by the universal term, Eq. (2.29), results in the transfer of energy and momentum between the depleton and the background. At zero temperature it takes the form of radiation of phonons by the accelerated impurity similar to the radiative damping in classical electrodynamics [59] and leads to the finite mobility of the depleton. For sufficiently weak forces the mobility, defined as the ratio of the drift velocity to the applied force, see Eq. (2.56), can be expressed via the equilibrium dispersion, Eq. (2.57), reminiscent of the Kubo linear response theory. The drift, however, is superimposed with essentially *non-linear* Bloch oscillations of the velocity. The amplitude of the oscillations is shown to vanish as the external force attains the upper critical force $F_{\max}$, reflecting the limit of validity for the description based on the

scale separation between the healing length and the phonon wavelength.

At finite temperatures the thermal phonons present in the system are scattered by the depleton leading to the viscous friction force, Eq. (2.73). This in turn leads to the appearance of the lower critical force $F_{\min}(T) \sim T^4$, which defines the minimum value of the external force where it is able to drive the Bloch oscillation sequence. In contrast to the situation in the vicinity of $F_{\max}$, the approach of F to $F_{\min}$ makes the Bloch oscillations disappear through the divergence of the period, Eq. (2.85). Below $F_{\min}$ the system enters the regime of non-oscillatory drift characterized by the velocity $V_{\rm D} < V_{\rm c}$, where all the momentum provided by the external force is dissipated into the phononic bath.

The viscous force contains valuable information about the fine details of the interactions between particles. In this work we have confirmed and extended the earlier observation [25] that the backscattering amplitude, given in terms of equilibrium properties by Eqs. (2.74), (2.75), vanishes if the depleton is an elementary excitation of an integrable model. This includes the dark soliton excitation of Lieb-Liniger model [63], spinons in the bosonic Yang-Gaudin model [27, 28] and an equal mass impurity in a free fermi gas [51]. The microscopic mechanism responsible for the absence of dissipation is due to destructive quantum interference between various two-phonon processes. It can be traced back to the absence of three-body processes lying at the heart of integrability in one dimension. In contrast, the radiative processes due to the presence of an external force are always present in the dynamics of the depleton. This is because the external potential is not, in general, compatible with the integrability.

Various dynamical regimes of depleton are summarized in the diagram of Fig. 2.8. At sufficiently low temperatures there is a wide parametric window $F_{\min} < F < F_{\max}$ for the external force in which the Bloch oscillations can be observed experimentally. At temperatures higher than the chemical potential the mobility of the particle becomes inversely proportional to temperature [24, 26] and moderates the growth of $F_{\min}$ (see Fig. 2.8). The above range of forces can be increased further by exploring the dependence of $F_{\min}$ and $F_{\max}$ on the interaction parameters. In particular, at integrable points $F_{\min}$ vanishes for *any* temperature. Consequently, the $T > 0$ mobility $\sigma_T \propto F_{\min}^{-1}$ is *inapplicable* to integrable impurity systems. For such systems the $T > 0$ mobility is given by Eq. (2.57) and is expressible through the exactly calculable dispersion relation.

Our approach to the dynamics of the depleton is essentially classical; the quantum mechanics enters only via parameters of the effective action. The equations of motion, Eqs. (2.46) neglect therefore the quantum and thermal fluctuations of the collective variables of the depleton. These fluctuations can be taken into account by either simulating the Langevin equation in the presence of equilibrium noises or by writing an appropriate Fokker-Planck equation for the distribution function. One of the most important consequences of the fluctuations is expected to be the smearing of the boundaries between the dynamical regimes in Fig. 2.8. We leave this as well as the question about the role of quantum fluctuation for further investigation. Another important extension of the present work would be the study of the finite size effects due to the trap geometry relevant for experiments with ultracold atoms.

Chapter 3

Heavy Impurities

In this Chapter we study the case where the impurity mass M exceeds a critical mass $M_{\rm c}$. This has important consequences for the notion of superfluid critical velocity in one spatial dimension. The dispersion develops cusps at momenta $\pi n j$, with j an odd integer, accompanied by metastable branches which result in dramatic changes of the impurity dynamics in the presence of an external driving force. In contrast to smooth Bloch oscillations for $M < M_{\rm c}$ which was discussed in Ch. 2, a heavy impurity climbs metastable branches until it reaches a branch termination point or undergoes a random tunneling event, both leading to an abrupt change in velocity and an energy loss. This is predicted to lead to a non-analytic dependence of the impurity drift velocity on small forces.

As with the case of light impurities, such drift is superimposed with oscillations of the velocity. In this case, however, the oscillations result not from the gradual change of the impurity effective mass from positive to negative but instead come from abrupt backscattering events associated with the presence of the metastable branches (which may have strictly positive effective mass). Such events occur with a certain frequency dictated by the external force, which is a consequence of the periodicity of the impurity dispersion. We remind that this ultimately stems from the fact that integer multiples of $2\pi n$ can be transferred to the gas at no energy cost in the thermodynamic limit.

The same picture of momentum transfered to the fluid at no energy cost leads to the prediction of vanishing Landau critical velocity in 1D [65, 66]. It was shown that an *infinitely massive* object moving with any nonzero velocity with respect to the

background nucleates phase slips corresponding to one quantum $2\pi n$ of total momentum transferred to the fluid. The finite rate of this process can then be related to the energy and momentum dissipation in the liquid, precluding superfluidity. On the other hand, a mobile impurity with *finite mass* M can propagate without dissipation at zero temperature with velocity given by slope of the dispersion $V = \partial E/\partial P$. Hence, the maximum slope of the dispersion defines a non-zero critical velocity for light mobile impurities.

The main result of this Chapter is the prediction that the above regimes of heavy and light impurities are separated by a quantum phase transition taking place at a critical mass $M_{\rm c}$, given by Eq. (3.3). We show that above the critical mass the many-body ground state in a total momentum sector P has cusps at $P = \pm\pi n, \pm 3\pi n, \ldots$, while the impurity dispersion develops a swallowtail structure with metastable branches shown in Fig. 3.1. In this case the true *thermodynamic* critical velocity $\mathcal{V}_{\rm c}$, given by the maximal slope of the many-body ground state, should be distinguished from the *dynamic* critical velocity $V_{\rm c}$ obtained from the maximal slope of the metastable branch. It can be shown that for $M \gg M_c$ the thermodynamic critical velocity is inversely proportional to M consistent with the infinite mass limit of Refs. [65, 66].

3.1 Metastability and two definitions of critical velocity

For a concrete example of how a metastable impurity dispersion can arise, let us take our fluid to be a weakly interacting Bose gas. At the mean field level, appropriate for weak interactions, the condensate wavefunction develops a phase drop Φ across the impurity located at X. In the limit of strong coupling between gas and impurity, the latter gives rise to the Josephson term

$$H_{\rm d}(\Phi) = -nV_{\rm c}\cos\Phi \tag{3.1}$$

in the impurity energy. Here $V_{\rm c}$ is the dynamical critical velocity which depends on the strength of the impurity-host coupling. The phase drop inevitably creates a background supercurrent contributing a term $n\Phi$ to the *total* momentum P. The total energy of the impurity and the background can then be written as

$$H(P,\Phi) = \frac{1}{2\mathcal{M}}(P - n\Phi)^2 + H_{\rm d}(\Phi) \tag{3.2}$$

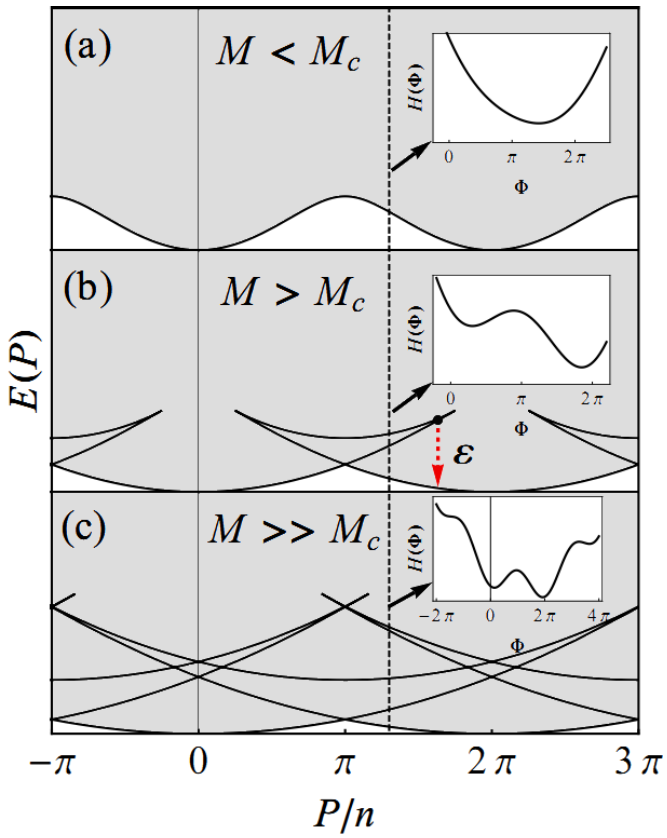

Figure 3.1: Dispersion law for an impurity in a 1D quantum fluid for various impurity masses. **(a)** $M < M_c$, $E(P)$ is a smooth function of P and H (inset, Eq. (3.2)) has a single minimum. **(b)** $M \gtrsim M_c$, there exists a metastable minimum. An impurity driven by a force climbs a metastable branch until tunneling or H loses its minimum. Each cycle releases energy ε to the system. **(c)** $M \gg M_c$, many minima co-exist.

The first term is the kinetic energy of the impurity moving with velocity $V = (P - n\Phi)/\mathcal{M}$, where $\mathcal{M}$ is the total mass of the impurity and induced depletion cloud. As we shall see one can assume $\mathcal{M} \simeq M$ for a sufficiently heavy impurity.

As explained in Ch. 2, the phase drop Φ represents a collective coordinate characterizing the state of the impurity equilibrated with the background. Its value is determined from the requirement of the minimum of the total energy (3.2) leading to the matching $P - n\Phi = MV_c \sin\Phi$ of the Josephson current $nV_c \sin\Phi$ to the current nV experienced by the impurity in its rest frame. For sufficiently large mass $M > M_c$ this equation has

several solutions corresponding to different arrangements of the impurity and the background. The total energy $H(P,\Phi)$ in Eq. (3.2) can therefore have minima for several values of the phase drop Φ for a given value of the total momentum P. Plotting the corresponding energies results in a typical swallowtail structure for the dispersion, see Fig. 3.1.

Following the global minimum $E_-(P)$ of the dispersion one sees that it develops cusps at the crossing points $P = \pm\pi n, \pm 3\pi n, \ldots$ corresponding to a first order transition as a function of the total momentum P. In addition to the true ground state $E_-(P)$ there is also a metastable branch $E_+(P)$ corresponding to local a minimum. The minima corresponding to $E_-(P)$ and $E_+(P)$ are separated by a maximum. At the termination points P_t the maximum merges with the local minimum at $\Phi = \Phi_\mathrm{t}$ and the metastable branch ceases to exist. The critical mass M_c for the swallowtail catastrophe can be estimated from the simple model Eq. (3.2) as

$$M_\mathrm{c} = \pi n/V_\mathrm{c} = Km(c/V_\mathrm{c}). \tag{3.3}$$

For a strongly repulsive impurity in a weakly interacting background $M_c \gg m$ since $K \gg 1$ and $c \gg V_\mathrm{c}$, justifying *a posteriori* the assumption $\mathcal{M} \simeq M$.

For $M \gg M_\mathrm{c}$ the termination point corresponds to $\sin\Phi_\mathrm{t} = \pm 1$ and the mass-independent velocity $\partial E_+/\partial P = \pm V_\mathrm{c}$. In contrast, the thermodynamic critical velocity, defined with the help of the stable branch $\mathcal{V}_\mathrm{c} = \partial E_-/\partial P$, behaves as $1/M$ resulting in zero critical velocity for infinitely heavy impurity [65, 66].

Quantum fluctuations can smear the transition by producing a mechanism for the decay of the metastable branch [36]. The metastable branch $E_+(P)$ is well defined as long as the decay rate $\Gamma(P)$ to the lower branch satisfies $\Gamma(P) \ll E_+(P) - E_-(P) \approx 2\mathcal{V}_\mathrm{c}|P - \pi n|$. We show below that $\Gamma(P)$ vanishes as a power law near the crossing points, $\Gamma(P) \propto |P - \pi n|^\alpha$ for $P \to \pi n$ with the exponent α given in Eq. (3.11). Self-consistency therefore requires $\alpha > 1$. Hence $\alpha = 1$ is the condition defining the transition between the two classes of dispersion curves, and corresponds to $M = M_c$ [36].

3.2 Heavy Impurity in a Weakly Interacting Bose Gas

The qualitative features discussed in the previous Section in no way depend upon the specific model Eq. (3.1). In this section we demonstrate that they occur generally in the

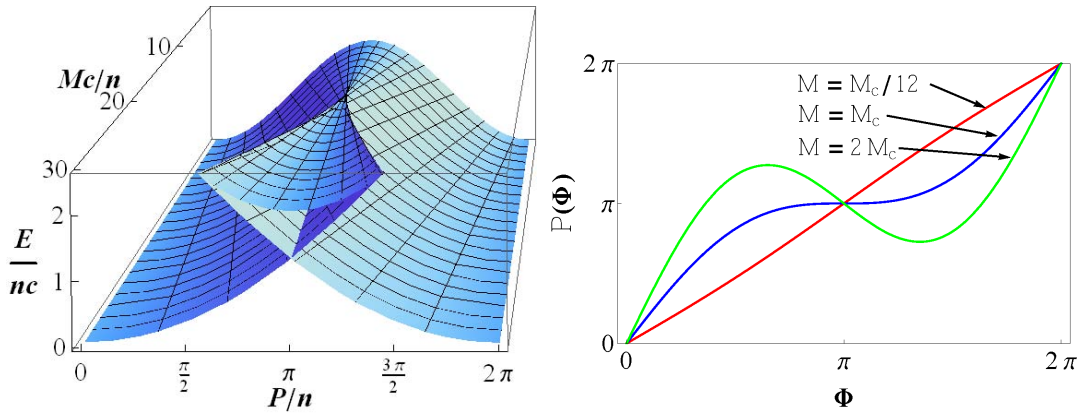

Figure 3.2: Top Panel: Variation of the impurity dispersion across the $M = M_c$ transition, exhibiting the swallowtail catastrophe. Here $V_c/c = 0.1$, $K = 10\pi$ and $M_c = 12n/c$ (see Eq. (3.5)). Bottom panel: Momentum $P(\Phi)$ for different masses, see Eq. (3.4). For $M > M_c$ there persists two extrema which merge and disappear at $M = M_c$.

dispersion relation of a particle moving in a Bose gas described by the Gross–Pitaevskii equation valid for arbitrary coupling between the gas and impurity, see Appendix A for details on how this model is solved.

To allow ourselves the generality of discussing a wide range of impurity masses, and for simplicity of illustration, we momentarily focus on the regime of strong coupling $G \gg c$. According to the results of Appendix A, we may determine the dependence of z and Φ_s on Φ to leading order in c/G. From Eqs. (A.15), (A.16) we find $z(\Phi) \simeq \frac{c}{G}\cos^2\frac{\Phi}{2}$ and $\Phi_s(\Phi) \simeq \pi - \frac{c}{G}\sin\Phi$ and hence,

$$P = n\Phi + \left(M - \frac{2n}{c}\right) V_c \sin\Phi. \tag{3.4}$$

Here the critical velocity is given by $V_c = \frac{c^2}{2G} \ll c$ [49, 60], and the Φ dependence of the velocity acquires the Josephson form: $V(\Phi) = V_c\sin\Phi$. The appearance of the critical mass occurs when $P = P(\Phi)$ is satisfied by multiple values of $\Phi(P)$. The functional form of $P(\Phi)$ for $M > M_c$ takes an "$\mathcal{N}$" shape, implying the existence of two extrema in the range $\Phi \in (0, 2\pi)$, see Fig. 3.2. As M crosses M_c from above, these extrema merge and disappear at $P = n\Phi = \pi n$. This observation allows to derive the critical mass within the above framework,

$$\left.\frac{\partial P}{\partial \Phi}\right|_{\Phi=\pi} = 0 \implies M_c = \frac{2n}{c}\left(1 + \frac{G}{c}\right) \approx \frac{mK}{\pi}\frac{c}{V_c}, \tag{3.5}$$

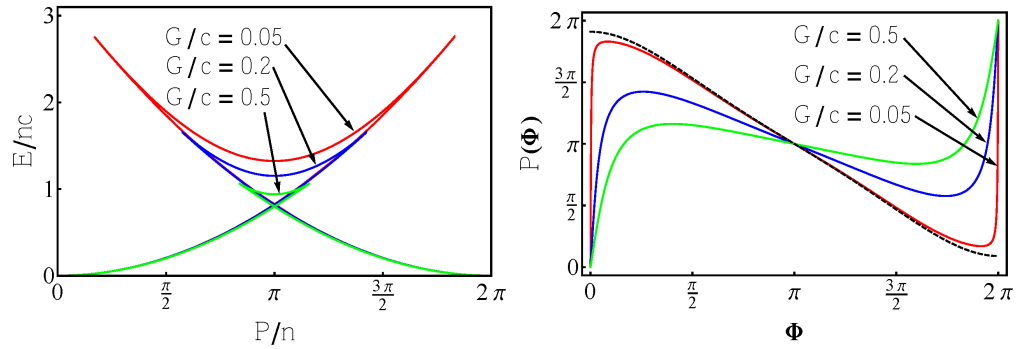

Figure 3.3: Top panel: Impurity dispersion at weak coupling with parameters $M/m = 60$, $K = 10\pi$, $G/c = 0.5$ (green), $G/c = 0.2$ (blue) and $G/c = 0.05$ (red). Bottom panel: Momentum P as a function of Φ having the same parameters listed above. The $G \to 0$ limit is well approximated by the gray soliton configuration (dashed): $P = n(\Phi - \sin\Phi) + Mc\cos\frac{\Phi}{2}$, except near $\Phi = 2\pi j$ for integer j, where the momentum is necessarily given by $P = 2\pi nj$.

in agreement with the parametric dependence Eq. (3.3).

The case of weak impurity coupling does not lend itself to convenient analytical analysis. For given $G/c < 1$, we thus solve the boundary Eqs. (A.15), (A.16) numerically to produce the dispersion law $E(P)$, see Fig. 3.3. For comparison to the strong coupling case, we also plot $P(\Phi)$ for various couplings $G/c < 1$. In the limit $G \to 0$, the impurity is dressed by an essentially unperturbed gray soliton (*i.e.*, the two solitons of Fig. A.1 are separated by a very small distance). This approximation breaks down near $\Phi = 2\pi j$ for integer j since we must have $P = 2\pi nj$. Consequently, there is a sharp deviation from the soliton configuration (dashed line in Fig. 3.3) near these points, making the functional form of $P(\Phi)$ difficult to characterize analytically. As a result of the numerical analysis, we see that even in the regime of weak coupling the appearance of multiple momenta extrema give rise to the observed swallowtail catastrophe of the energy dispersion and is thus not restricted to the Josephson limit.

3.3 Decay of the Metastable Branch

We now briefly recapitulate the framework developed in Ch. 2, which we shall use to describe the metastable branch and its decay in the general case. The moving depleton,

i.e. impurity dressed by the liquid depletion, is characterized by a number of particles N expelled from its core in addition to the phase drop Φ. The depleton's dynamics is specified by the following Hamiltonian

$$H(P,\Phi,N)=\frac{1}{2\mathcal{M}}(P-n\Phi)^2+\mu N+H_{\rm d}(\Phi,N). \tag{3.6}$$

Here $H_{\rm d}$ is the Φ-periodic energy function of the depletion cloud, μ is the chemical potential of the liquid in the absence of the impurity and $\mathcal{M}=M-mN$. In the limit of strongly repulsive impurity the dynamics of N is frozen and $H_{\rm d}(\Phi,N)$ reduces to the simple Josephson form Eq. (3.1). If the mass $\mathcal{M}$ is sufficiently large, the Hamiltonian (3.6) (being almost a periodic energy function of Φ) possesses many metastable minima in addition to the absolute one.

We wish to determine the tunneling rate from the above mentioned metastable minima to the ground state branch at the same momentum P. Such tunneling is accompanied by a change in the phase drop $\Delta\Phi$ and number of depleted particles ΔN, despite the momentum of both states being equal. Therefore one must know the Lagrangian governing the dynamics of the collective variables Φ and N. As shown in Ch. 2 the effective action governing the phonons is given by

$$S_{\rm ph}=\frac{1}{\pi}\int {\rm dtdx}\left[-\partial_x\vartheta\partial_t\varphi-\frac{c}{2K}(\partial_x\vartheta)^2-\frac{cK}{2}(\partial_x\varphi)^2\right], \tag{3.7}$$

while their coupling to the depleton degrees of freedom takes a universal form,

$$S_{\rm int}=\int {\rm d}t\left[-\dot{\Phi}\ \vartheta(X,t)/\pi-\dot{N}\varphi(X,t)\right]. \tag{3.8}$$

It is the phonon subsystem which must supply the macroscopic momentum $n\Delta\Phi$ and take away ΔN particles from the depleton. Near the point $P=\pi n$, the phonons have only a small amount of energy ε with which to do this. This low-probability event, or 'under-the-barrier' evolution of the phononic system, can be described in imaginary time by performing the Wick rotation $t\to -i\tau$ in Eqs. (3.7), (3.8).

The tunneling rate $\Gamma(\bar{\tau})$ is given by the exponentiated action $S(\bar{\tau})$ evaluated on the trajectory where the system tunnels for an imaginary time $\bar{\tau}$ from one minimum to the other. For $\alpha>1$ where tunneling is an irrelevant perturbation, we may safely neglect higher order processes involving tunneling back and forth between the minima and focus on the single tunneling event. Starting from Eqs. (3.7), (3.8) (after the Wick rotation

$t \to -i\tau$) one integrates the imaginary time Luttinger liquid action with linear coupling to arrive at the tunneling action

$$S(\bar{\tau}) = -\frac{1}{2}\int \mathrm{d}x\mathrm{d}x'\mathrm{d}\tau\mathrm{d}\tau' \vec{J}^{\dagger}_{x,\tau}(\bar{\tau})\hat{D}(x-x',\tau-\tau')\vec{J}_{x',\tau'}(\bar{\tau}) \tag{3.9}$$

where $\vec{J}^{\dagger}_{x,\tau}(\bar{\tau}) = \delta(x-X(\tau))(\dot{\Phi},\dot{N}) = \delta(x-X(\tau))[\delta(\tau)-\delta(\tau-\bar{\tau})](\Delta\Phi,\Delta N)$ describes the tunneling trajectory between minima having configurations which differ in phase by $\Delta\Phi$ and number of expelled particles ΔN and $\hat{D}(x,\tau)$ is the matrix imaginary time phononic propagator. The latter is determined by inverting the matrix operator of the quadratic Luttinger liquid action in the form $S_{\mathrm{LL}} = -\frac{1}{2}\int \mathrm{d}x\mathrm{d}\tau \vec{\chi}^{\dagger}\hat{D}^{-1}\vec{\chi}$, where $\vec{\chi}^{\dagger} = (\vartheta/\pi,\varphi)$.

Substituting the above tunneling trajectories into Eq. (3.9) with the imaginary time propagator

$$\hat{D}(x,\tau) = \frac{1}{4\pi}\begin{bmatrix} \frac{K}{\pi}\ln\left(\frac{c^2\tau^2+x^2}{l^2}\right) & \ln\left(\frac{c\tau-ix}{c\tau+ix}\right) \\ \ln\left(\frac{c\tau-ix}{c\tau+ix}\right) & \frac{\pi}{K}\ln\left(\frac{c^2\tau^2+x^2}{l^2}\right) \end{bmatrix}, \tag{3.10}$$

we find $S(\bar{\tau}) = (1+\alpha)\ln(c\bar{\tau}/l)$ where $l \gtrsim (mc)^{-1}$ is a short distance cut-off beyond which the point-particle description of the depleton breaks down and $\alpha = 2K\left[\left(\frac{\Delta\Phi}{2\pi}\right)^2 + \left(\frac{\Delta N}{2K}\right)^2\right] - 1$. The X dependence of the action is neglected because it enters as $X(\tau) - X(\tau') \approx V(\tau-\tau') \ll c(\tau-\tau')$.

The energy-dependent tunneling rate is found with the help of the Fourier transformation, $\Gamma(\varepsilon) \sim \int \mathrm{d}t e^{-S(it)}e^{i\varepsilon t}$, where the analytical continuation to real energy $i\varepsilon \to \varepsilon$ is accompanied by the Wick rotation $\tau \to it$. Substituting $S(\tau)$ given above and using the identity $\int \mathrm{d}t e^{i\varepsilon t}(it)^{-(1+\alpha)} = \frac{2\pi\Theta(\varepsilon)}{\Gamma(1+\alpha)}\varepsilon^{\alpha}$, we find for the tunneling rate

$$\Gamma(\varepsilon) \sim \varepsilon^{\alpha};\ \alpha = 2K\left[\left(\frac{\Delta\Phi}{2\pi}\right)^2 + \left(\frac{\Delta N}{2K}\right)^2\right] - 1. \tag{3.11}$$

Writing $\varepsilon = 2\mathcal{V}_{\mathrm{c}}|P-\pi n|$ gives the momentum dependent tunneling rate advertised earlier.

It is worth noticing that the preceding discussion of tunneling from the metastable branch actually sets the stage for a much broader discussion of tunneling probabilities in 1d quantum liquids. While a comprehensive review of this subject lies outside the scope of this dissertation (see [40] for a recent review), it is nevertheless instructive to see how the main features of the response functions emerge within the depleton theory. Moreover, our construction based on the collective coordinates N, Φ lends a

certain intuition which may be less transparent in other approaches. We include a brief discussion of these aspects in Appendix B.4.

The logarithmic behavior of the tunneling action is valid only on the long time-scale $\tau \gtrsim l/c$, implying the validity of Eq. (3.11) is restricted to the regime of small ε close to $P = \pi n$. In such a case the velocities of the upper and lower branches of the dispersion are essentially opposite and close to $\pm\mathcal{V}_{\rm c}$, while the change in number of particles ΔN, being an even function of velocity, is negligible. As a result one arrives at the exponent $\alpha = 2K(\Delta\Phi/2\pi)^2 - 1$. This single collective coordinate limit, *i.e.* $\Delta N = 0$, agrees with the previous result of Ref. [67] (cf. Eq. (7.20) therein) based on a phenomenological model of tunneling between two minima in the presence of coupling to an environment. Their results also show that a finite temperature T acts as a low energy cut-off, namely $\Gamma \sim T^\alpha$, $\varepsilon \ll T$ (see Eqs. (5.30), (7.18) of Ref. [67]).

Higher order processes involve tunneling back and forth between the two minima that become degenerate for $\varepsilon = 0$, leading to an effective spin-boson or anisotropic Kondo description [36]. The inclusion of such processes is only necessary if $\alpha < 1$, meaning that tunneling is a relevant perturbation. This leads to the rounding out of the cusp in the dispersion $E_-(P)$ at $P = \pi n$, and the disappearance of the metastable branch. Thus $\alpha = 1$ is the exact condition determining the critical mass $M = M_c$. Note that at criticality we have $1/\sqrt{K} = \Delta\Phi/2\pi < 1$. Hence, the transition is possible only if $K > 1$, in agreement with Ref. [36]. The marginal case when $K = 1$, $\Delta\Phi = 2\pi$ occurs when $M \to \infty$, as we now discuss.

In the infinite mass limit with fixed velocity $V = P/M$ Eq. (3.6) becomes essentially a washboard potential, Fig. 3.1c, $H \underset{M\to\infty}{\longrightarrow} nV\Phi + H_{\rm d}(\Phi)$ (change ΔN between adjacent minima goes to zero in this limit). Thus the change $\Delta\Phi$ between the adjacent minima is exactly 2π, while the energy difference is $\varepsilon = 2\pi nV$. As a result, one finds $\alpha = 2K - 1$ and the power law dependence of the tunneling rate $\Gamma \sim V^{2K-1}$ on the velocity in full agreement with the result of Ref. [65, 66].

In the limit of large energy detuning, *i.e.*, away from $P = \pi n$, the tunneling rate does not take the form (3.11). In this region the barrier is small and the impurity emerges from under it with only slightly less energy, despite the large detuning between the branches (see Fig. 3.1 insets). Therefore most of the descent from the upper branch corresponds to viscous relaxation in real time and not an under-the-barrier tunneling

trajectory. Thus, near the termination momentum $P_{\rm t} \simeq MV_{\rm c}$, the potential may be approximated by a cubic polynomial. The dissipative tunneling through such a potential was described in Ref. [52], leading to the escape rate $\Gamma \propto e^{-\bar{S}}$, where

$$\bar{S} = 2K \frac{P_{\rm t} - P}{\sqrt{M^2 V_{\rm c}^2 - n^2}}. \tag{3.12}$$

We see that for both large and small energy detuning, Eqs. (3.11), (3.12) the tunneling action scales with the Luttinger parameter K.

3.4 Dynamics in the Presence of an External Force

One way to explore the metastable branches of the dispersion is by applying an external force F to the impurity and studying the ensuing dynamics. For sufficiently strong force the driven impurity overshoots the ground state branch and follows the metastable branch until it either tunnels or reaches the termination point $P_{\rm t}$ (see Fig. 3.1). The energy dissipated per cycle, ε, must be supplied by external force: $FV_{\rm D} = \varepsilon/\tau_{\rm B}$ resulting in the drift velocity $V_{\rm D} = \varepsilon/2\pi n$.

Tunneling is negligible when $\Gamma\tau_{\rm B} \ll 1$, which occurs if the force is sufficiently large. In such a case the external force drives the impurity all the way up to the termination point $P_{\rm t}$. It then loses the energy minimum and relaxes to the lower branch, emitting phonons. As a result, the energy dissipated per cycle and thus drift velocity are essentially independent of the applied force. This is in stark contrast to the case of $M < M_c$, where the phonon emission due to dipole radiation gives rise to a linear in F drift velocity and hence a *finite* impurity mobility $\sigma = V_{\rm D}/F$, see Ch. 2.

The impurity velocity takes the form of a saw-tooth trajectory, experiencing a slow build-up and a sudden drop when the velocity reaches $V_{\rm c}$, see Fig. 3.4. As a function of the mass, $V_{\rm D}$ saturates to the critical velocity in the limit $M \to \infty$. This is most easily seen by noting that in such a limit the energy drop occurs between two adjacent and essentially parallel parabolas: $\varepsilon = 2\pi n V_{\rm D} = P^2/2M - (P - 2\pi n)^2/2M \to 2\pi n V_{\rm c}$. On the same grounds, the amplitude of the saw-tooth oscillations is a decreasing function of M going to zero in the infinite mass limit.

Quantum effects become dominant only if the time spent on a metastable branch is

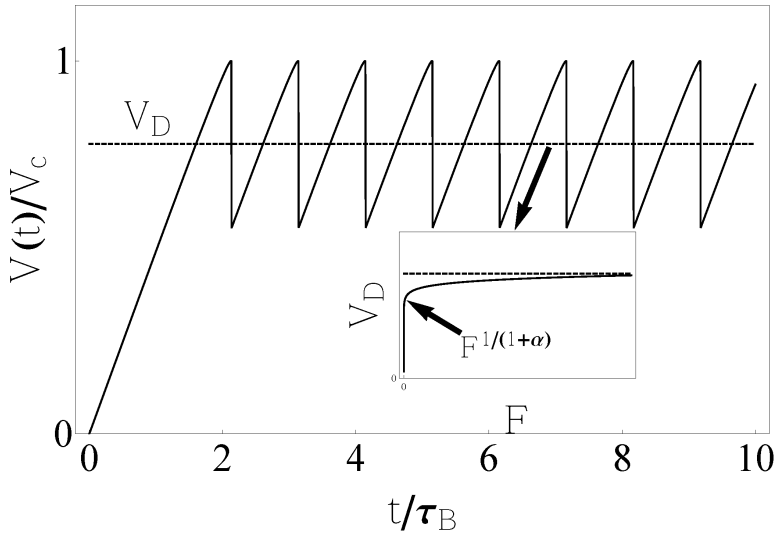

Figure 3.4: Impurity velocity (solid) in units of the dynamic critical velocity $V_{\rm c}$ as a function of time in units of the period $\tau_{\rm B} = 2\pi n/F$. The drift velocity is denoted by $V_{\rm D}$ (dashed) and is displayed in the inset as a function of the applied force. Due to quantum tunneling near $P = \pi n$, the drift velocity goes to zero as a power law with exponent $1/(\alpha+1)$ (solid, inset) given by Eq. (3.15) for $F < F_{\rm c}$ and approaches the semi-classical result for $F > F_{\rm c}$ (dashed, inset).

comparable with the inverse tunneling rate: $\Gamma\tau_{\rm B} \gtrsim 1$. Thus, the effect of quantum tunneling plays a role only for very small forces. In this limit, the impurity is likely to tunnel at a momentum immediately above $P = \pi n$, right when it enters the metastable branch. The probability to tunnel per unit time is given by $\dot{\mathcal{P}}(t) = \Gamma(t)\mathrm{Exp}\left[-\int_0^t dt'\Gamma(t')\right]$, which follows from the assumption that the process is Markovian. By parameterizing the average over time by an average over momenta one finds

$$\langle\varepsilon\rangle = \int_{n\pi}^{P_t} dP\varepsilon(P)\frac{\Gamma(P)}{F}\mathrm{Exp}\left[-\int_{n\pi}^{P}dP'\frac{\Gamma(P')}{F}\right] \tag{3.13}$$

$$= \int_0^{F_\pi/F} dx\varepsilon(P(x))e^{-x}. \tag{3.14}$$

Here we introduced the dimensionless variable $x(P) = \int_{n\pi}^{P} dP'\Gamma(P')/F$ along with $F_\pi = \int_{n\pi}^{P_t} dP'\Gamma(P')$. Due to the exponential decay of the kernel in Eq. (3.13), the integral is cut at $x_c = \min\{1, F_\pi/F\}$. As a result, one obtains the approximation $\langle\varepsilon\rangle \sim x_c\varepsilon(P_c)$, where P_c satisfies $x_c = \int_{n\pi}^{P_c} dP\Gamma(P)/F$. For $F \ll F_\pi$, we have $x_c = 1$ and hence P_c may

be solved by writing $P_c = n\pi + \delta P$ for small, yet undetermined, δP. Expanding Γ near $n\pi$ as $\Gamma = \Gamma_\pi[(P - n\pi)\mathcal{V}_c/mc^2]^\alpha$, we find $\delta P = \frac{mc^2}{\mathcal{V}_c}(F/F_c)^{\frac{1}{1+\alpha}}$ and $F_c = \frac{\Gamma_\pi mc^2}{\mathcal{V}_c(1+\alpha)} \approx \frac{\Gamma_\pi Mc}{2K^2}$ for large M. Thus,

$$\langle \varepsilon \rangle = mc^2 \left(\frac{F}{F_c}\right)^{\frac{1}{1+\alpha}} \implies V_{\rm D} = \frac{c}{K}\left(\frac{F}{F_c}\right)^{\frac{1}{1+\alpha}}. \tag{3.15}$$

The non-analytic dependence of the drift on small forces is the result of the cusp of the ground state energy at $P = \pi n$ and implies the divergence of the mobility $\sigma = V_{\rm D}/F$ as $F \to 0$ across the $M = M_c$ transition (see inset of Fig. 3.4). At finite temperature T the mobility is *not* given by $\sigma \sim T^{-\alpha}$ as might be expected due to the finite tunneling rate $\Gamma \sim T^\alpha$ near the cusp. Strictly speaking, it is given by $\sigma \sim T^{-4}$ due to two-phonon thermal Raman scattering [23, 25] which results in velocity saturation *below* $\mathcal{V}_{\rm c}$ as $F \to 0$. In practice, therefore, it is necessary to work at sufficiently low temperatures and finite drives to overcome such saturation and allow the impurity to explore the full range of momentum where metastable branches become important.

In conclusion, we have shown that the dispersion relation of a mobile impurity undergoes a sudden change when the mass of the impurity exceeds a certain critical value. The latter depends on the interaction parameter within the host liquid and thus may be varied experimentally. The predicted transition can be probed by applying an external force and monitoring either impurity velocity or excitations of the host liquid. The change of dispersion also affects the oscillation frequency and dissipation of the impurity in the trapping potential. With investigations of impurity motion in 1D atomic gases now underway, we hope that these predictions will guide future experiments.

Chapter 4

Casimir Interaction between Impurities

In this Chapter we move beyond the single impurity limit to discuss inter-impurity correlation effects induced by the quantum liquid. We show that virtual phonons scatter off impurities and mediate a long-range interaction, analogous to the Casimir effect. In one dimension the effect is universal and the induced interaction decays as $1/r^3$, much slower than the van der Waals interaction $\sim 1/r^6$, where r is the impurity separation. The sign of the effect is characterized by the product of impurity-phonon back-scattering amplitudes, introduced in Ch. 2, which take a universal form and have been seen to vanish for several integrable impurity models. Thus, if the impurity parameters can be independently tuned to lie on opposite sides of such integrable points, one can observe an attractive interaction turned into a repulsive one. We derive semiclassical equations of motion for the impurities which show that the Casimir interaction is the real part of the total induced interaction. The existence of the imaginary part can be understood via the Kramers-Kronigs relation and is responsible for a *correlated* friction. This effect can lead to an enhancement or suppression of the center of mass damping, depending on the relative separation of the impurities.

4.1 Qualitative Aspects of the Casimir Interaction

The concept of zero-point energy has fascinated minds ever since the inception of quantum mechanics. Beyond being merely an inconsequential redefinition of the ground state energy, it was shown by Casimir [68] that *changes* in the zero-point energy can lead to observable forces between uncharged conducting plates. Although usually discussed in the context of quantized electromagnetic fields, zero-point fluctuations of essentially *any* medium with long-range correlations induces long-range interactions between perturbing objects that modify the spectrum of fluctuations [69]. In 1d, the low-lying excitations are quantized sound modes whose gapless nature is expected to give rise to a long-range interaction. As we show, impurities immersed in an *interacting* cold atom environment experience such an interaction due to scattering of virtual phonons, the same mechanism lying at the heart of the analogous photon-induced Casimir effect. In addition, the cold-atom analog of the interaction has the advantage of being continuously tunable both in magnitude and in *sign*, a task which is hardly achievable in a linear electromagnetic medium [70].

In most studies of Casimir interactions the analysis is restricted to *static* configurations of objects or bounding surfaces. The impurities in quantum liquids are typically free to propagate under the influence of the induced interactions. Therefore they must be regarded as *mobile*, and in certain circumstances should be distinguished from their static counterparts characterized by infinite effective mass. As we discuss below, for a system of repulsively interacting fermions in 1d this leads to a *qualitatively* different asymptotic behavior of the induced interaction between impurities.

Using an effective low-energy theory, we find a Casimir interaction between mobile impurities in a 1d quantum liquid given by

$$U_{\rm Cas}(r) = -mc^2 \frac{\Gamma_1 \Gamma_2}{32\pi} \frac{\xi^3}{r^3}, \tag{4.1}$$

where the dimensionless parameters $\Gamma_{1,2}$ are related to the impurity-phonon backscattering amplitudes[1] introduced in Ch. 2 and discussed in detail below.

Owing to the enhanced role of fluctuations in 1d, the Casimir interaction exhibits a decay law $\sim 1/r^3$ which is much slower than the van der Waals interaction between

[1] For convenience we have defined $\Gamma = m(c^2 - V^2)\Gamma_{+-}$, see Appendix B.3.1

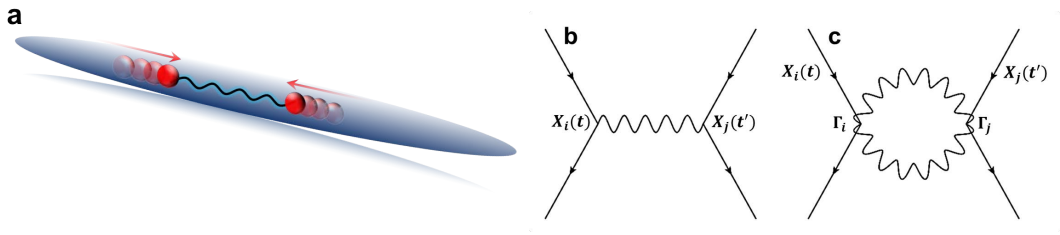

Figure 4.1: Casimir interaction between mobile impurities in a quantum liquid. **a**. Schematic depiction of two impurities experiencing an induced Casimir attraction mediated by phonon fluctuations of a one-dimensional quantum liquid. **b**. Single-phonon exchange (wavy line) leading to a spatially local inter-impurity interaction (impurities i, j are denoted by straight lines with coordinates $X_{i,j}$). **c**. Two-phonon exchange responsible for the long-range Casimir interaction between impurities (see Eqs. (4.9), (4.10) for the corresponding Lagrangian).

neutral atoms $U_{\rm vdW}(r) \sim 1/r^6$ [71]. As shown in Ch. 2, we also find that Γ acquires a universal form in terms of independently measurable thermodynamic characteristics. At special points in parameter space where the underlying model becomes integrable, the thermodynamics can be extracted exactly, thus yielding the back-scattering amplitude, which has been seen to vanish identically in several of these special cases, $\Gamma = 0$ [25, 26, 29, 30]. This has important implications for spinor condensates, which lie close to the integrable $SU(2)$ symmetric point, for which particles in different hyperfine states have equal masses and nearly equal interaction constants. It opens the possibility of observing an attractive interaction turned into a repulsive one when the impurity parameters are independently tuned to lie on opposite sides of the integrable point.

Our results should be contrasted with the works of [43, 72, 73] who considered the limit of infinitely heavy impurities embedded in a 1d quantum liquid. They concluded that (a) repulsively interacting fermions mediate an interaction whose smooth component [74] scales as $1/r$ and (b) repulsively interacting bosons (or attractively interacting fermions) do not mediate a smooth long-range interaction. In the case of *mobile* impurities we find that the induced interaction is different from (a) & (b) and is instead given by Eq. (4.1). Moreover, even *static* impurities in repulsively interacting bosonic liquids are subject to induced interactions of the form given by Eq. (4.1), in contradiction with (b).

Conclusions (a) & (b) were reached by appealing to the scaling theory of the effective

impurity strength [61]. The latter shows a non-trivial energy dependence in the presence of a quantum liquid due to its non-linear (*i.e.,* interacting) nature. The physics behind this is that, in addition to direct scattering off the impurity, excitations of the liquid may also scatter indirectly off the local density distortion induced by the impurity. This mechanism gives rise to a renormalization of the low-energy effective impurity strength: for a system of repulsively interacting fermions the impurity is renormalized into a perfectly reflecting barrier [61], while for bosons the impurity instead becomes perfectly transparent (hence (b)).

However the Casimir effect comes *not* from the ultimate low-energy impurity strength, but rather relies on the participation of an *energy band* of quantum fluctuations, whose width is set by c/r. As a result, there is a long-range Casimir force even in the case where the impurity strength renormalizes towards zero. Moreover such a flow towards zero impurity strength is a universal feature of mobile impurities in any environment, both bosonic and fermonic. This is because at energy scales below the recoil energy $E_{\rm R} \sim k_{\rm F}^2/M$ the impurity essentially decouples from (super-flows in) the host liquid [23]. This renders broad universality of our result – Eq. (4.1) (the only exception being infinite mass objects in repulsive fermonic environment, interacting with $1/r$ potential, [43, 72]).

4.2 Effective Low-Energy Model

We now develop the effective model leading to Eq. (4.1). Our approach, although fully equivalent to the depleton framework of Ch. 2, takes a slightly more direct route to the desired result and is more convenient in the absence of an external force. It effectively amounts to integrating out small fluctuations of the collective coordinates N, Φ to arrive at a theory in terms of P, X alone.

In the absence of excitations, a system of impurities in a quantum liquid can be described by the Lagrangian $L_{\rm imp} = \sum_j [P_j \dot{X}_j - E_j(P_j, n)]$, where X_j, P_j are impurity coordinates and momenta, respectively, and E_j are the exact single-impurity periodic dispersion relations.

As discussed in Ch. 2, the relevant low-energy excitations of the quantum liquid are

phonons whose dynamics are encoded in the phonon Lagrangian,

$$L_{\rm ph} = -\int_x \left[\rho\partial_t\varphi + \frac{n+\rho}{2m}(\partial_x\varphi)^2 + \frac{mc^2}{2n}\rho^2 + \frac{\alpha}{3!}\rho^3\right] \tag{4.2}$$

The quadratic (Luttinger liquid) part of the Lagrangian describes a linearly dispersing hydrodynamic mode, $\omega(q) = c|q|$. The cubic non-linear terms $\rho(\partial_x\phi)^2$ and ρ^3 are retained, as they turn out to be essential in deriving the correct impurity-phonon back-scattering amplitude Γ [25, 26, 30].

The impurity-phonon coupling can then be derived by employing a "weak-coupling" expansion in phonon amplitude [23]. This description is valid at low energies where the impurity becomes essentially transparent. The expansion may be achieved by noting [22, 25, 26, 30] that an impurity in the presence of a long wavelength phonon sees an essentially *global* modification of the density $n + \rho(X)$ and supercurrent $u(X)$. One thus concludes that in the frame moving with velocity $u(X)$, the impurity energy is $E(P - Mu(X), n + \rho(X))$. A Galilean transformation then gives laboratory interaction energy: $E_{\rm lab}(P, u, n+\rho) = E(P - Mu, n+\rho) + Pu - \frac{1}{2}Mu^2$, where the phonon fields are taken at the location of the impurity. The left-hand side describes the additional energy cost associated with exciting the liquid in the presence of the impurity, thus expressing the impurity-phonon coupling through the exact impurity dispersion relation.

To describe scattering between impurities and phonons one start from the Lagrangian $L = L_{\rm imp-ph} + L_{\rm ph}$ where

$$L_{\rm imp-ph} \;=\; \sum_j \left[P_j(\dot{X}_j - u_j) - E_j(P_j - M_j u_j, n+\rho_j) + \frac{1}{2}M_j u_j^2\right], \tag{4.3}$$

and ρ_j, u_j are phonon fields taken at the location of the $j^{\rm th}$ impurity. We now perform a canonical transformation to remove terms linear in phonon amplitude,

$$\tilde{\rho} \;=\; \rho + \sum_j N_j\delta(x - X_j), \tag{4.4}$$

$$\tilde{u} \;=\; u + \frac{1}{m}\sum_j \Phi_j\delta(x - X_j), \tag{4.5}$$

$$\tilde{P}_j \;=\; P_j - \Phi_j\tilde{\rho}_j - mN_j\tilde{u}_j. \tag{4.6}$$

Here N_j, Φ_j are yet undetermined parameters which, as we discuss below, correspond respectively to the number of depleted particles and phase drop induced by the $j^{\rm th}$

mobile impurity. Substituting Eqs. (4.4-4.6) into Eqs. (4.2), (4.3) and expanding to the second order in $\tilde{\rho}, \tilde{u}$ gives (suppressing tildes) $L = L_{\rm imp} + L_{\rm ph} + \sum_j L_{{\rm int},j} - \frac{1}{2}\sum_{i\neq j} U_{\rm loc}$, where $U_{\rm loc}$ is given below and

$$\begin{aligned} L_{{\rm int},j} &= -\left(P_j - n\Phi_j - (M_j - mN_j)\dot{X}_j\right) u_j - \left(\partial_n E_j - (mc^2/n)N_j + \Phi_j \dot{X}_j\right)\rho_j \\ &- \frac{1}{2}(\rho_j, u_j)\hat{E}_j''\begin{pmatrix} \rho_j \\ u_j \end{pmatrix}. \end{aligned} \tag{4.7}$$

One now sees that the terms linear in ρ, u can be eliminated by demanding that N_j, Φ_j satisfy the equations: $P_j = n\Phi_j + (M_j - mN_j)\dot{X}_j$, $\partial_n E_j = (mc^2/n)N_j - \Phi_j \dot{X}_j$, which appeared in Ch. 2.

The second order terms are written in terms of the Hessian matrix (suppressing index j),

$$\hat{E}'' = \begin{bmatrix} \partial_n^2(E-\mu N) + 2\Phi\partial_n V + \frac{\Phi^2}{M^*}, & -\frac{M-mN}{M^*}(\Phi + 2M^*\partial_n V) \\ -\frac{M-mN}{M^*}(\Phi + 2M^*\partial_n V), & \frac{(M-mN)(M-mN-M^*)}{M^*} \end{bmatrix}, \tag{4.8}$$

where $V(P,n) = \partial_P E(P,n)$ and $M^* = [\partial_P^2 E(P,n)]^{-1}$. Finally, after rotation to the chiral phonon basis, $\chi_\pm = \vartheta/\sqrt{\pi K} \pm \varphi\sqrt{K/\pi}$, we find

$$L_{\rm ph} = \frac{1}{2}\sum_{\beta=\pm}\int_x \left[\chi_\beta(c\partial_x^2 + \beta\partial_{x,t}^2)\chi_\beta\right]; \tag{4.9}$$

$$L_{\rm int} = \sum_j \frac{\Gamma_j}{m}\partial_x\chi_+(X_j,t)\partial_x\chi_-(X_j,t), \tag{4.10}$$

where Γ_j is the off-diagonal component of the rotated Hessian matrix and is thus identified with the back-scattering amplitude corresponding to the $j^{\rm th}$ impurity. It represents the impurity-induced scattering matrix element between right and left moving chiral phonons [76], and is discussed in more detail below.

The spatially *local* contribution to the inter-impurity potential, mediated by single-phonon exchange, is given by $U_{\rm loc}(X_i - X_j) = -c\gamma_{ij}\,\delta(X_i - X_j)$ where

$$\gamma_{ij} = \frac{\delta_{i,+}\delta_{j,+}}{2\pi}\left(1 - \frac{V_i + V_j}{2c}\right) + \frac{\delta_{i,-}\delta_{j,-}}{2\pi}\left(1 + \frac{V_i + V_j}{2c}\right). \tag{4.11}$$

Here $\frac{\delta_\pm}{\sqrt{\pi}} = -\sqrt{\frac{K}{\pi}}\Phi \mp \sqrt{\frac{\pi}{K}}N$ are the phonon scattering phase shifts induced by the mobile impurity. As shown previously in Refs. [38, 39, 40, 54], the scattering phase

shifts may be expressed in terms of the thermodynamic characteristics, *i.e.,* partial derivatives of the exact impurity dispersion relation $E(P,n)$. By solving for N and Φ above (with $\dot{X}=V$) we find

$$\frac{\delta_\pm}{\pi}=\mp\frac{1}{\sqrt{K}}\frac{1}{1\mp V/c}\left[\frac{n\partial_n E}{mc^2}\pm\frac{P-MV}{mc}\right], \tag{4.12}$$

which acquires the form presented in Refs. [38, 40, 54].

4.3 Equations of Motion: Multiple Impurities

Focusing now on the long-range component of the induced inter-impurity interaction, one may average the interaction, Eq. (4.10), over the quadratic chiral action Eq. (4.9), see Fig. (4.1) for a diagrammatic representation. This procedure gives the leading large distance, $r\gg\xi$, component of the inter-impurity interaction, *not* restricted to the regime of weak impurity coupling. It also incorporates the leading small temperature, $T\ll mc^2$, dissipative effects which are encoded in the semiclassical equations of motion,

$$\dot{P}_i=-\sum_j\partial_{X_i}U\left(\frac{\dot{X}_i+\dot{X}_j}{2},X_i-X_j\right), \tag{4.13}$$

$$U(V,X)=\frac{1}{2}\,\Gamma_i\Gamma_j\int\frac{dq}{2\pi}\,\Pi(q,qV)\,\mathrm{e}^{iqX}. \tag{4.14}$$

Here $\Pi(q,\omega)$ is the polarization operator of the phonon gas, related to the Fourier transform of the retarded response function $\theta(t)\langle[\rho^2(x,t),\rho^2(0,0)]\rangle$. The causality structure of $\Pi(q,\omega)$ allows one to express $U(V,X)$ in terms of even and odd components: $U=U_+ + U_-$. Here $U_\pm(V,-X)=\pm U_\pm(V,X)$ correspondingly depend on the real and imaginary parts of $\Pi(q,\omega)$, which in turn are connected via the Kramers-Kronigs relation $\mathrm{Re}\Pi(q,\omega)=\frac{1}{\pi}\int\frac{d\omega'}{\omega'-\omega}\mathrm{Im}\Pi(q,\omega')$. The imaginary part is given by

$$\mathrm{Im}\Pi(q,\omega)=\frac{q^2-\omega^2/c^2}{64c}\left[\coth\frac{cq+\omega}{4T}-\coth\frac{cq-\omega}{4T}\right]. \tag{4.15}$$

Restricted to the impurity trajectory, $\omega=qV$, one sees that $\mathrm{Im}\Pi(q,qV)$ is an odd function of q while the real part is an even function. From Eq. (4.14), we then

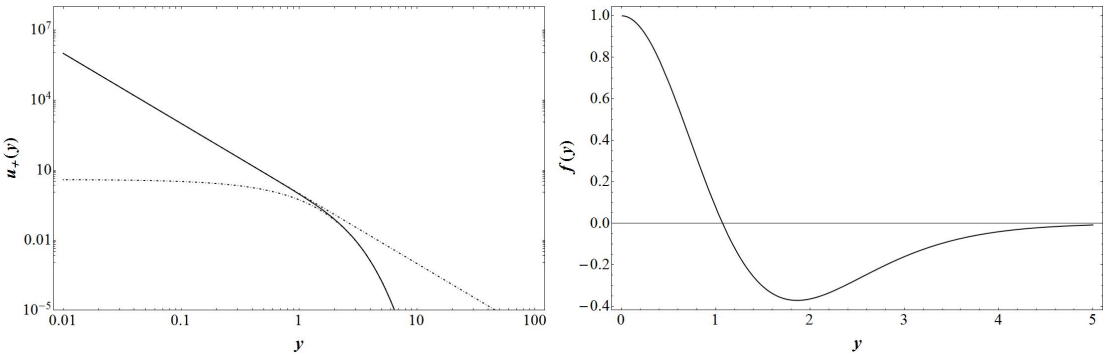

Figure 4.2: Top panel: Log-log plot of the function $u_+(y)$ (solid curve, Eq. (4.18)). It interpolates between the asymptotic limits: $u_+(y) = 1/y^3$ for $y \ll 1$ and $u_+(y) = 4\mathrm{e}^{-2y}$ for $y \gg 1$ (dashed line and curve, respectively) described by Eqs. (4.1) and (4.21). Bottom panel: Dimensionless function $f(y)$, Eq. (4.20), controlling the correlation correction to the center of mass friction, see Eqs. (4.22).

have $U_+(V,X) \propto \int_q \cos(qX)\mathrm{Re}\Pi(q,qV)$ and $U_-(V,X) \propto \int_q \sin(qX)\mathrm{Im}\Pi(q,qV)$. Using Eq. (4.15) we obtain

$$\begin{aligned} U_+(V,X) &= -mc^2\frac{\Gamma_i\Gamma_j}{64\pi}\left(1-V^2/c^2\right) \\ &\times \left[\frac{1}{1-V/c}\frac{\xi^3}{L_+^3}\frac{\cosh\frac{X}{L_+}}{\sinh^3\frac{|X|}{L_+}} + \frac{1}{1+V/c}\frac{\xi^3}{L_-^3}\frac{\cosh\frac{X}{L_-}}{\sinh^3\frac{|X|}{L_-}}\right] \end{aligned} \tag{4.16}$$

$$U_-(V,X) = -mc^2\frac{\Gamma_i\Gamma_j}{64\pi}\left(1-V^2/c^2\right)\left[\frac{\xi^3}{L_-^3}\frac{\cosh\frac{X}{L_-}}{\sinh^3\frac{X}{L_-}} - \frac{\xi^3}{L_+^3}\frac{\cosh\frac{X}{L_+}}{\sinh^3\frac{X}{L_+}}\right]. \tag{4.17}$$

Here $L_\pm = \frac{c\mp V}{2\pi T}$ are the Doppler shifted thermal lengths in the co-moving (+) and counter-propagating (−) frames. The leading order expansion in small velocity $V/c \ll 1$ is given by $U_+(0,X) = -mc^2\frac{\Gamma_i\Gamma_j}{32\pi}\frac{\xi^3}{L_T^3}u_+(X/L_T)$ and $U_-(V,X) = -mc^2\frac{\Gamma_i\Gamma_j}{120\pi}\frac{V}{c}\frac{\xi^3}{L_T^3}u_-(X/L_T)$, where

$$u_+(y) = \frac{\cosh y}{\sinh^3 y}, \tag{4.18}$$

$$u_-(y) = \frac{45}{4}\frac{y\left(\coth^2 y - \frac{1}{3}\right) - \coth y}{\sinh^2 y}. \tag{4.19}$$

The inter-impurity potential is given by $U_{\mathrm{Cas}} = U_+(0,r)$, which is related to Eq. (4.18) and interpolates between the asymptotic limits described by Eqs. (4.1) and (4.21), see

Fig. (4.2). The function $f(y)$ entering Eq. (4.22) is given by $f(y) = \partial_y u_-(y)$, see Fig. (4.2). Using Eq. (4.19), one finds

$$f(y) = 15\,\mathrm{csch}^2 y\left[1 + (1 - y\coth y)\left(1 + 3\,\mathrm{csch}^2 y\right)\right], \tag{4.20}$$

so that f changes sign at $y = r/L_T = 1.07$.

The first effect of finite temperature is that the coherent nature of virtual phonon scattering is suppressed at separations beyond the temperature length $L_T = c/2\pi T$. This results in the exponential suppression of the Casimir interaction at large distances $r > L_T$,

$$U_{\mathrm{Cas}}(r) = -mc^2\frac{\Gamma_1\Gamma_2}{8\pi}\frac{\xi^3}{L_T^3}\mathrm{e}^{-2r/L_T}. \tag{4.21}$$

The power-law scaling of Eq. (4.1), valid for $\xi < r < L_T$, is thus only meaningful deep in the quantum regime, $L_T \gg \xi$ or $T \ll mc^2$.

The second effect is that *real* excitations of the phonon background in general lead to impurity momentum relaxation, which manifests itself as damping in Eq. (4.13). This is due to two-phonon Raman scattering discussed in Ch. 2.5. It may be seen in the simplest case of two slow, $\dot{X}_j \ll c$, symmetric impurities ($\Gamma_1 = \Gamma_2 = \Gamma$) where the equations of motion can be written in compact form using center of mass coordinates,

$$\dot{p} = -\frac{\kappa}{2}\dot{r} - \frac{\partial U_{\mathrm{Cas}}(r)}{\partial r}; \quad \dot{P} = -2\kappa\dot{R}\left[1 + f(r/L_T)\right]. \tag{4.22}$$

Here $r = X_1 - X_2$, $R = \frac{1}{2}(X_1 + X_2)$, $p = \frac{1}{2}(P_1 - P_2)$, $P = P_1 + P_2$, $\dot{X}_i = \partial_{P_i}E(P_i)$ and $f(y)$ is a dimensionless function (related to U_-) with asymptotic behavior $f(y) = 1$ for $y \ll 1$ and $f(y) = -15y\mathrm{e}^{-2y}$ for $y \gg 1$ [26]. The damping coefficient κ is given by Eq. (4.23) and is discussed below.

Equation (4.22) shows that in addition to standard terms of the form $\dot{P}_i = -\kappa\dot{X}_i$, there is also a correlation correction to the center of mass damping which emerges from coherent two-phonon exchange processes. A similar effect was derived in Ref. [26] in the context of dark soliton dynamics and leads to an effective center of mass damping which depends on the relative separation: for $r \lesssim L_T$ the damping is essentially twice as strong, whereas for $r \gtrsim L_T$ ($f < 0$) it becomes slightly suppressed. Here we demonstrate that this a generic phenomena, not restricted to solitons in weakly interacting condensates.

The damping coefficient in Eq. (4.22) is given by

$$\kappa = (mc)^2 \frac{2\pi^3 \Gamma^2}{15} \left(\frac{T}{mc^2} \right)^4 . \tag{4.23}$$

The T^4 scaling of κ (equivalent to the inverse linear response mobility) first appeared in the context of single impurity dynamics in Ref. [23], see Ch. 2.5.

It is worth emphasizing that the exact coefficient entering Eq. (4.23) involves the same parameter Γ as in Eqs. (4.1), (4.21). This is because both the Casimir interaction and the damping coefficient are controlled by the same underlying scattering mechanism: the virtual excitations are responsible for $U_{\rm Cas}$ while the real processes lead to collective damping of the center of mass. Remarkably, the two effects are related by the causality structure inherent in Eq. (4.14).

The other main achievement of the theory is that it allows one to express the exact back-scattering amplitude Γ in terms of partial derivatives of the exact single-impurity dispersion relation [25, 26, 29, 30]. The general expression for Γ is not essential to the present discussion and can be found in previous works as well as in the Appendix B.3. What is crucial is the observation that for several physically relevant models Γ changes sign across integrable points in parameter space.

To demonstrate this we briefly recall the weakly interacting Bose gas with impurities having nearly the same mass and coupling constants G as the background gas g, relevant to spinor Bose condensates. In that case the system is near the integrable $SU(2)$ symmetric point ($M = m$, $G = g$) known as the Yang-Gaudin model [27, 28]. In this case it has been shown that $\Gamma = \frac{G}{c}\,(mG/Mg - 1)$ (see Appendix B.3.1 or Refs. [25, 29]). One thus sees that if two separated impurities can be independently tuned to lie on opposite sides of integrability (say with $M = m$, $G_1 > g$ and $G_2 < g$), one can achieve a *repulsive* Casimir interaction, instead of an attractive one.

4.4 Experimental Realization

The analysis utilized above also follows through entirely for *static* impurities in 1d interacting *bosonic* (or attractively interacting fermionic) systems. This offers possibly the most straightforward way to verify the $1/r^3$ law (although in this case, to authors' knowledge, one does not have a possibility of tuning through integrability, as in the case

of mobile impurities). To this end one would pin two impurites with the help of a state-dependent optical lattice [77] or a species selective dipole potential [7], and perform rf spectroscopy on individual impurity atoms [43, 78]. As a function of their separation, one can then measure the corresponding line shifts of suitable internal hyperfine energy levels.

To estimate the magnitude of the Casimir effect we focus on the strongly-interacting Tonks limit where the energy scale mc^2 is largest. For the experiment of Ref. [7] one finds a density of ^{87}Rb atoms $n \approx 7\,(\mu\mathrm{m})^{-1}$ with a typical interaction strength of $mg/\hbar^2 n \approx 1$. With temperatures as low as $T = 300\,\mathrm{nK}$ and a speed of sound $c \approx 1\,\mathrm{cm/s}$ this leads to $mc^2/\hbar \approx 138\,\mathrm{kHz}$ and $k_\mathrm{B}T/mc^2 \approx 0.29$. Thus the magnitude of the potential at the closest applicable separation $r = \xi \approx 1/n \approx 0.14\,\mu\mathrm{m}$ is $U_\mathrm{Cas}(\xi) \approx -1\,\mathrm{kHz}$, while for $r = 5L_T \approx 0.39\,\mu\mathrm{m}$ one finds $U_\mathrm{Cas}(5L_T) \approx -1\,\mathrm{Hz}$, indicating 3 orders of magnitude variation over a $\sim 0.25\,\mu\mathrm{m}$ range of separations. The magnitude of the effect $\sim 1\,\mathrm{kHz}$ is thus within an experimentally accessible range, with the scale of applicable separations increasing as one goes deeper into the quantum degenerate regime, $T \ll mc^2$.

In conclusion, we have shown that mobile impurities immersed in a 1d quantum liquid are subject to a long-range Casimir interaction, universally given by Eq. (4.1). This happens in spite of the fact that they become transparent at low energies. For several integrable impurity models, the amplitude of impurity-phonon back-scattering vanishes, leading to the absence of Casimir interactions in those systems. Finally, the strength of the effect is estimated to be within the resolution of current cold atom experiments, opening the possibility of observing the Casimir effect in a highly tunable, non-linear environment.

Chapter 5

Conclusion and Discussion

5.1 Overview of the Dissertation

Impurity physics in condensed matter has a long and rich history which has taught us an enormous amount about quantum transport. The lessons learned continue to guide our exploration of new systems. In this dissertation we have shown how new capabilities in the field of ultracold atoms has opened a new door for impurity physics, where the dynamical degrees of freedom associated with impurities takes front stage. This setup allows one to manipulate and probe the impurity degrees of freedom in real space & time and monitor the influence of a variety of tunable quantum environments.

We focused on the mobile impurity problem in a 1d quantum liquid, where several novel phenomena have been shown to emerge that have no higher dimensional counterparts. These include lattice-free Bloch oscillations of the impurity velocity and power-law threshold behavior of the impurity spectral function. The Bloch oscillations are made possibilie by the remarkable fact that in 1d the impurity dispersion relation $E(P)$ is a *periodic* function of momentum with period $2\pi n$. The latter may be identified as the many-body ground-state energy of the system with total momentum P. It follows from two generic properties of the quantum liquid spectrum in the absence of the impurity: acoustic at small P and gapless at momenta $2\pi nj$, for integer j. The first property ensures that it is always energetically favorable to channel small momentum to the impurity motion, $P^2/2M^* < c|P|$, while the second property implies that this picture must fail at the momentum scale $2\pi n$, where the system remains gapless.

Adiabatic continuity of the ground-state with parameter P thus implies a complicated crossover at a certain momentum scale, where the impurity becomes strongly hybridized with excitations of the host even at weak coupling. In Appendix A we analyzed two extreme models which illustrate this behavior first hand: weakly interacting bosons A.2 and free fermions A.3. They demonstrate the development of a non-perturbative bound-state between the impurity and a hole-like excitation of the host. The negative mass of the latter object dominates in the case of light impurities and leads to the effective "Umklapp" mechanism at momentum $\pm\pi n$ where the velocity vanishes. As discussed in Ch. 3, for heavy impurities whose mass exceeds a critical value the "Umklapp" process is ineffective and leads to a qualitative change (quantum phase transition) of the dispersion near πnj for odd integer j.

As a result of these properties, the impurity dynamics at low-energy is inaccessible to any order of perturbation theory in the impurity-host coupling. We therefore adopted an effective theory which can capture these non-perturbative features from the start. In Ch. 2 we developed this approach by noting that the low-energy response of the system must consist of the dressed impurity (depleton) plus small energy excitations of the quantum liquid. Using gauge and Galilean invariance we are able to deduce how the impurity energy must be transformed in the presence of long wavelength phonons, thus providing the depleton-phonon interaction energy.

This framework allows one to study the radiation losses incurred by an accelerating impurity driven by an external force. In the case of light impurities, $M < M_{\rm c}$, the relation between the drift velocity and external force is linear, allowing a definition of the impurity mobility: $V_{\rm D} = \sigma F$. We have derived an exact expression for the mobility in terms of independently measurable thermodynamic characteristics. The latter can be computed exactly for special values of parameters which render the model integrable. At finite temperature we derived an expression for the thermal friction associated with two-phonon Raman scattering. In addition to the T^4 scaling predicted by previous authors, we determine the exact coefficient of the thermal friction and show that it vanishes at points of exact integrability. This supports the idea that an integrable system cannot thermalize: owing to an extensive number of conserved quantities, the dynamics become strongly constrained.

In Ch. 3 we discussed the quantum phase transition associated with the impurity

mass exceeding a critical threshold, $M > M_c$. Using an illustrative model of impurity coupled to a weakly interacting condenstate, we found that above the critical mass the dispersion exhibits a swallowtail structure in which the ground-state develops cusps at momenta πnj for odd integer j. Such cusps are accompanied by metastable branches in the continuum which significantly alter the dynamical response of impurities to an external force. It leads to a non-analytic dependence of the drift velocity on the external force, implying a divergence in the mobility across the transition. Obtaining this result was facilitated by studying the tunneling rate out of the metastable branch, which also allowed us to identify the exact condition determining the location of the phase transition. We used this to elucidate the nature of the $M \to \infty$ limit and found agreement with previous results on static impurities. At the same time we were able to establish a connection with the orthogonality catastrophe associated with various other impurity tunneling protocols in 1d quantum liquids.

Finally, we considered the case of several impurities propagating in a 1d quantum liquid. Quantum coherent excitations of the latter can be exchanged by the former to give rise to interesting inter-impurity correlation effects. The main point was to emphasize the existence of a long-range interaction between separate impurities arising from scattering of virtual phonons in analogy to the Casimir effect. Although typically discussed in the case of perfectly reflecting objects, we showed that the effect exists even for objects which become transparent at zero energy transfer. This is due to the fact that the Casimir effect relies on the integration over the full energy band of quantum fluctuations, whose bandwidth is set by the inverse separation, c/r. This gives rise to a univeral, inverse cube interaction for mobile impurities which also applies to static impurities if the Luttinger parameter of the background is large, $K > 1$.

The Casimir interaction manifests itself in the semiclassical equations of impurity motion as the real part of an interaction potential. Its Kramers-Kronig partner (imaginary part) is responsible for a correlated friction of impurities, which enters as a suppression or enhancement of the center of mass viscosity depending on the relative separation. Remarkably, since both the Casimir interaction and dissipation are causally connected, vanishing of the latter implies vanishing of the former. As a result, the Casimir interaction is absent at points in parameter where the underlying model becomes integrable. This allows the intriguing possibility to tune an attractive interaction into a repulsive

one if the impurity parameters can be independently tuned to lie on opposite sides of an integrable point. We estimated the strength of the Casimir interaction to be within the current resolution of cold atom experiments and proposed a setup in which our results can be verified.

5.2 Outlook

The problem of describing dynamics in 1d quantum liquids has seen tremendous progress in recent years due to the development of certain effective field theories which address the shortcomings of standard approaches. For example, even in the case of "exactly solvable" models, it is well-known that extracting a dynamical response is an extremely difficult task (even though the spectrum is rather easy to obtain). The other established paradigm is that of the Luttinger liquid approach which suffers from several rather severe limitations: (i) it is essentially constructed of linear excitations (phonons) and thus lacks a mechanism for relaxation. (ii) it linearizes the true non-linear spectrum and predicts incorrect exponents of the momentum-resolved dynamic reponse functions even at low energies. (iii) it disregards effects associated with integrability of the underlying model. All of these issues are addressed in detail within the framework presented in this dissertation.

Despite its achievements, our results have several shortcomings of their own. One of the main unexplored areas is to understand the role of fluctuations on the impurity dynamics. We believe that one of the biggest qualitative changes fluctuations will introduce is the attentuation of the Bloch oscillation cycle. Indeed, different realizations of impurity trajectories are expected to gradually dephase, thus leading to a decay in time of the average oscillation signal. A few essential questions are: (a) What is the associated decay time? (b) Is the decay envelope is an exponential function or power-law? (c) Does it depend on whether the mass is heavy or light? The power-law scenario is an intriguing one which may be intimately related to the power-law behavior of the impurity spectral function[1] . Results from the Boltzmann approach of Ref. [42] have pointed towards an exponential law, but this was restricted to large forces in a free fermi gas. We leave these questions to future work.

[1] I am indebted to M. Knap for suggesting this interesting possibility.

The other limitation of our approach is that, by construction, it deals only with the leading low-energy response. It therefore remains an open problem as to what may occur at larger forces, or under other far-from-equilibrium protocols. Results from the Boltzmann approach of Ref. [42] have shown that there may exist a critical force separating a regime of incoherent drift from an unbounded acceleration of the impurity. Whether this effect can be generalized beyond the free fermionic host or can be understood as an example of a certain kind of dynamical phase transition remains open for future investigations.

We have also focused exclusively on the simplest case where both the impurity and background particles are considered spinless. Understanding spin transport in the case where both the impurity and the host have spin dynamics would be an interesting and important extension of the present work. We know that for a spinless host the Bloch oscillation mechanism occurs via strong impurity-hole or impurity-soliton hybridization in the density sector. Whether a similar strongly correlated state can occur in the spin sector, similar to the Kondo effect, is an open question. Another interesting question is whether the existence of spin-charge separation in 1d bears any consequence for the dynamics of the impurity spin or coordinate.

As always, new capabilities lead to the challenge and promise of new and exciting problems. The cold atom realization of synthesizing and dynamically manipulating impurity degrees of freedom in tunable quantum environments is one example which has met this challenge. We hope the aforementioned problems, as well as the concepts and results presented in this dissertation, will motivate and help guide future studies of impurity dynamics.

References

[1] I. Bloch, J. Dalibard, and W. Zwerger, Rev. Mod. Phys. **80**, 885 (2008).

[2] S. Palzer, C. Zipkes, C. Sias, and M. Köhl, Phys. Rev. Lett. **103**, 150601 (2009)

[3] C. Zipkes, S. Palzer, C. Sias, and M. Köhl, Nature **464**, 388 (2010)

[4] S. Schmid, A. Härter, and J. H. Denschlag, Phys. Rev. Lett. **105**, 133202 (2010)

[5] P. Wicke, S. Whitlock, and N. J. van Druten, arXiv:1010.4545 (2010)

[6] J. Catani, L. DeSarlo, G. Barontini, F. Minardi, and M. Inguscio, Phys. Rev. A **77**, 011603 (2008).

[7] J. Catani, G. Lamporesi, D. Naik, M. Gring, M. Inguscio, F. Minardi, A. Kantian, and T. Giamarchi, Phys. Rev. A **85**, 023623 (2012).

[8] H. Moritz, T. Stöferle, M. Köhl, and T. Esslinger, Phys. Rev. Lett. **91**, 250402 (2003)

[9] T. Stöferle, H. Moritz, C. Schori, M. Köhl, and T. Esslinger, Phys. Rev. Lett. **92**, 130403 (2004)

[10] C. D. Fertig, K. M. OHara, J. H. Huckans, S. L. Rolston, W. D. Phillips, and J. V. Porto, Phys. Rev. Lett. **94**, 120403 (2005)

[11] T. Kinoshita, T. Wenger, and D. S. Weiss, Science **305**, 1125 (2004)

[12] T. Kinoshita, T. Wenger, and D. S. Weiss, Nature **440**, 900 (2006)

[13] C. Weitenberg *et. al.*, Nature **471**, 319 (2011).

[14] T. Fukuhara *et. al.*, Nat. Phys. **9**, 235 (2013).

[15] L. D. Landau and I. M. Khalatnikov, Zh. Eksp. Teor. Fiz. **19**, 637 (1949)

[16] L. D. Landau and I. M. Khalatnikov, Zh. Eksp. Teor. Fiz. **19**, 709 (1949)

[17] J. Bardeen, G. Baym, and D. Pines, Phys. Rev. Lett. **17**, 372 (1966)

[18] J. Bardeen, G. Baym, and D. Pines, Phys. Rev. **156**, 207 (1967)

[19] G. Baym, Phys. Rev. Lett. **17**, 952 (1966)

[20] G. Baym, Phys. Rev. Lett. **18**, 71 (1967)

[21] C. Ebner, Phys. Rev. **156**, 222 (1967)

[22] G. Baym and C. Ebner, Phys. Rev. **164**, 235 (1967)

[23] A. H. Castro Neto and M. P. Fisher, Phys. Rev. B **53**, 9713 (1996)

[24] A. Muryshev, G. V. Shlyapnikov, W. Ertmer, K. Sengstock, and M. Lewenstein, Phys. Rev. Lett. **89**, 110401 (2002)

[25] D. M. Gangardt and A. Kamenev, Phys. Rev. Lett. **102**, 070402 (2009)

[26] D. M. Gangardt and A. Kamenev, Phys. Rev. Lett. **104**, 190402 (2010)

[27] C. N. Yang, Phys. Rev. Lett. **19**, 1312 (1967)

[28] M. Gaudin, Phys. Lett. A **24**, 55 (1967)

[29] M. Schecter, D. M. Gangardt, and A. Kamenev, Ann. Phys. (N.Y.) **327**, 639 (2011).

[30] K. A. Matveev and A. V. Andreev, Phys. Rev. B **86**, 045136 (2012).

[31] J. N. Fuchs, D. M. Gangardt, T. Keilmann, and G. V. Shlyapnikov, Phys. Rev. Lett. **95**, 150402 (2005)

[32] K. A. Matveev and A. Furusaki, Phys. Rev. Lett. **101**, 170403 (2008)

[33] D. K. K. Lee and J. M. F. Gunn, Phys. Rev. B **46**, 301 (1992)

[34] F. M. Cucchietti and E. Timmermans, Phys. Rev. Lett. **96**, 210401 (2006)

[35] M. Bruderer, A. Klein, S. R. Clark, and D. Jaksch, Phys. Rev. A **76**, 011605 (2007)

[36] A. Lamacraft, Phys. Rev. B **79**, 241105 (2009)

[37] M. B. Zvonarev, V. V. Cheianov, and T. Giamarchi, Phys. Rev. Lett. **99**, 240404 (2007)

[38] A. Kamenev and L. I. Glazman, Phys. Rev. A **80**, 011603 (2009)

[39] M. B. Zvonarev, V. V. Cheianov, and T. Giamarchi, Phys. Rev. B **80**, 201102 (2009)

[40] A. Imambekov, T. L. Schmidt, and L. I. Glazman, Rev. Mod. Phys. **84**, 1253 (2012).

[41] M. Schecter, A. Kamenev, D. M. Gangardt, A. Lamacraft, Phys. Rev. Lett. **108**, 207001 (2012).

[42] O. Gamayun, O. Lychkovskiy, and V. Cheianov, arXiv:1402.6362.

[43] A. Recati, J. N. Fuchs, C. S. Peca, and W. Zwerger, Phys. Rev. A **72**, 023616 (2005).

[44] M. Schecter, A. Kamenev, Phys. Rev. Lett. **112**, 155301 (2014).

[45] M. Schecter, A. Kamenev, and D. M. Gangardt, arXiv:1404.4433.

[46] T. Tsuzuki, J. Low. Temp. Phys. **4**, 441 (1971)

[47] V. N. Popov, *Functional Integrals and Collective Excitations* (Cambridge University Press, 1988)

[48] F. M. D. Haldane, Phys. Rev. Lett. **47**, 1840 (1981)

[49] V. Hakim, Phys. Rev. E **55**, 2835 (1997)

[50] L. P. Pitaevskii and S. Stringari, *Bose-Einstein Condensation* (Clarendon Press, Oxford, 2003)

[51] H. Castella and X. Zotos, Phys. Rev. B **47**, 16186 (1993)

[52] A. O. Caldeira and A. J. Leggett, Ann. of Phys. **149**, 374 (1983)

[53] D. M. Gangardt and G. V. Shlyapnikov, Phys. Rev. Lett. **90**, 010401 (2003)

[54] A. Imambekov and L. Glazman, Phys. Rev. Lett. **100**, 206805 (2008)

[55] L. Keldysh, Sov. Phys. JETP **20**, 1018 (1965)

[56] A. Kamenev and A. Levchenko, Adv. Phys. **58**, 197 (2009)

[57] D. E. Pelinovsky, Y. S. Kivshar, and V. V. Afanasjev, Phys. Rev. E **54**, 2015 (1996)

[58] L. D. Landau and E. M. Lifshitz, *The Classical Theory of Fields*, 4th ed., Course of Theoretical Physics, Vol. 2 (Butterworth-Heinemann, 1975)

[59] V. L. Ginzburg, *Applications of Electrodynamics in Theoretical Physics and Astrophysics*, 3rd ed. (Gordon and Breach Science Publishers, 1989)

[60] D. Taras-Semchuk and J. M. F. Gunn, Phys. Rev. B **60**, 13139 (1999)

[61] C. L. Kane and M. P. A. Fisher, Phys. Rev. B **46**, 15233 (1992)

[62] D. L. Maslov and M. Stone, Phys. Rev. B **52**, R5539 (1995)

[63] E. H. Lieb and W. Liniger, Phys. Rev. **130**, 1605 (1963)

[64] Integrability of Gross-Pitaevskii equation is a semiclassical manifestation of the exact quantum integrability of the Lieb-Liniger model defined by the quantum version of the Lagrangian (A.1). The grey soliton considered here is a weak-coupling analogue of the so-called Lieb II mode. The absence of dissipation of the Lieb II mode for the entire range of the interaction parameter will be demonstrated elsewhere.

[65] H. P. Büchler, V. B. Geshkenbein, and G. Blatter, Phys. Rev. Lett. **87**, 100403 (2001)

[66] G. E. Astrakharchik and L. P. Pitaevskii, Phys. Rev. A **70**, 013608 (2004)

[67] A. J. Leggett, S. Chakravarty, A. T. Dorsey, M. P. A. Fisher, A. Garg, and W. Zwerger, Rev. Mod. Phys. **59**, 1 (1987).

[68] H. B. G. Casimir, Proc. K. Ned. Akad. Wet. **51**, 793 (1948).

[69] M. Kardar and R. Golestanian, Rev. Mod. Phys. **71**, 4 (1999).

[70] J. M. Obrecht, R. J. Wild, M. Antezza, L. P. Pitaevskii, S. Stringari, and E. A. Cornell, Phys. Rev. Lett. **98**, 063201 (2007).

[71] Based on a phase-space argument we expect that in dimension d the induced interaction scales as $U_{\rm Cas}(r) \sim 1/r^{2d+1}$, see Eq. (4.14). In this work we focus on the case $d = 1$ where, in addition to the Casimir effect being strongest at large separations, integrability of the underlying model also plays an important role.

[72] J. N. Fuchs, A. Recati, and W. Zwerger, Phys. Rev. A **75**, 043615 (2007).

[73] P. Wächter, V. Meden, and K. Schönhammer, Phys. Rev. B **76**, 045123 (2007).

[74] The authors of Refs. [72, 73] also found a purely *oscillatory* component with period $1/n$ coming from double-barrier tunneling resonances. Since this component will be suppressed if impurity coordinates fluctuate on the scale of $1/n$ (*e.g.,* for mobile impurities or for an ensemble of 1d tubes with slightly different impurity separations), we focus solely on the *smooth* component of the induced interaction.

[75] M. Bruderer, A. Klein, S. R. Clark, and D. Jaksch, Phys. Rev. A **76**, 011605(R) (2007).

[76] In principal there are also terms proportional to $(\partial_x \chi_\pm(X_j, t))^2$ but they do not contribute to the impurity equations of motion. This is because the physically relevant processes are those in which the relative number of right and left movers changes, *i.e.,* those described by Eq. (4.10).

[77] B. Gadway, D. Pertot, R. Reimann, and D. Schneble, Phys. Rev. Lett. **105**, 045303 (2010).

[78] H. Moritz, T. Stöferle, K. Güenter, M. Köhl, and T. Esslinger, Phys. Rev. Lett. **94**, 210401 (2005).

[79] P. O. Fedichev, A. E. Muryshev, and G. V. Shlyapnikov, Phys. Rev. A **60**, 3220 (1999)

[80] I. E. Mazets, T. Schumm, and J. Schmiedmayer, Phys. Rev. Lett. **100**, 210403 (2008)

[81] S. Shevchenko, Sov. J. Low Temp. Phys. **14**, 553 (1988)

[82] V. V. Konotop and L. Pitaevskii, Phys. Rev. Lett. **93**, 240403 (2004)

[83] A. S. Campbell, Ph.D. Thesis, University of Birmingham (2012).

Appendix A

Illustrative Models

A.1 Grey Solitons

The dynamic properties of one-dimensional bosons of mass m weakly interacting via a repulsive short range potential proportional to coupling constant g can be studied within the Gross-Pitaevskii description using the following Lagrangian

$$L = \int \mathrm{d}x \left(i\bar{\psi}\partial_t\psi - \frac{1}{2m}\left|\partial_x\psi\right|^2 - \frac{g}{2}\left|\psi\right|^4 + \mu\left|\psi\right|^2 \right) . \tag{A.1}$$

Here ψ is the quasi-condensate wavefunction corresponding to the asymptotic density $|\psi(\pm\infty, t)|^2 = n$ and vanishing supercurrent at infinity. The condition of weak interactions is $mg/n \ll 1$. Minimizing the action defined by the Lagrangian Eq. (A.1) leads to the Gross-Pitaevskii equation,

$$i\partial_t\psi = \left(-\frac{\partial_x^2}{2m} + g|\psi|^2 - \mu \right)\psi. \tag{A.2}$$

Substituting a constant solution $\psi_0 = \sqrt{n}$ one obtains the chemical potential $\mu = gn = mc^2$ related to the sound velocity $c = \sqrt{gn/m}$. In addition to the uniform solution, the Gross-Pitaevskii equation (A.13) admits a one-parameter family of solutions

$$\psi_{\mathrm{s}}(x - Vt; \Phi_{\mathrm{s}}) = \sqrt{n}\left(\cos\left(\frac{\Phi_{\mathrm{s}}}{2}\right) - i\sin\left(\frac{\Phi_{\mathrm{s}}}{2}\right)\tanh\left(\frac{x - Vt}{l}\right)\right), \tag{A.3}$$

known as grey solitons [46, 50]. They can be visualized as a dip moving with velocity V, having a core size $l = 1/m\sqrt{(c^2 - V^2)}$. The solution, Eq. (A.3) is characterized by

the total phase drop and number of expelled particles related to the velocity as

$$\Phi_{\rm s}(V,n) = 2\arctan\frac{\sqrt{c^2-V^2}}{V},\ N_{\rm s}(V,n) = \int {\rm d}x\ \left(n - |\psi_{\rm s}(x)|^2\right) = \frac{2}{g}\sqrt{c^2-V^2}\,. \quad \text{(A.4)}$$

The momentum and energy of the soliton are given by [46, 81, 82]

$$P_{\rm s} = n\Phi_{\rm s} - mN_{\rm s}V\,, \qquad E_{\rm s} = \frac{4}{3}cn\sin^3(\Phi_{\rm s}/2) = \frac{mg^2}{6}N_{\rm s}^3, \quad \text{(A.5)}$$

which allows one to define the Lagrangian

$$L_{\rm s}(V,n) = (n\Phi_{\rm s} - mN_{\rm s}V)V - \frac{mg^2}{6}N_{\rm s}^3. \quad \text{(A.6)}$$

Using the soliton Lagrangian (A.6) and putting $M = 0$ in Eqs. (2.17) and (2.18) one sees immediately that the variables in (A.4) coincide with the collective variables Φ, N. Therefore the grey soliton can be viewed as a model for a *massless* impurity consisting of a depletion cloud only.

We invert Eqs. (A.4) which yields

$$V_0 = \frac{gN}{2\tan\frac{\Phi}{2}}, \qquad n_0 = \frac{mgN^2}{4\sin^2\frac{\Phi}{2}}\,. \quad \text{(A.7)}$$

Using Eq. (2.20) and Eqs. (A.6), (A.7) with $L_{\rm s} = L_{\rm d}$ and $N_{\rm s} = N$ yields the internal energy, Eq. (2.23) of the soliton,

$$H_{\rm d}(N,\Phi) \;=\; \frac{mg^2}{6}N^3 + N\left(\frac{mV_0^2}{2} - gn_0\right) = \frac{mg^2N^3}{8}\left(\frac{1}{3} - \frac{1}{\sin^2\Phi/2}\right). \quad \text{(A.8)}$$

The matrix of second derivatives *at the equilibrium solution* reads

$$\mathsf{H} = \begin{pmatrix} H_{\Phi\Phi} & H_{\Phi N} \\ H_{N\Phi} & H_{NN} \end{pmatrix} = \begin{pmatrix} -cn\frac{1+\cos^2\Phi/2}{\sin\Phi/2} & 2mc^2\frac{\cos\Phi/2}{\sin\Phi/2} \\ 2mc^2\frac{\cos\Phi/2}{\sin\Phi/2} & -\frac{m^2c^3}{n}\frac{1+\cos^2\Phi/2}{\sin\Phi/2} \end{pmatrix} \quad \text{(A.9)}$$

The backscattering amplitude Γ_{+-}, calculated with the help of Eq. (B.18), vanishes identically due to the integrability [64] of the Gross-Pitaevskii equation (A.2).

As it was shown in [24, 79] a weak cubic non-linearity $-(\alpha/6)|\psi|^6$ in the Lagrangian (A.1) breaks the integrability of the model. Cubic terms describe three-body interactions which arise from virtual transitions to higher transverse states of a tightly confined one-dimensional liquid [80]. Here we extend the results in Ref. [26] and calculate the

amplitude of the corresponding dissipation processes for the whole range of soliton velocities.

The corresponding correction to the Lagrangian, Eq. (A.6) of the soliton can be calculated to the leading order by evaluating it with the unperturbed solution,

$$\delta L_{\rm d} = -\frac{\alpha}{6}\int {\rm d}x \left(|\psi_{\rm d}(x)|^2 - n\right)^3 = \frac{8}{45}\frac{\alpha n^3}{mc}\left(1-\frac{V^2}{c^2}\right)^{5/2} = \frac{\alpha m^2 g^2}{180}N^5 = -\delta H_{\rm d}. \quad \text{(A.10)}$$

Here we have used the expression Eq. (A.4) for the number of expelled particles N to calculate the correction to the energy, relying on the theorem of small increments. The corresponding change in the matrix (A.9) of second derivatives

$$\delta \mathsf{H} = -\frac{\alpha m^2 g^2}{9}N^3 \times \begin{pmatrix} 0 & 0 \\ 0 & 1 \end{pmatrix} \quad \text{(A.11)}$$

can be used to determine the leading correction to Γ_{+-} using Eq. (B.18). Rewriting the latter expression in terms of velocity one finds

$$\Gamma_{+-} = -\frac{8}{9}\frac{\alpha n^2}{m^2 c^4}\left(1-\frac{V^2}{c^2}\right)^{1/2}, \quad \text{(A.12)}$$

in agreement with the results of Ref. [26].

A.2 Impurity in a weakly interacting liquid

To model the impurity coupled to a weakly interacting superfluid at $T = 0$, the Gross-Pitaevskii equation, Eq. (A.2) is modified in the presence of a delta function potential moving with constant velocity V as

$$i\partial_t \psi = \left(-\frac{\partial_x^2}{2m} + g|\psi|^2 - \mu + G\delta(x - Vt)\right)\psi. \quad \text{(A.13)}$$

For $G > 0$, the soliton solution, Eq. (A.3) still satisfies Eq.(A.13) except at the location of the impurity. Thus, one may construct a solution to Eq.(A.13) by matching *two* soliton solutions, Eq. (A.3) at the location of the impurity, as shown in Fig. A.1. The proper solutions of Eq, (A.13) can thus be written

$$\psi(y) = \begin{cases} \psi_{\rm s}(y + x_0; \Phi_{\rm s})e^{i\Phi_0/2}, & y > 0 \\ \psi_{\rm s}(y - x_0; \Phi_{\rm s})e^{-i\Phi_0/2}, & y < 0 \end{cases} \quad \text{(A.14)}$$

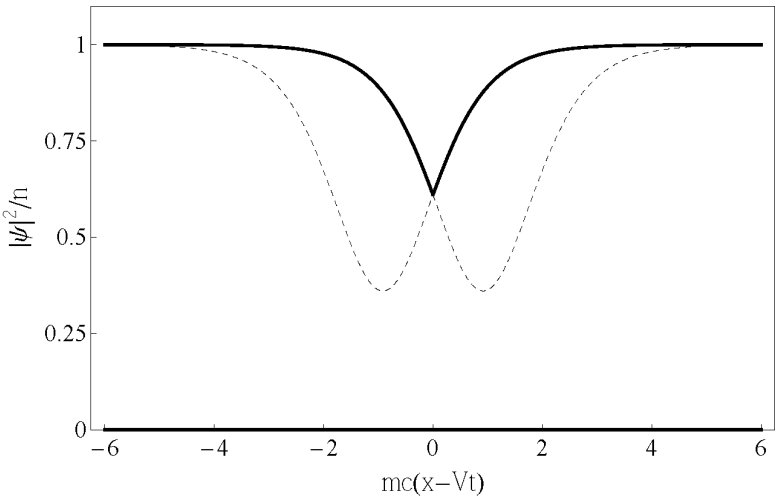

Figure A.1: Superfluid density in the presence of an impurity moving with velocity $V/c = 0.6$ and coupling $G/c = 0.1$ (solid line). The dashed lines correspond to the double soliton solution Eq.(A.3) used to construct Eq.(A.14).

where $y = x - Vt$ and the velocity is related to the phase $\Phi_{\rm s}$ as $V/c = \cos(\Phi_{\rm s}/2)$, parameterizing the soliton configuration, Eq. (A.3). The solutions $\psi_{\pm}$ to the right (left) of the impurity satisfy the boundary conditions: $\psi_+(0) = \psi_-(0)$, $\psi'_+(0) - \psi'_-(0) = 2mG\psi(0)$. Using (A.14), the boundary conditions give rise to the following two equations for Φ_0 and $z = \tanh(x_0/l)$

$$\tan\left(\frac{\Phi_0}{2}\right) = z\,\tan\left(\frac{\Phi_s}{2}\right) \tag{A.15}$$

$$\sin^3\left(\frac{\Phi_{\rm s}}{2}\right)(1-z^2)\,z = \frac{G}{c}\left[\cos^2\left(\frac{\Phi_{\rm s}}{2}\right) + z^2\sin^2\left(\frac{\Phi_{\rm s}}{2}\right)\right]. \tag{A.16}$$

Equations (A.15), (A.16) permit a solution only for $V < V_c(G/c)$ where V_c is some critical velocity that depends only upon the parameter G/c [49, 60]. This can be seen by considering the right and left hand sides of the second equation (A.16). While the left hand side is bounded by the maximum at $z_{\rm max} = 1/\sqrt{3}$, the right hand side grows quadratically with z and therefore the solution exists only for a limited range of Φ_s, which leads to the above-mentioned limitation on velocity.

For this reason we choose to parameterize the solution, Eq.(A.14), by the *total* phase drop across the impurity, $\Phi = \Phi_s - \Phi_0$, which happens to permit a solution for *any* Φ. Thus, upon solving Eqs. (A.15), (A.16) one finds the relations $z = z(\Phi, G/c)$

and $\Phi_{\rm s} = \Phi_{\rm s}(\Phi, G/c)$. It can easily be seen from Eqs. (A.15), (A.16) that these functions are periodic in Φ. The number of expelled particles and momentum can be calculated and expressed through the phase Φ as

$$N = \int dx(n - |\psi|^2) = 2\kappa(1-z)\sin\frac{\Phi_s}{2}; \qquad P = n\Phi + (M - mN)V, \tag{A.17}$$

The energy may also be calculated and expressed in terms of Φ as

$$\begin{aligned} E &= \frac{1}{2}MV^2 + \int dx \left[\frac{|\partial_x\psi|^2}{2m} + \frac{g}{2}(n-|\psi|^2)^2\right] + G|\psi(0)|^2 && \text{(A.18)} \\ &= \frac{1}{2}MV^2 + \frac{4}{3}nc\,\sin^3\frac{\Phi_s}{2}\left[1 - \frac{3}{4}z - \frac{1}{4}z^3\right]. && \text{(A.19)} \end{aligned}$$

Alternatively, we may solve for $\Phi = \Phi(P)$ by inverting the second of Eqs. (A.17). Substituting it into the energy function, Eq. (A.18) one obtains the dispersion relation $E(P)$ plotted in Fig. 1.3 for the impurity in a weakly interacting bose liquid.

In the weak coupling regime $G/c \ll 1$ the critical velocity can be obtained by neglecting the z-dependence of the r.h.s. of Eq. (A.16). This is justified *a posteriori* if the solution satisfies $\Phi_{\rm s} \ll 1$. Expanding the trigonometric functions and using $z_{\max} = 1/\sqrt{3}$ on the l.h.s one obtains $(\Phi_{\rm s}/2)^3 = (3\sqrt{3}/2)\,G/c$, which justifies our approximation. We thus have the critical velocity

$$\frac{V_{\rm c}}{c} = 1 - \frac{1}{2}\left(\frac{\Phi_{\rm s}}{2}\right)^2 = 1 - \frac{3}{4}\left(\frac{\sqrt{2}G}{c}\right)^{2/3}. \tag{A.20}$$

Solving Eqs. (A.15), (A.16) for arbitrary velocity or momentum is cumbersome and we resort to numerical methods.

In the strong coupling limit $G \gg c$ we determine the dependence of z and $\Phi_{\rm s}$ on Φ to order c/G. This is done by writing $\Phi_{\rm s} \simeq \pi + \frac{c}{G}\Phi_{\rm s}^{(1)}$ and $z \simeq \frac{c}{G}z^{(1)}$ and finding coefficients $\Phi_{\rm s}^{(1)}$ and $z^{(1)}$ from Eqs. (A.15), (A.16). We have

$$z(\Phi) \simeq \frac{c}{G}\cos^2\frac{\Phi}{2}; \qquad \Phi_s(\Phi) \simeq \pi - \frac{c}{G}\sin\Phi\,. \tag{A.21}$$

Using Eqs. (A.21), (A.17) one has

$$V \simeq \frac{c^2}{2G}\sin\Phi; \qquad N \simeq 2\kappa\left(1 - \frac{c}{G}\cos^2\frac{\Phi}{2}\right). \tag{A.22}$$

The first equation has the Josephson form with the critical velocity $V_c = c^2/2G$ in the strong coupling limit. It is also clear from the second equation that in the leading approximation N is a constant $N \simeq 2\kappa$. This results in the Josephson form for the energy, Eq. (2.24).

At $V = 0$ the equations (A.15), (A.16) simplify considerably by putting $\Phi_s = \pi$. There are two solutions,

$$z_0 = \sqrt{1 + \left(\frac{G}{2c}\right)^2} - \frac{G}{2c}\,, \qquad z_\pi = 0\,, \tag{A.23}$$

The z_0 root corresponds to $\Phi = 0$. The z_π root corresponds to the dark soliton solution with $\Phi = \pi$, which persists for $G > 0$ because the density vanishes at the impurity location, *i.e.*, there is no additional energy cost to put the impurity in the center of a dark soliton.

A.3 Impurity in a free fermion gas: existence of the impurity-hole bound state

The physics of the adiabatic supercurrent creation facilitated by solitons works best in the regime of weak interactions, where the quasi-condensate description of the background particles is most reliable. As the interactions within the background increase, it is well-known that this description should be essentially replaced by a picture of free-fermions[1] – a system which manifestly lacks both superfluid and crystalline order.

Consider a state of the system with total momentum $P > 0$. If $P < P_0 \equiv \min\{Mv_F, k_F\}$, the low energy states are those where most of the momentum is carried by the impurity. Indeed, the impurity kinetic energy $P^2/(2M)$ is less than that of soft particle-hole excitations above the Fermi sea $\sim v_F P$. In the opposite limit $P > P_0$ the low energy states are those where *hole excitations* carry a significant fraction of the entire momentum P. The many-body ground state adiabatically connects between these two limits, signaling strong impurity-hole hybridization at $P > P_0$. In a recent work, we were able to show that this leads to the non-perturbative formation of an

[1] For infinite repulsion, bosons satisfy a hard-core constraint analogous to the Pauli principle. The anti-symmetry of fermionic wave-function is immaterial if the impurity only couples to its square, as in the case of density-density coupling. Of course, one may also simply start from free fermions.

impurity-hole *bound-state* even for arbitrarily small coupling. In agreement with our general arguments, the resulting dispersion relation $E(P)$ is indeed a periodic function of momentum P with the period $2k_F = 2\pi n$.

We start from the Hamiltonian of $N_{\rm tot}$ free fermions created by $c_p^\dagger$, weakly coupled to a quantum impurity with the coordinate X through the density-density interaction:

$$\hat{H} = -\frac{1}{2M}\frac{\partial^2}{\partial X^2} + \sum_p \frac{p^2}{2m} c_p^\dagger c_p + \gamma \frac{n^2}{m N_{\rm tot}} \sum_{p,q} c_p^\dagger c_{p+q} e^{iqX} \tag{A.24}$$

where $0 < \gamma \ll 1$ is a dimensionless coupling constant.

Consider a state of the system with total momentum $P > 0$. If $P < P_0 \equiv \min\{Mv_F, k_F\}$, the low energy states are those where most of the momentum is carried by the impurity. Indeed, the impurity kinetic energy $P^2/(2M)$ is less than that of soft particle-hole excitations above the Fermi sea $\sim v_F P$. In the opposite limit $P > P_0$ the low energy states are those where *hole excitations* carry a significant fraction of the entire momentum P. The many-body ground state adiabatically connects between these two limits, signaling strong impurity-hole hybridization at $P > P_0$. Indeed, consider a subspace of the full many-body space, which contains a single hole excitation with momentum $0 < k < 2k_F$ in addition to the impurity with momentum $P - k$ (this restriction is justified in the limit $\gamma \ll 1$). The basis vectors of this subspace are

$$|k; P\rangle = e^{i(P-k)X} c_{k_F}^\dagger c_{k_F - k} |\text{Fermi Sea}\rangle \,. \tag{A.25}$$

The corresponding Schrödinger equation $\sum_{k'} \langle k; P|\hat{H}|k'; P\rangle \psi_P(k') = E\psi_P(k)$ takes the form of the two-particle problem with the *attractive* delta-interaction (formally the attraction arises from anti-commuting the fermionic operators in the last term in Eq. (A.24)),

$$\left[\frac{(P-k)^2}{2M} + E_h(k)\right]\psi_P(k) - \frac{\gamma n}{m}\int_0^{2k_F} \frac{dk'}{2\pi}\,\psi_P(k') = E\psi_P(k), \tag{A.26}$$

where $E_h(k) = v_F k - k^2/(2m)$ is the hole kinetic energy (we measure E relative to $NE_F/3 + \gamma n^2/m$). This problem admits a unique bound-state solution, whose energy $E = E_b(P)$ is found from the integral equation

$$\int_0^{2k_F} \frac{dk'}{\frac{(P-k')^2}{2M} + E_h(k') - E_b(P)} = \frac{2\pi m}{\gamma n} \,. \tag{A.27}$$

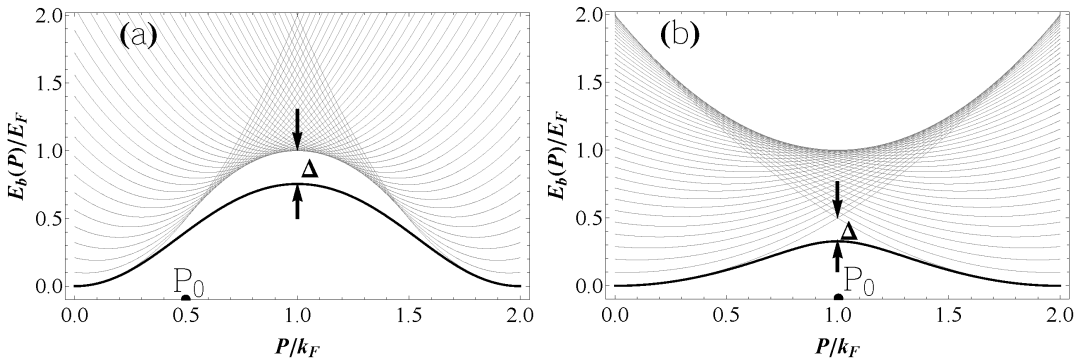

Figure A.2: The bound-state $E_b(P)$, Eq. (A.27), (thick black line) and scattering continuum $\frac{(P-k)^2}{2M} + E_h(k)$ for a set of k (thin gray lines) for the light impurity $\eta = 1/2$ (a) and heavy impurity $\eta = 2$ (b). In both cases $\gamma = 0.7$.

Its solution represents a non-perturbative correction to the bare impurity dispersion. We plot $E_b(P)$, along with the continuum of the scattering states, in Fig. A.2 for the case of light, $\eta = M/m < 1$, and heavy, $\eta > 1$ impurity. The gap Δ between the bound-state and the continuum is found to be $\Delta/E_F \sim \gamma^2\eta/(1-\eta)$ for $\eta < 1 - \gamma/\pi^2$ and $P_0 \leq P$, while $\Delta/E_F \sim \exp\{-\pi^2(\eta-1)/\eta\gamma\}$ for $\eta > 1 + \gamma/\pi^2$. For an almost equal mass case $|1-\eta| < \gamma/\pi^2$, one finds $\Delta/E_F \sim \gamma$. We also note that for $\eta = 1$, integrability of Eq. (A.24) allows access to the exact many-body ground state energy [36] $E_0(P \sim k_F) = E_F - \frac{2\pi^2}{3\gamma}\frac{(P-k_F)^2}{2m}$. Remarkably, as one may verify from Eq. (A.27), $E_b(P \sim k_F) + \gamma n^2/m = E_0(P \sim k_F)$ for $\gamma \ll 1$, justifying our Hilbert space truncation.

The hard gap between the bound-state and the continuum is an artifact of restricting the particle in Eq. (A.25) to be created right at the Fermi momentum k_F. Allowing for slight deviation $c^\dagger_{k_F} \to c^\dagger_{k_F+p}$, introduces interaction of the bound-state with low energy, $\sim v_F p$, excitations. It is known [36, 38, 40, 54] that such interaction transforms the bound-state into the *quasi* bound-state with the power-law (instead of the pole) correlation function, see Appendix B.4. These low energy excitations are responsible for radiation losses and thus for linear mobility σ. They do not, however, destroy the quasi bound-state and associated Bloch oscillations at small applied force.

The Bloch oscillations are destroyed if a large enough force $F > F_{\max}$ is applied to the impurity. The physics of this process is that of the Landau-Zener transition between the bound-state and the continuum at $P \approx P_0 = k_F \min\{\eta, 1\}$. One may thus

estimate the crossover force as $F_{\max} \sim \Delta^2/v$, where $v = v_F \min\{1, 1/\eta\}$. This leads to the following estimate for the maximal force, preserving (nearly) adiabatic bound-state dynamics

$$F_{\max} \propto \frac{k_F^3}{m} \begin{cases} \left(\frac{\gamma^2\eta}{1-\eta}\right)^2, & \eta < 1 - \frac{\gamma}{\pi^2}; \\ \eta \left(\frac{\eta-1}{\eta}\right)^2 \mathrm{e}^{-\frac{2\pi^2(\eta-1)}{\gamma\eta}}, & \eta > 1 + \frac{\gamma}{\pi^2}, \end{cases} \tag{A.28}$$

while for $|1-\eta| < \gamma/\pi^2$, one finds $F_{\max} \propto k_F^3\gamma^2/m$. For $F < F_{\max}$ both light and heavy impurities exhibit Bloch oscillations along with the drift [29], whose velocity scales linearly with the force $v_D = \sigma F$.

In Ch. 3 and Ref. [36] it was shown that for a heavy impurity *away* from the Tonks-Girardeau limit, there exists a phase transition at a critical value of the impurity mass: for $M < M_c$ the ground-state is a smooth function of momentum, while for $M > M_c$ the ground-state exhibits a cusp singularity at momenta $P = (1+2j)k_F$ for integer j (in the Tonks-Girardeau limit $M_c \to \infty$). In the latter case the impurity "overshoots" the intersection points at $P = (1+2j)k_F$ and has to emit phonons to reach the ground state. In Ch. 3 this was seen to lead to an enhanced dissipation and thus to super-linear drift velocity

$$v_D \propto F^{1/(1+\alpha)}, \tag{A.29}$$

where $\alpha \approx 2K - 1$ for $\gamma \ll 1$ and K is the Luttinger parameter of the host.

Notice that in the Tonks-Girardeau limit the validity of the $v_D = \sigma F$ response for $\eta > 1$ is limited to an exponentially small force (A.28). This scale originates from the exponentially narrow region of momenta, where the bound-state exhibits the avoided crossing behavior, Fig. A.2(b). For $F > F_{\max}$ the impurity overshoots the avoided crossing and follows the "wrong" parabola before emitting phonons and returning to the ground state. Thus, for $F > F_{\max}$ one may apply Eq. (A.29) with $K = 1$ – appropriate for the Tonks gas. This leads to $v_D \propto \sqrt{F}$, in full agreement with The Boltzmann equation approach of Ref. [42]. For $F < F_{\max}$, the dynamics of the impurity-hole quasi-bound state is important and is entirely missed in the Boltzmann approach. An important extension of Ref. [42] is that the super-linear drift (A.29) is to be expected for moderately heavy impurities $m < M < M_c$ in an intermediate range of forces where the linear mobility $v_D = \sigma F$ is inapplicable.

Appendix B

Technical Calculations

B.1 Derivation of dissipative action

Gaussian integration of the interaction term Eq. (2.38) using the following phononic propagators

$$\begin{aligned} -i\Big\langle \chi_{\rm cl}(x,t)\chi^\dagger_{\rm cl}(x',t')\Big\rangle &= \mathsf{D}^K(x-x',t-t'),\ -i\Big\langle \chi_{\rm q}(x,t)\chi^\dagger_{\rm cl}(x',t')\Big\rangle = \mathsf{D}^A(x-x',t-t') \\ -i\Big\langle \chi_{\rm cl}(x,t)\chi^\dagger_{\rm q}(x',t')\Big\rangle &= \mathsf{D}^R(x-x',t-t'),\ -i\Big\langle \chi_{\rm q}(x,t)\chi^\dagger_{\rm q}(x',t')\Big\rangle = 0 \end{aligned} \tag{B.1}$$

leads to the quadratic nonlocal action

$$\begin{aligned} S_{\rm eff} &= 2\int {\rm d}t{\rm d}t'\ \dot\Lambda^\dagger_{\rm cl}(t)\ \partial_t\Big[\Delta^R(t-t')-\Delta^A(t-t')\Big]\ \Big[\Lambda_{\rm q}(t')+\mathsf{V}^{-1}\dot\Lambda_{\rm cl}(t')X_{\rm q}(t')\Big] \\ &+ 2\int {\rm d}t{\rm d}t'\ \Big[\Lambda^\dagger_{\rm q}+X_{\rm q}\dot\Lambda^\dagger_{\rm cl}\mathsf{V}^{-1}\Big]_t\ \partial_t^2\Delta^K(t-t')\ \Big[\Lambda_{\rm q}+\mathsf{V}^{-1}\dot\Lambda_{\rm cl}X_{\rm q}\Big]_{t'}\ , \end{aligned} \tag{B.2}$$

where $\Delta^{R,A,K}(t)=\mathsf{D}^{R,A,K}(Vt,t)$ are phonon propagators restricted to the impurity trajectory.

Inverting the matrix in Eq. (2.33) and taking the appropriate analytic structure in the complex ω plane we obtain the Fourier components of the retarded and advanced propagators,

$$\mathsf{D}^R(q,\omega)=\Big[\mathsf{D}^A(q,\omega)\Big]^\dagger=\int dxdt\ e^{-iqx+i\omega t}\,\mathsf{D}^R(x,t)=\frac{1}{2}\begin{pmatrix}\frac{1}{q(\omega-cq+i0)} & 0\\ 0 & -\frac{1}{q(\omega+cq+i0)}\end{pmatrix} \tag{B.3}$$

This leads to

$$\mathsf{D}^R(q,\omega) - \mathsf{D}^A(q,\omega) = \frac{\pi}{iq}\begin{pmatrix}\delta(\omega - cq) & 0\\ 0 & -\delta(\omega + cq)\end{pmatrix} \tag{B.4}$$

and, subsequently,

$$\begin{aligned}\partial_t\Big[\Delta^R - \Delta^A\Big] &= \frac{1}{4\pi}\int \mathrm{d}q\,\mathrm{d}\omega\, e^{i(qV-\omega)t}\left(\frac{qV-\omega}{q}\right)\begin{pmatrix}\delta(\omega - cq) & 0\\ 0 & -\delta(\omega + cq)\end{pmatrix} &\text{(B.5)}\\ &= -\frac{1}{2}\delta(t)\mathbb{I}, &\text{(B.6)}\end{aligned}$$

where $\mathbb{I}$ is the 2×2 identity matrix.

The noise terms, *i.e.* the second line of Eq. (B.2), are controlled by the Keldysh component D^K and its derivatives. Assuming thermal equilibrium of phonons in the laboratory frame, and using Fluctuation-Dissipation Theorem, we have

$$\mathsf{D}^K(q,\omega) = \coth\left(\frac{\omega}{2T}\right)\Big(\mathsf{D}^R(q,\omega) - \mathsf{D}^A(q,\omega)\Big). \tag{B.7}$$

Using Eq. (B.4) we find the Fourier component of the Keldysh propagator restricted to the impurity trajectory

$$\begin{aligned}\Delta^K(\omega) &= \int\frac{\mathrm{d}q}{2\pi}\coth\left(\frac{\omega+qV}{2T}\right)\Big(\mathsf{D}^R(q,\omega+qV) - \mathsf{D}^A(q,\omega+qV)\Big)\\ &= \frac{1}{2i\omega}\begin{pmatrix}\coth\frac{\omega}{2T}\frac{c}{c-V} & 0\\ 0 & \coth\frac{\omega}{2T}\frac{c}{c+V}\end{pmatrix}, &\text{(B.8)}\end{aligned}$$

Substituting its Fourier transform it into Eq. (B.2) and taking a double time derivative leads to the second term in Eq. (2.40).

B.2 Solution of equation of motion for a strongly coupled impurity

We write the sinusoidal forms for the velocity and the phase of the depleton

$$V(t) = V_{\mathrm{D}} + V_{\mathrm{B}}\sin(\omega_{\mathrm{B}}t + \delta_V); \qquad \dot{\Phi}(t) = \omega_{\mathrm{B}}(1 + A\cos(\omega_{\mathrm{B}}t + \delta_\Phi)), \tag{B.9}$$

depending on *a priori* unknown parameters $V_{\rm D}, V_{\rm B}, \omega_{\rm B}, \delta_V, \delta_\Phi, A$ and substitute them into Eq. (2.61). One first arrives at the following relations between the time *independent* components.

$$n\omega_{\rm B} = F - \frac{1}{2}\frac{\kappa V_{\rm D}\omega_{\rm B}^2}{c^2 - V_{\rm D}^2}; \qquad \kappa\omega_{\rm B}/2n = V_{\rm D} \implies \omega_{\rm B}/2mc^2 = V_{\rm D}/c \tag{B.10}$$

Solving these equations one obtains $V_{\rm D}$ and $\omega_{\rm B}$ given by Eq. (2.64). In the limit $F \ll F_{\rm max} = 2nmc^2$ we recover the linear dependence $V_{\rm D}/c = F/F_{\rm max}$. The leading order deviation from linearity is given by

$$V_{\rm D}/c \approx \frac{F}{F_{\rm max}}\left(1 - \frac{F^2}{F_{\rm max}^2}\right). \tag{B.11}$$

Substituting the ansatz (B.9) into the first of Eqs. (2.61) gives a relation between the time *dependent* components,

$$\begin{aligned} 0 &= A\left[n\omega_{\rm B} + \frac{\kappa\omega_{\rm B}^2 V_{\rm D}}{c^2 - V_{\rm D}^2}\right]\cos(\omega_{\rm B}t + \delta_\Phi) \\ &+ V_{\rm B}(M - mN)\omega_{\rm B} \\ &\times \left[\cos(\omega_{\rm B}t + \delta_V) + \frac{1}{2}\frac{\kappa\omega_{\rm B}}{M - mN}\frac{c^2 + V_{\rm D}^2}{(c^2 - V_{\rm D}^2)^2}\sin(\omega_{\rm B}t + \delta_V)\right], \end{aligned} \tag{B.12}$$

where we neglected terms $\mathcal{O}(A^2)$, $\mathcal{O}(V_{\rm B}^2)$ and $\mathcal{O}(AV_{\rm B})$ to keep the calculation to first order in V_c/c, as both $V_{\rm B}$ and A will be seen to scale with V_c/c. The second term in brackets in Eq. (B.12) is simplified employing the formula

$$\cos x + \alpha \sin x = -\sqrt{1 + \alpha^2}\cos(x + \pi/2 + \arctan(1/\alpha)). \tag{B.13}$$

In order to cancel the term $\propto \cos(\omega_{\rm B}t + \delta_\Phi)$, we require a definite relation between the phases and amplitudes. The constraint for the phase is $\delta_V + \pi/2 + \arctan(1/\alpha) = \delta_\Phi$. From Eq. (B.12) we have

$$\alpha = \frac{1}{2}\frac{\kappa\omega_{\rm B}}{M - mN}\frac{c^2 + V_{\rm D}^2}{\left(c^2 - V_{\rm D}^2\right)^2} = \frac{m\kappa}{M - mN}\frac{1 + V_{\rm D}^2/c^2}{\left(1 - V_{\rm D}^2/c^2\right)^2}\frac{V_{\rm D}}{c}. \tag{B.14}$$

The equality of amplitude implies a relation between A and $V_{\rm B}$, namely

$$A = \frac{V_{\rm B}}{c}\frac{M - mN}{m\kappa}\sqrt{1 + \alpha^2}\left(\frac{1 - V_{\rm D}^2/c^2}{1 + V_{\rm D}^2/c^2}\right). \tag{B.15}$$

Finally, we substitute the ansatz into the second of Eqs. (2.61) to obtain

$$\left[AV_{\mathrm{D}} + \frac{\alpha V_{\mathrm{B}}}{\sqrt{1+\alpha^2}}\right]\cos(\omega_{\mathrm{B}}t+\delta_\Phi) + \frac{V_{\mathrm{B}}}{\sqrt{1+\alpha^2}}\sin(\omega_{\mathrm{B}}t+\delta_\Phi) = -V_c\sin(\omega_{\mathrm{B}}t+\Phi_0), \quad \text{(B.16)}$$

where we used $\sin(\omega_{\mathrm{B}}t+\delta_V) = -\frac{1}{\sqrt{1+\alpha^2}}\left(\sin(\omega_{\mathrm{B}}t+\delta_\Phi)+\alpha\cos(\omega_{\mathrm{B}}t+\delta_\Phi)\right)$ and Φ_0 is some initial phase of Φ which comes from integrating the second of Eqs. (B.9). Using Eq. (B.13) again finally gives

$$V_{\mathrm{B}} = V_c\frac{1-V_{\mathrm{D}}^2/c^2}{\sqrt{1+V_{\mathrm{D}}^4/\alpha^2c^4}} = V_c\frac{1-V_{\mathrm{D}}^4/c^4}{\sqrt{\left(1+V_{\mathrm{D}}^2/c^2\right)^2+\left(\frac{M-mN}{\kappa m}\right)^2\left(1-V_{\mathrm{D}}^2/c^2\right)^4V_{\mathrm{D}}^2/c^2}}, \quad \text{(B.17)}$$

where V_{D} is given by Eq. (2.64). As expected, V_{B} is an even function of F since V_{D} is odd. For small $F \ll F_{\max}$ Eq. (B.17) gives Eq. (2.64).

B.3 Calculation of the backscattering amplitude Γ_{+-}

Using the transformation Eq. (2.35) we have $\mathsf{\Gamma} = 2\mathsf{T}^\dagger\mathsf{H}^{-1}\mathsf{T}$ which leads to

$$\Gamma_{+-} = \frac{1}{\det\mathsf{H}}\left(\kappa H_{NN} - \frac{1}{\kappa}H_{\Phi\Phi}\right). \quad \text{(B.18)}$$

The matrix of second derivatives

$$\mathsf{H} = \begin{pmatrix} H_{\Phi\Phi} & H_{\Phi N} \\ H_{N\Phi} & H_{NN}\end{pmatrix} \quad \text{(B.19)}$$

is calculated at equilibrium values of Φ and N, which we denote in this Appendix by Φ, N instead of Φ_0, N_0 for brevity. Differentiating Eq. (2.11) and taking into account Eq. (2.10) for the dependence of the velocity V on Φ and N at constant momentum P, one can rewrite Eq. (B.19) as

$$\mathsf{H} = \frac{1}{M-mN}\begin{pmatrix} n^2 & -nmV \\ -nmV & m^2V^2\end{pmatrix} - \frac{1}{\det\Omega}\begin{pmatrix} N_\mu & -\Phi_\mu \\ -N_j & \Phi_j\end{pmatrix} \quad \text{(B.20)}$$

The last term in this equation represents the matrix of second derivatives of $H_{\mathrm{d}}(\Phi, N)$. Owing to a property of Legendre transformations, we have expressed it as the inverse of the Hessian matrix,

$$\Omega = \begin{pmatrix} \Omega_{jj} & \Omega_{j\mu} \\ \Omega_{\mu j} & \Omega_{\mu\mu}\end{pmatrix} = \begin{pmatrix} \Phi_j & \Phi_\mu \\ N_j & N_\mu\end{pmatrix} \quad \text{(B.21)}$$

of the thermodynamical potential $\Omega'_{\rm d}(j',\mu')$. Hereafter we drop the primes over Ω, j and μ for clarity. In writing Eq. (B.21) we used Eq. (2.5) to express the double derivatives as derivatives of the equilibrium values Φ and N with respect to the underlying values of the supercurrent and chemical potential.

Using the relations $mV = \partial\mu/\partial V$, $n = -\partial j/\partial V$ in the first term of Eq. (B.20) simplifies considerably the determinant

$$\det \mathsf{H} = \frac{1}{\det\Omega}\left(1 - \frac{1}{M-mN}\left[m^2V^2N_\mu + n^2\Phi_j - mnV(N_j+\Phi_\mu)\right]\right) \quad \text{(B.22)}$$

$$= \frac{1}{\det\Omega}\frac{M^*}{M-mN}. \quad \text{(B.23)}$$

by using the effective mass Eq. (2.19) of the equilibrated impurity. We use this fact and invert the matrix in Eq. (B.20) by a standard procedure and find for the off-diagonal matrix element

$$\Gamma_{+-} = \frac{1}{\kappa M^*}\Big[(M-mN)\left(\kappa^2\Phi_j - N_\mu\right) + n^2\left(1-V^2/c^2\right)\left(\Phi_j N_\mu - \Phi_\mu N_j\right)\Big]. \quad \text{(B.24)}$$

In the heavy particle limit $M \simeq M^* \gg m$ only the first term in the square bracket survives. In this limit Γ_{+-} can be identified with backscattering amplitude of a static impurity $\Gamma_{+-} = \Gamma_\infty = \kappa\Phi_j - \kappa^{-1}N_\mu = -\left(\partial_V\Phi + m\partial_n N\right)/mc$. To obtain this result we inverted the relations in Eq. (2.16),

$$\begin{pmatrix}\partial_j\\ \partial_\mu\end{pmatrix} = \frac{1}{m\left(c^2-V^2\right)}\begin{pmatrix}-mc^2/n & mV\\ -V & n\end{pmatrix}\begin{pmatrix}\partial_V\\ \partial_n\end{pmatrix}, \quad \text{(B.25)}$$

and used the identity $n\partial_n\Phi - mV\partial_n N = V\partial_V\Phi - (mc^2/n)\partial_V N$. The latter is obtained from equality of the mixed derivatives of the Lagrangian $L(V,n)$, obtained by differentiating Eqs. (2.17), (2.18) by n and V, respectively. The second term in the square brackets in Eq. (B.24) is transformed by applying (B.25). Combining it with the term $\Gamma_\infty\,(M-mN)/M^*$ yields Eq. (2.74).

To deal with equilibrium functions $\Phi(P,n)$, $N(P,n)$ obtained for a given momentum P rather than velocity V we use the fact that $\partial_V = M^*\partial_P$ and the following relation for the derivatives with respect to the density

$$\left(\partial/\partial n\right)_V = \left(\partial/\partial n\right)_P - M^*\left(\partial V/\partial n\right)_P\partial_P\,. \quad \text{(B.26)}$$

Differentiating Eqs. (2.17),(2.18) with respect to P and n at constant momentum leads to

$$\begin{pmatrix}\partial_P\Phi\\ \partial_P N\end{pmatrix} = \frac{1}{m\,(c^2-V^2)}\begin{pmatrix}mc^2/n & mV\\ V & n\end{pmatrix}\begin{pmatrix}(M^*-M+mN)/M^*\\ \partial_n V+\Phi/M^*\end{pmatrix} \quad \text{(B.27)}$$

$$\begin{pmatrix}\partial_n\Phi\\ \partial_n N\end{pmatrix} = \frac{1}{m\,(c^2-V^2)}\begin{pmatrix}mc^2/n & mV\\ V & n\end{pmatrix}\begin{pmatrix}-\Phi-(M-mN)\partial_n V\\ \Phi\partial_n V+(\alpha_d-\alpha N)\end{pmatrix}, \quad \text{(B.28)}$$

where $\alpha_d = \partial_n^2 E$. Substituting Eq. (B.26) into Eq (2.74), using the effective mass, Eq. (2.19) together with Eq. (B.27) we arrive at Eq. (2.75). Alternatively one may wish to express Γ_{+-} directly in terms of derivatives of the dispersion law $E(P,n)$ with the result,

$$\begin{aligned}\Gamma_{+-} &= -\frac{1}{cn}\frac{1}{1-V^2/c^2}\left[\frac{M-mN}{m}+\frac{n^2}{mc^2}(\alpha_d-\alpha N)\right.\\ &- \left.\frac{(M-mN)^2-m^2\kappa^2\Phi^2}{mM^*}+2m\kappa^2\Phi\partial_n V\right] \end{aligned} \quad \text{(B.29)}$$

In the limit of small velocities, the terms proportional to Φ can be neglected and this expression becomes identical to Eq. (3) in Ref.[25] with $N = 1-\delta_l$.

B.3.1 Expression for Γ

As first shown in Refs. [25, 26, 29, 30], the back-scattering amplitude $\Gamma = m(c^2-V^2)\Gamma_{+-}$ can be expressed in terms of partial derivatives of the exact dispersion. Since $\delta_\pm$ also depend on partial derivatives of the same dispersion, one can partially simplify the expression for Γ by using together Eqs. (4.8) & (4.12). This yields a relatively compact form for the scattering amplitude,

$$\Gamma = -\frac{n}{c}\partial_n^2\left(E-\frac{M}{m}\mu\right)-\frac{m}{M^*}\frac{\tilde\delta_+\tilde\delta_-}{\pi}-m\sqrt{K}\left[\frac{\tilde\delta_+}{\pi}\partial_n(c-V)-\frac{\tilde\delta_-}{\pi}\partial_n(c+V)\right],$$

where $\tilde\delta_\pm = \delta_\pm \pm \frac{M}{m}\frac{\pi}{\sqrt{K}}$. At small momentum one finds

$$\Gamma = \frac{n}{c}\partial_n^2\tilde\mu-\frac{n}{M^*c^3}\left(\partial_n\tilde\mu\right)^2-\frac{2n}{c^2}(\partial_n c)(\partial_n\tilde\mu), \quad \text{(B.30)}$$

where $\tilde\mu = E(0,n)-\frac{M}{m}\mu$. For a generic $SU(2)$ symmetric gas with equal coupling constants and masses ($M=m$), one has $E(0,n)=\mu(n) \implies \tilde\mu = 0$, and thus

$\Gamma = 0$ (note that in this case $\Gamma = 0$ actually holds for *arbitrary* momenta, as can be checked using the exact Bethe Ansatz solution for $E(P, n)$). For a gas of weakly interacting particles with local interactions of strength g between background particles and G between background and impurity, one finds $\mu = ng = mc^2$, $E(0, n) = nG$ and $M^* \approx M$ to leading order in g, G. Using Eq. (B.30) then gives $\Gamma = \frac{G}{c}(mG/Mg - 1)$. One thus sees explicitly that $\Gamma \to 0$ at the $SU(2)$ symmetric point: $M = m$ and $G = g$.

B.4 Impurity Spectral Function and Orthogonality Catastrophe

The discussion of Ch. 3.3 puts us in a position to heuristically discuss various tunneling or absorption probabilities in 1d quantum liquids. The latter is proportional to the imaginary part of a certain correlation function, which in the case of impurity tunneling defines its spectral function: $A(P, \omega)$, given by the Fourier transform of $\langle 0|\Psi_P(t)\Psi_P^\dagger(0)|0\rangle$. Here $\Psi_P^\dagger$ creates an impurity with momentum P and $|0\rangle$ represents the ground state of the system in the absence of the impurity.

Roughly speaking, the problem may be reduced to the probability of an impurity tunneling from the initial state with $N = 0, \Phi = 0$ and energy ω to the ground-state with finite $N(P)$, $\Phi(P)$ and energy $E(P)$. Applying this formulation of the problem to the results of Ch. 3.3 we find according to Eq. (3.11)

$$A(P, \omega) \propto \Theta\left[\omega - E(P)\right]\left[\omega - E(P)\right]^{\alpha(P)}, \tag{B.31}$$

where Θ is the Heaviside step function and $\alpha(P)$ is taken from Eq. (3.11) with $\Delta N = N(P)$ and $\Delta\Phi = \Phi(P)$.

The power-law threshold behavior of the impurity spectral function is a ubiquitous feature of correlation functions in 1d. The existence of a lower edge, $E(P)$, is a consequence of kinematical constaints in 1d, while the the power-law behavior of the spectral density directly above it stems from the orthogonality catastrophe. Such effects and their universality are discussed extensively in Refs. [36, 38, 39, 40, 54]. The dispersion $E(P)$ and exponent $\alpha(P)$ are non-universal functions of momentum which depend on the specific model and the correlation function under consideration. In the case of the impurity tunneling threshold, the exponent $\alpha(P)$ agrees with the exponents $\mu_d(P)$ of

Ref. [38] and $\alpha(P)-1$ of Ref. [36] once one identifies the relation between N, Φ and the scattering phase shifts $\delta_{\pm}$, see Eq. (4.12).

If instead one is interested in the spin-flip probability in a ferromagnetic spinor condensate, for example, the appropriate correlation function first extracts a spin-up particle and then replaces it with a spin-down particle. The difference is that now the depletion cloud of the initial state is, in effect, already missing the extracted particle: $N \to N-1$. The correct exponent in this case is thus $\alpha_{\rm flip}(P) = \alpha(N(P)-1, \Phi(P))$, which agrees with the exponents $\mu_m(P)$ of Ref. [38] and $\Delta(P)$ of Ref. [39]. Since the impurity tends to deplete the surrounding fluid the spin-flip protocol leads to a larger overlap between initial and final states, thus reducing the corresponding orthogonality effect, $\alpha_{\rm flip} < \alpha$ [83].

A similar rule of thumb can be used to determine the exponents outside the principal momentum interval $|P| < \pi n$. In that case one realizes that when $P \to P + 2\pi n j$ the phase drop likewise increases as $\Phi \to \Phi + 2\pi j$, for integer j. Therefore, tunneling at large momenta, such that $-\pi n < P - 2\pi n j < \pi n$, is determined by the exponent $\alpha(N(P^*), \Phi(P^*) + 2\pi j)$, where $P^* = P - 2\pi n j$ and $|P^*| < \pi n$. Although the spectrum remains periodic, the exponent α increases with large $|j|$. This is again a manifestation of the orthogonality effect: the final state describes a fluid carrying an additional momentum $2\pi n j$, which has progressively less overlap with the initial state in which the fluid is at rest [38, 83].